The Activity and Metabolism of Recombinant Lecithin:Cholesterol Acyltransferase in vivo

by

STAN TERRY SHAW

B.M.L.Sc., The University of British Columbia, 1989

A THESIS SUBMITTED IN PARTIAL FULFILLMENT OF

THE REQUIREMENTS FOR THE DEGREE OF

DOCTOR OF PHILOSOPHY

IN THE FACULTY OF GRADUATE STUDIES

(Department of Pathology)

We accept this thesis as conforming

to the required standard

THE UNIVERSITY OF BRITISH COLUMBIA

July, 1996

©Stan Shaw, 1996

In presenting this thesis in partial fulfilment of the requirements for an advanced degree at the University of British Columbia, I agree that the Library shall make it freely available for reference and study. I further agree that permission for extensive copying of this thesis for scholarly purposes may be granted by the head of my department or by his or her representatives. It is understood that copying or publication of this thesis for financial gain shall not be allowed without my written permission.

Department of _Pathology_

The University of British Columbia
Vancouver, Canada

Date _16 Aug '96_

Abstract

Lecithin:cholesterol acyltransferase (LCAT; phosphatidylcholine-sterol acyltransferase, EC 2.3.1.43) is the plasma enzyme responsible for the formation of the majority of cholesteryl esters in human plasma. Its role in regulating plasma lipoprotein metabolism has been recognized for many years. However, despite extensive research, our knowledge of the structure and function of this enzyme is incomplete. With this in mind, the purpose of this thesis was to utilize a molecular biology approach to better understand the structure of LCAT through analysis of predicted amino acid sequences and to utilize our ability to produce active recombinant LCAT to study the metabolism of LCAT *in vivo*. Specifically, we set out to:

- Clone rabbit LCAT cDNA.
- Constitutively express rLCAT in a stable cell line
- Produce radiolabeled, biologically active rLCAT
- Determine the metabolic turnover rate of rLCAT *in vivo*.

In order to achieve these aims, we cloned and expressed full length rabbit rLCAT and near full-length porcine rLCAT.The near full-length porcine cDNA was obtained from screening a porcine λ-GT 11 library. Together with previously published sequence data from other species, the information obtained from the cloned porcine LCAT cDNA enabled us to design a set of consensus primers which were used to amplify overlapping nucleotide sequences from reverse-transcribed rabbit liver RNA.

The nucleotide sequence identity of the rabbit LCAT cDNA sequence was 93% when compared to human LCAT . All major predicted structural features found in human LCAT were found in the rabbit sequence. This includes the lipase consensus region, the predicted N-linked glycosylation sites and potential bridged Cys residues.

The rabbit LCAT cDNA was cloned into a pNUT expression vector, stably transfected into BHK cells and the enzymatically active recombinant protein was purified from the culture media. Characterization of the recombinant rabbit LCAT demonstrated that it was activated by both human and rabbit apo A-I and the Km of unesterified cholesterol in HDL analog substrates was 72.8 nmol/mL. All methods for radioiodination of the rLCAT (e.g.,Bolton-Hunter, Chloramine-T and Iodobeads) resulted in an enzymatically inactive protein. However, endogenous incorporation of [^{3}H]-leucine into BHK cells produced radiolabeled rLCAT with unaltered esterification activity. When incubated with plasma, 44.3% of [^{3}H]-rLCAT was bound to lipoprotein fractions separated by size-exclusion chromatography. In vivo metabolic studies of rabbits injected with [^{3}H]-rLCAT showed two catabolic components; the largest, with a half-life of 2.1-5.8 hours, and a second with a half-life of 52.7-62.6 hours. Interestingly, rabbits injected with enzymatically inactive [^{125}I]-rLCAT demonstrated no significant difference between the two components when compared to the turnover of [^{3}H]-rLCAT. Since enzyme activity is maintained despite the failure of the majority of added rLCAT to bind to HDL *in vitro* and *in vivo*, the evidence suggests that esterification activity by LCAT does not require the enzyme to be permanently associated with plasma lipoproteins.

In conclusion, this thesis provided novel information regarding the molecular organization of rabbit and porcine LCAT and the properties (*in vitro*) and catabolism of the recombinant enzyme (*in vivo*) in the New Zealand rabbit. These studies extend the growing body of knowledge of the structure and function of LCAT. In addition, the unexpectedly high initial rate of turnover of the rLCAT *in vivo* provides valuable insights into the utility of rLCAT for enzyme replacement therapy.

Table of Contents

Table of Contents (con't)

Tables

Figures

Figures (con't)

Abbreviations

ACAT	acyl coenzyme A:cholesterol acyltransferase
apo	apolipoprotein
BHK	baby hamster kidney
CE	cholesteryl ester
CER	cholesterol esterification rate
CETP	cholesteryl ester transfer protein
CHO	Chinese hamster ovary
CLD	classic LCAT ceficiency (total LCAT deficiency)
COS	transformed monkey kidney cell
cDNA	complementary DNA
DEAE	diethylaminoethyl
DHFR	dihydrofolate reductase
DMEM	Dulbecco's modified Eagle medium
DMSO	dimethylsulfoxide
DNA	deoxyribonucleic acid
DPPC	dipalmitoylphosphatidylcholine
dATP	deoxyadenosine triphosphate
dCTP	deoxycytidine triphosphate
dGTP	deoxyguanosine triphosphate
dTTP	deoxythymidine triphosphate
EDTA	ethylenediamine tetra-acetic acid
Endo H	endoglycosidase H
FA	fatty acid
FBS	fetal bovine serum

FED	fish eye disease
HDL	high density lipoprotein
HEPES	N-2-hydroxyethylpiperazine-N'-2-ethanesulfonic acid
HL	hepatic lipase
IDL	intermediate density lipoprotein
LAT	lysolecithin acyltransferase
LCAT	lecithin:cholesterol acyltransferase
LDL	low density lipoprotein
LPL	lipoprotein lipase
Lp	lipoprotein
mRNA	messenger RNA
PC	phosphatidylcholine
PCR	polymerase chain reaction
PL	phospholipid
PLTP	phospholipid transfer protein
PNP	*p*-nitrophenol
POPC	palmitoyloleoylphosphatidylcholine
RNA	ribonucleic acid
RNAse	ribonuclease
rHDL	reconstituted high density lipoprotein
rLCAT	recombinant lecithin:cholesterol acyltransferase
SDS	sodium dodecylsulfate
TC	total cholesterol
TG	triglyceride
UC	uneseterified cholesterol
VHDL	very high density lipoprotein
VLDL	very low density lipoprotein

Amino Acid Designations

Amino Acid	Single Letter	Three Letter
Alanine	A	Ala
Arginine	R	Arg
Asparagine	N	Asn
Aspartic acid	D	Asp
Cysteine	C	Cys
Glutamic acid	E	Glu
Glutamine	Q	Gln
Glycine	G	Gly
Histidine	H	His
Isoleucine	I	Ile
Leucine	L	Leu
Lysine	K	Lys
Methionine	M	Met
Phenylalanine	F	Phe
Proline	P	Pro
Serine	S	Ser
Threonine	T	Thr
Tryptophan	W	Trp
Tyrosine	Y	Tyr
Valine	V	Val

ACKNOWLEDGMENTS

Chapter 1

INTRODUCTION

1.   INTRODUCTION

Lecithin:cholesterol acyltransferase (LCAT; phosphatidylcholine-sterol acyltransferase, EC 2.3.1.43) is the plasma enzyme responsible for the formation of the majority of cholesteryl esters in human plasma. Its role in regulating plasma lipoprotein metabolism has been recognized for many years; however, despite extensive research, our knowledge of the structure and function of this enzyme is incomplete. With this in mind, the purpose of this thesis was to utilize a molecular biology approach to understand the structure of LCAT through analysis of predicted amino acid sequences and to utilize our ability to produce active recombinant LCAT to study the metabolism of LCAT in vivo.

In this introduction, I have attempted to provide an accurate summary of our knowledge of LCAT to date. In addition, I include a review of the structure and function of high density lipoproteins (HDL), since the metabolism of LCAT is clearly related to the metabolism of this plasma lipoprotein.

1.1   Plasma Lipoproteins

1.1.1   Lipoprotein Structure

Cholesterol is transported in the plasma via a complex mixture of lipids and proteins which form water-miscible lipoproteins. These lipoproteins are composed of a surface monolayer consisting of proteins (known as apoproteins), phospholipids and unesterified cholesterol and an inner neutral lipid core of cholesteryl ester and triacylglycerol. The structure and metabolism of lipoproteins is determined largely by the protein content and composition. Apolipoproteins, are amphipathic and contain both polar and nonpolar properties. Several of these apolipoproteins have multiple functional roles in lipid metabolism acting as enzyme reaction cofactors, promotion of lipid transfer reactions and ligands which bind to specific cell membrane receptors.

The classification of plasma lipoproteins has been traditionally based on their relative buoyant density (see table 1). The average size of each lipoprotein class is inversely proportional to its hydrated density with the least dense class, chylomicrons, having the largest size. Each class is a heterogeneous group of related species which encompass a range of densities and size but with a similar apoprotein composition. Very low density lipoprotein (VLDL) is synthesized and secreted in the liver and has a relative density of d<1.006 g/mL. The formation of VLDL is regarded as the initial stage in the complex process underlying the transport and metabolism of endogenous lipids. Low Density lipoproteins (LDL), d=1.006-1.063 g/mL, is the form of lipid most closely identified with accelerated atherosclerosis (Goldstein and Brown, 1987). This lipoprotein is produced through the metabolism of VLDL and is involved in the "forward" delivery of cholesterol from the liver to peripheral tissues. The major apoprotein of LDL is apolipoprotein B (apo B). The molecular size of the form found in LDL (termed apo B-100) which is synthesized in the liver, is greater than that found in chylomicrons (apo B-48), synthesized in the intestine in humans. Specific receptors on the cell surface recognize apo B and mediate the uptake and distribution of LDL cholesterol to peripheral cells. The major apoprotein of small dense lipoproteins, HDL and VHDL, is apoprotein A-I. Unlike LDL, in which only one apoprotein is present (apo B-100), all other classes of lipoproteins contain mixtures of several other proteins, designated as apoprotein A, C, D, E, F and H.

1.1.2   HDL Structure and Heterogeneity

HDL is a heterogeneous mixture of lipoproteins ranging in size between 7.0 and 10nm and a molecular weight of 200-400kDa (Eisenberg, 1984). HDL are classically defined as lipoproteins with relative densities between 1.063 and 1.21 (Havel *et al.,* 1955). Approximately 50% of HDL is protein by weight (in humans, mainly apo A-I and apo A-II). The rest of HDL is lipid, mainly phospholipids, free and esterified cholesterol , and triglyceride. HDL particles vary in apoprotein and lipid composition,

Table 1. Plasma lipoproteins. Adapted from Segrest (1994)

Lipoprotein	Abbreviation	Diameter (nm)	Density (g/mL)	Major Lipids*	Major Apolipo-proteins
Chylomicrons	Chylo, CM	75-100	0.93	TG	B48, E, C, A-I, A-II, A-IV
Very low Density	VLDL	30-80	0.93-1.006	TG	B-100) E, C
Intermediate Density	IDL	25-35	1.006-1.019	TG	B-100) E, C
Low Density	LDL	18-25	1.019-1.063	CE	B-100
High Density	HDL	5-12	1.063-1.21	Cholesterol, CE, phospholipid	A-I, A-II, C

*TG, Triglyceride; CE, cholesteryl ester

size and hydrated density. Discrete HDL subclasses, HDL_2 (in humans, d=1.063-1.125g/mL) and HDL_3 (1.125-1.21 g/mL) are isolated from other lipoproteins using the latter property using differential ultracentrifugation (Patsch JR, *et al.,*1980). Similar HDL subfractions have also been isolated from serum using differential dextran sulfate-magnesium chloride precipitation (Burstein *et al.,* 1989).

Further subpopulations of HDL particles have been isolated through a variety of techniques including, agarose gel electrophoresis, polyacrylamide gradient gel electrophoresis and immunoaffinity chromatography. In agarose gel electrophoresis, plasma proteins separate into distinct bands, i.e, albumin (the most anodic), $\alpha 1$- and

α2- globulins, β-globulins and γ-globulins (the most cathodic). Following agarose gel electrophoresis, the major fraction of HDL migrates with α-mobility and is therefore classified as α-HDL. Approx. 5% of total HDL migrates with preβ-mobility (preβ-HDL) (Kunitake *et al.*, 1985). These two major electrophoretic subfractions have been further characterized by polyacrylamide gradient gel used as the second dimension in two-dimensional electrophoresis. This technique separates α-HDL into two subfractions, (α-HDL$_2$ and α-HDL$_3$ and β-HDL into three subfractions (pre-β_1-HDL, pre-β_2-HDL and pre-β_3-HDL) (Fielding *et al.,* 1991). At least five subclasses of HDL, have been isolated using non-denaturing polyacrylamide gradient gel electrophoresis. Two of these subclasses HDL$_{2a}$ and HDL$_{2b}$ are of lower density, while the rest, HDL$_{3a,}$ HDL$_{3b}$ and HDL$_{3c}$ are of higher density (Blanch *et al.,* 1981). Using selective-affinity chromatography, a sub-population of lipoproteins containing apo A-I but, unlike the majority of HDL, having pre-β electrophoretic mobility has been isolated (Kunitake ST *et al.,* 1985).

HDL subclasses have also been defined by apoprotein content. Sequential immunoaffinity chromatography was first employed by Cheung and Albers to isolate two populations of apo A-I containing lipoproteins from plasma of normal individuals (Cheung *et al.,* 1984). Since then, monoclonal antibodies to apo A-I, A-II and A-IV have been used to isolate four types of lipoproteins (Lp A-I, Lp A-I:A-II, Lp A-I:A-IV and Lp A-IV) (Fruchart *et al.,* 1993). Apo A-I was found to be the major protein in Lp A-I, Lp A-I:A-II and Lp A-I:A-IV. All particles contained a similar proportion of protein to Lp A-I:IV and Lp A-IV contain lower cholesterol but higher triglyceride levels than Lp A-I and Lp A-I:I-II. Most plasma apo A-I (65%) and A-II (98%) are contained in Lp A-I:A-II particles. Most apo A-IV (83%) is found in Lp A-IV. Additional protein constituents were identified in the isolated lipoproteins by applying SDS-polyacrylamide gel electrophoresis followed by immunoblots. Each type of particle contained cholesteryl ester transfer protein (CETP), lecithin:cholesterol acyltransferase (LCAT)

and apo D. The majority of CETP, a protein which promotes the exchange of HDL cholesteryl esters for triglyceride in LDL and VLDL particles, was isolated in Lp A-I, Lp A-IV and Lp A-I:A-IV. The production of cholesteryl esters derived from HDL , phospholipids and unesterified cholesterol due to LCAT activity was found to be highest in Lp A-IV particles, with lesser activity in Lp A-I:A-IV and Lp A-I (Fruchart *et al.,* 1993). however, differences were found in the lipid content (see Table I).

Table 2. Protein, apolipoprotein and lipid composition of Lp A-I, Lp A-I:A-II, Lp A-IV, Lp A-IV and Lp A-I:A-IV particles. Adapted from Fruchart *et al.,* (1993).

Mass (%)	Lp A-I	Lp A-I:A-II	Lp A-IV	Lp A-IV:A-I
Proteins	62.0±7.4	65.2±7.3	70.2±20.1	61.3±9.4
Lipids				
TC	11.8±4.1	11.5±3.9	4.2±3.5	8.0±3.8
UC	2.8±1.1	1.6±1.1	0.4±0.2	1.2±1.1
TG	5.0±2.2	3.8±1.8	9.4±6.8	9.6±5.7
PL	21.2±4.4	19.5±4.3	16.2±10.5	21.1±6.9
Apolipoproteins				
AI	97.6±2.5	67.4±13.3	-	57.8±14.4
A-II	-	31.4±13.5	0.4±0.7	10.2±2.7
A-IV	2.1±2.4	1.0±1.9	99.6±0.8	31.5±21.0
C-III	0.3±0.3	1.2±0.2	0.1±0.1	0.4±0.1

Lp= lipoprotein; TC=total cholesterol; FC=free cholesterol; TG=triglycerides; PL=phospholipids. Values are given as mean ± standard deviation.

1.1.3   HDL Metabolism

Plasma HDL is thought to be produced either directly by the liver and intestine or may originate as a degradation product of chylomicron catabolism (Eisenberg, 1984). The newly formed "nascent" HDL particles, which may be discoidal or spherical, are rich in protein and contain only small amounts of lipid. They display pre-β electrophoretic mobility on agarose gels and contain phospholipids, unesterified cholesterol and triglyceride. Secreted hepatic nascent HDL consists of both Lp A-I and Lp A-I:A-II

while intestinal nascent HDL contains only apo A-I and apo A-IV particles (Forte *et al.,* 1989; Brewer *et al.,* 1990). Catabolic products of chylomicrons and other triglyceride-rich lipoproteins produce discoidal HDL through the extracellular activity of lipoprotein lipase (LPL) (Tall and Small, 1978). This results in the excess production of phospholipid and apolipoprotein surface components from which discoidal HDL particles, rich in phospholipid, apo A-I and apo Cs are derived .

1.2   Reverse Cholesterol Transport

The risk of coronary heart disease and its inverse correlation with plasma HDL levels has been well established through epidemiological studies (e.g., Miller *et al.,* 1975; Gordon *et al.,* 1977; Espeland *et al.,* 1994; Atger *et al.,* 1995). This association has been supported by pharmacological intervention trials in which increased HDL levels were associated with a reduced risk of coronary heart disease (Manninen *et al.,* 1988). Thus, increased HDL is thought to protect against vascular lipid accumulation and the development of atherosclerosis. The role of HDL, therefore, in reducing the risk of coronary artery disease (CAD) is generally thought to be due to its capacity to act as an acceptor of tissue cholesterol and to promote its esterification and transfer to lower density lipoproteins for rapid uptake by the liver. This hypothesis, known as reverse cholesterol transport, was originally described by Glomset (Glomset, 1968). Reverse cholesterol transport is composed of four distinct elements: efflux of free cholesterol from peripheral tissues, esterification of cholesterol in HDL, transfer to other lipoproteins and final transport to the liver (figure 1).

1.2.1   Cholesterol efflux

The initial phase of reverse cholesterol transport is the transport of

unesterified cholesterol between cell membranes and lipoproteins. Several mecha-

nisms have been proposed to explain how efflux from cells might occur: 1) aqueous

diffusion of cholesterol in the extracellular fluid (Phillips *et al.,* 1980) 2) binding of

HDL to cell surface receptors resulting in cholesterol translocation and efflux (Oram

JF, 1990) 3) cholesterol efflux mediated through apolipoproteins (Rothblat *et al.,*

1992) and 4) acceptor retroendocytosis (Schmitz *et al.,* 1985).   It is likely that no

single mechanism may be fully responsible for cholesterol efflux between cell types.
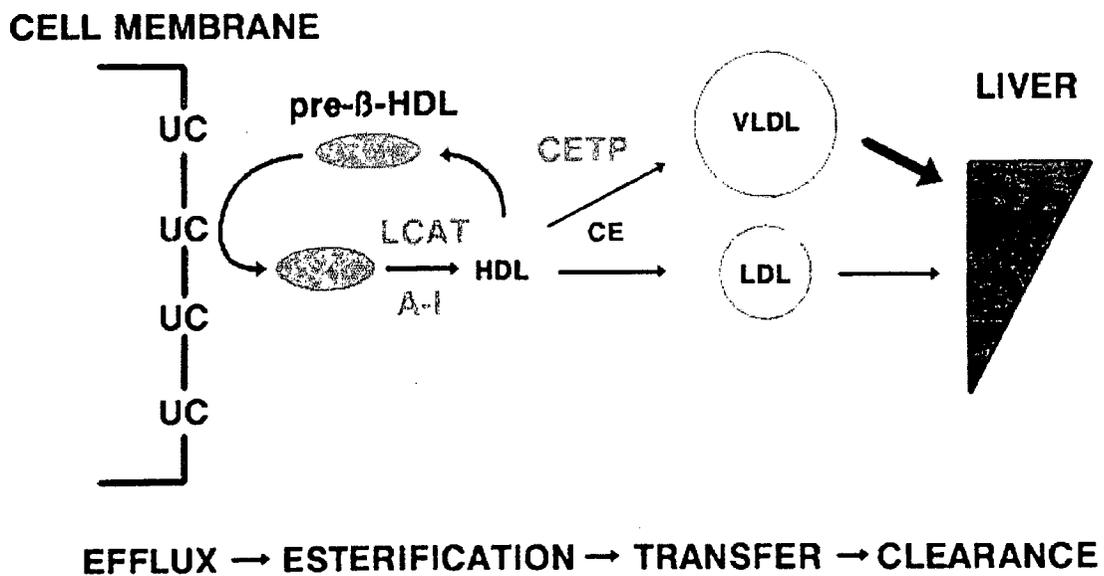
Figure 1. Reverse Cholesterol Transport. UC = unesterified cholesterol; CE= cholesteryl esters; HDL= high density lipoprotein; LDL= low density lipoprotein; VLDL= very low density lipoprotein; LCAT= lecithin cholesteryl acyl transferase; A-1 = apoprotein A-I; CETP = cholesteryl ester transfer protein.

Small discoidal HDL with pre-β electrophoretic mobility on agarose gel electrophoresis has been shown to be one of the most efficient acceptors of cholesterol from cell membranes (Castro and Fielding, 1988) . Recent evidence based on reconstituted HDL (rHDL) discoidal complexes shows a positive correlation between discoidal particle size and cholesterol efflux from fibroblasts (Agnani and Marcel, 1993). The pre-β HDL subfraction, depleted in cholesterol but rich in phospholipid and protein, is similar to nascent HDL directly synthesized by the liver and intestine or produced through catabolism of triglyceride-rich lipoproteins. The major apolipoprotein in this HDL subfraction is apo A-I. Studies of the Apo A-I amphipathic helix region suggest that a hinged region of the molecule may extend into the aqueous phase (Segrest et al., 1992) and that this portion may facilitate the diffusion of cholesterol into the acceptor lipoprotein by anchoring the lipoprotein to the plasma membrane and allowing the interaction with specific lipid domains (Rothblat et al., 1992). It is postulated that changes in apo A-I conformation due to accumulation of unesterified cholesterol accumulating within the discoidal complex causes disassociation of the lipoprotein from the cell membrane.

A separate HDL receptor-mediated pathway for cholesterol efflux and translocation has been proposed by Oram (1990). Studies supporting this model provide evidence that Apo A-I and A-IV may be recognized by specific cell surface receptors which stimulate translocation of intracellular cholesterol to the membrane through a signal-transduction pathway (Steinmetz et al., 1990; Mendez et al., 1991). Although this mechanism may have a role in cholesterol homeostasis, the low affinity and high capacity of the HDL receptors identified in these studies suggest this pathway cannot be responsible for the majority of cholesterol efflux from peripheral cells.

An HDL-receptor has now been identified in Chinese hamster ovary cells which can mediate selective HDL-cholesterol uptake (Acton et al., 1996). The mouse SR-BI receptor, a cell surface molecule previously cloned in hamster and reported to

bind native and chemically modified LDL, was shown to mediate cell association but not degradation of HDL. Although the role and importance of this receptor on reverse cholesterol transport is not clear, the identification of a specific receptor in the uptake of HDL-cholesterol is an important first step in understanding the mechanism through which HDL delivers cholesterol in reverse cholesterol transport.

1.2.2   Maintenance of a cholesterol concentration gradient.

A least two possible mechanisms have been proposed through which a concentration gradient may occur between cell membranes and HDL. The first mechanism, esterification of unesterified HDL cholesterol by LCAT, was originally proposed by Glomset (1970). The transfer and esterification of cholesterol derived from peripheral cells has been examined by pulse-chase studies with [^{3}H]-cholesterol-loaded fibroblasts. Unesterified cholesterol was taken up by small discoidal HDL with pre-β mobility, termed pre-β_1 particles. The incorporated unesterified cholesterol is quickly transferred from pre-β_1 to larger pre-β HDL particles, pre-β_2 and pre-β_3. The transfer of unesterified cholesterol between HDL subfractions appears to be specific and rapid, suggesting that this process is not due to simple diffusion. The pre-β_3 HDL subfraction is the major site of esterification by LCAT (Castro and Fielding, 1988; Francone *et al.,* 1989).

Recent evidence suggests that unesterified cholesterol derived from peripheral cells is only a small component of unesterified cholesterol involved in the LCAT reaction. The major source of unesterified cholesterol is the pool of apo B-containing particles, LDL and VLDL (Fielding and Fielding, 1981; Park *et al.,* 1987; Huang *et al.,* 1993). Some unesterified cholesterol derived from the larger LDL pool is thought to be redistributed to α-HDL and is subsequently esterified by LCAT (Fielding *et al.,* 1991). The transfer of LDL-derived unesterified cholesterol to HDL and the production of cholesteryl esters has been shown to be adversely affected by decreased LCAT esterification activity. Together with unesterified cholesterol taken up by dis-

coidal HDL from peripheral cells, to be esterified by LCAT, these LCAT-dependant mechanisms of transport provides an effective redistribution of cholesterol to the larger, α-HDL pool.

Pulse-chase studies have shown, however, a small component of unesterified cholesterol located on LDL to originate from cell-membrane derived cholesterol via HDL subfractions and ultimately to α-HDL. This suggests that a second, LCAT-independant, alternative pathway exists through which the cholesterol concentration gradient may be maintained between cell membranes and HDL. Unesterified choles-terol located on LDL that was not redistributed to HDL may be eventually transported to the liver for uptake via hepatic LDL receptors (Hung *et al.,* 1993).

1.2.3   Transfer to other lipoproteins and clearance of cholesterol by the liver

In many species, including man, cholesterol esterification is followed by the transfer of esterified cholesterol to other HDL subspecies or lower density lipoproteins by cholesteryl ester transfer protein (CETP). This transfer, which exchanges triglyceride for cholesteryl esters, provides rapid clearance of cholesterol via LDL and VLDL-remmants through hepatic apo B and apo E receptors. In species with little or no CETP activity, alternative pathways for the uptake of HDL in the rat include apo E receptor recognition and internalization of HDL particles (Glass *et al.,* 1985). Stud-ies by Kadowki *et al.* (1992) using perfused rat livers suggest that hepatic uptake of HDL cholesteryl esters and triglycerides require the presence of hepatic lipase (HL). HL-mediated uptake appear to be due to hydrolysis of HDL phospholipid rather than hydrolysis of triglyceride. Additionally, there is some *in vitro* evidence using cultured hepatocytes that a specific CETP-independant acceptor protein or lipoprotein may enable transfer of HDL cholesteryl esters onto the cell (Rinninger *et al.,* 1988).

1.2.4   HDL Remodelling

Lipids and apoproteins are cycled in a complex inter-conversion of HDL particles. The conversion of nascent discoidal HDL into spherical HDL is mediated by the esterification of cholesterol on the surface of the particle by LCAT and the movement of esterified cholesterol to the core to form HDL_3 (See figure 2). Unesterified cholesterol and phospholipid released from triglyceride-rich lipoproteins due to LPL activity and the simultaneous activity of LCAT result in the conversion of HDL_3 to produce HDL_2, a larger particle rich in esterified cholesterol (Patsch *et al.,* 1978).

Figure 2. Schematic drawing of HDL remodelling. CETP, cholesteryl ester transfer protein; FA, fatty acid; HL, hepatic lipase; LCAT, lecithin:cholesterol acyltransferase; LPL, lipoprotein lipase; PL, phospholipid; TG, triglyceride; UC, unesterified cholesterol.
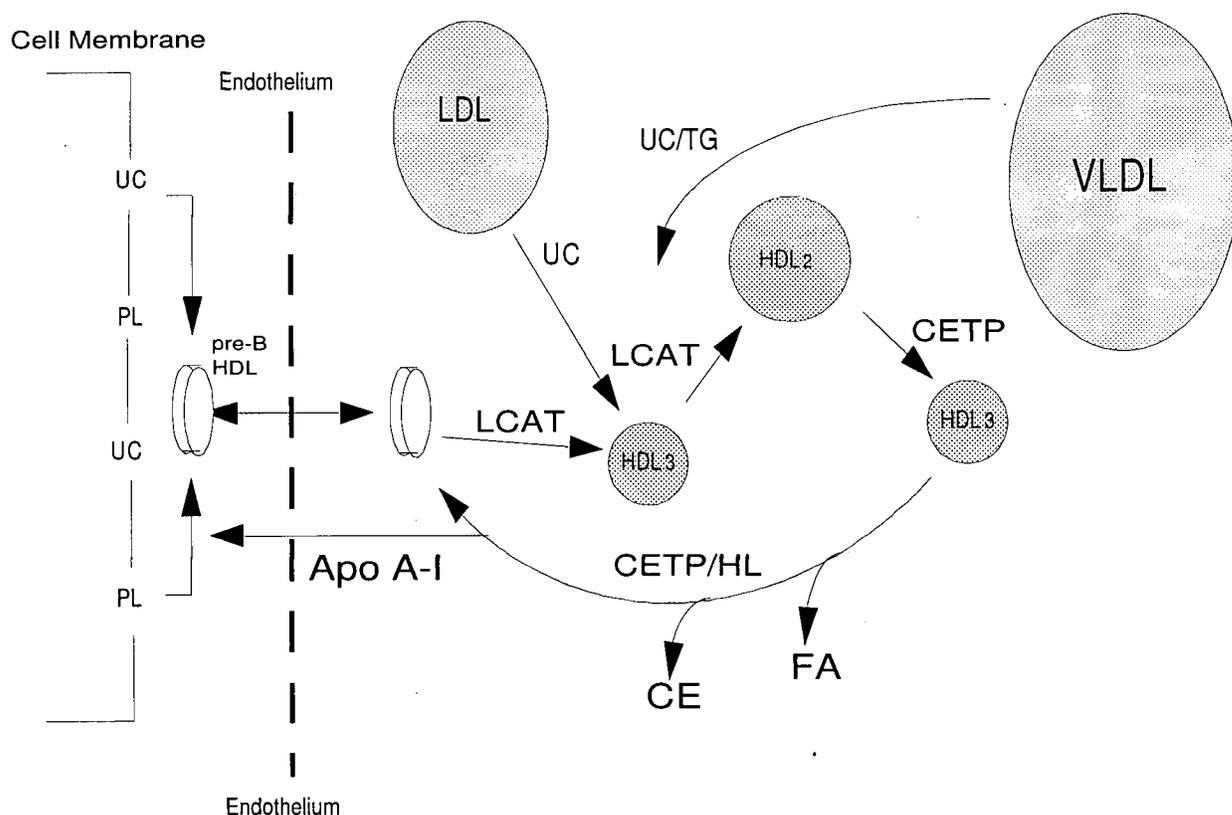
Several pathways exist by which HDL cholesterol esters are removed from the circulation. The dominant pathway in man is thought to involve CETP (Glomset 1970; Miller, 1984). A second pathway involves apo E (Miller *et al.,* 1985). In this hypothesis, cholesterol esters accumulate due to the esterification activity of LCAT in HDL. As HDL matures, resulting in an enlarged particle, apo E is progressively incorporated at the expense of apo A-I. Apo E then targets HDL for hepatic uptake. In addition to uptake of apo E in the general HDL pool, independently produced apo E-rich HDL particles may also mediate the clearance of cholesteryl esters in the liver. In humans, however, the rate of direct clearance of HDL apoproteins in the liver is low, suggesting that this route is a small contributor to total HDL cholesteryl ester efflux (Shepherd *et al.,* 1984). A third route, known as "selective uptake" involves the direct uptake of HDL cholesteryl esters without the endocytosis of HDL particles by the liver . This route is responsible for uptake of the majority of HDL cholesteryl esters in rats (Glass *et al.,* 1985).

The relative importance of these pathways vary between animal species. In rabbits, plasma CETP activity towards endogenous substrates is approximately four times that of humans, suggesting that this pathway is responsible for the clearance of the majority of HDL cholesteryl esters. Using multiple, simultaneously administered lipoprotein tracers, compartmental analysis of plasma decay curves has demonstrated this to be the case, resulting in the irreversible removal of approximately 67% of HDL-derived cholesteryl esters from LDL and VLDL following transfer via CETP (Goldberg *et al.,* 1991). Approximately 22% of HDL cholesteryl esters were removed by selective uptake, while irreversible clearance of HDL particles accounted for only 10% of total HDL cholesterol clearance. In contrast, rats (which lack CETP) clear approximately 90% of HDL cholesteryl esters in the liver via the selective uptake pathway (Glass *et al.,* 1985).

1.3 Lecithin Cholesterol Acyltransferase (LCAT)

1.3.1 Physical Properties of LCAT

LECITHIN   LYSOLECITHIN

CH₂O – *saturated fatty acid*   CH₂O – *saturated fatty acid*

CHO – *unsaturated fatty acid*   CHOH

CH₂O – P – choline   CH₂O – P – choline
         OH   OH

Phospholipase A2

———————————— LCAT ————————————→

Acyltransferase

CHOLESTEROL   CHOLESTERYL ESTER

HO   *unsaturated fatty acid*
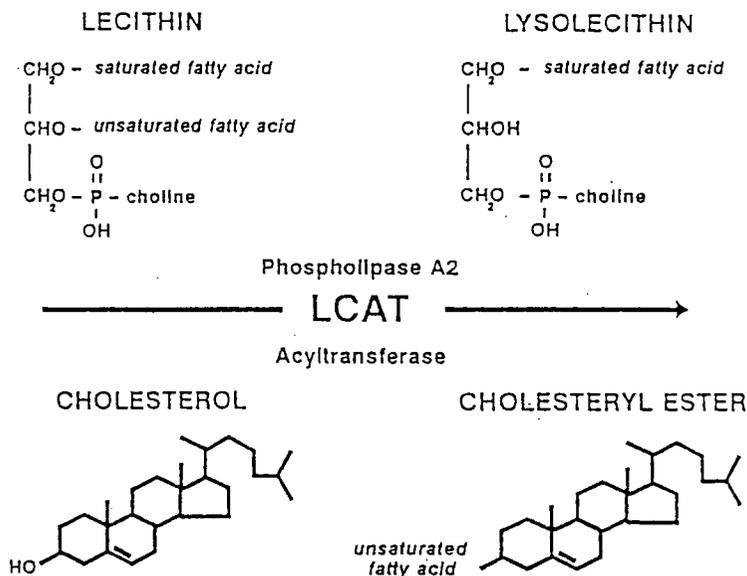
Figure 3. Schematic drawing of the LCAT reaction.

Lecithin:cholesterol acyltransferase (E.C. 2.3.1.43) (LCAT) catalyzes the transfer of an *sn*-2 fatty acid from phosphatidyl choline to the 3-hydroxyl group of cholesterol to produce lysophophatidylcholine and cholesteryl ester (Figure 3). The enzyme is unusual in that this single polypeptide sequence catalyzes both sequential reactions. LCAT is a glycoprotein with an apparent molecular weight of 67,000 daltons (Fielding, *et al.*, 1972a). It is secreted by the liver into the plasma where it is primarily associated with HDL, the major site of cholesterol esterification (Fielding and Fielding 1971; Chen and Albers, 1982). However, evidence provided by several investigators has shown that LCAT may act directly on lower density lipoproteins (Barter *et al.*, 1984, Barter *et al.*, 1985). Several investigators have determined that, under *in vitro* conditions similar to those found *in vivo*, apoprotein A-I (apo A-I), the major protein constituent of HDL, is the principle activator of cholesterol esterification by LCAT (Fielding and Fielding 1972a, Soutar *et al.*, 1975, Albers *et al.*, 1979, Matz

14

and Jonas 1982). Over 90% of LCAT activity is removed from plasma by anti-apo A-I immunoaffinity chromatography (Pritchard *et al.,* 1988) suggesting that there is both a functional and physical association between these two proteins.

LCAT has been purified to homogeneity from plasma in several laboratories including our own. The human gene for LCAT has been sequenced (McLean, *et al.,* 1986a) and contains 5 introns and 6 exons. Human LCAT mRNA consists of 1550 nucleotides and is primarily synthesized in the liver (McLean *et al.,* 1986b). The expressed protein includes a 24 amino acid hydrophobic leader sequence. The mature protein contains 416 amino acids with a calculated molecular weight of 47,090 and consists of a single polypeptide. The apparent molecular weight of LCAT is 65,000 to 69,000, due to glycosylation (Fielding, 1972a; Marcel, 1982). Approximately 25% of the total molecular mass of LCAT is glycosylated, which may explain its observed solubility in water despite a hydropathic index higher than other plasma lipoproteins, including apo A-I (Chong *et al.,* 1983).

Predictions of the major structural and functional regions of the enzyme have been made from analysis of the primary amino acid sequence and peptide alignment of human LCAT (Yang *et al.,* 1987). This includes a phospholipase homologous region similar to other known lipases (Brenner, 1988; Francone *et al.,* 1991). A hexapeptide (residues 178 to 183) is identical to the amino acid sequence found at the interfacial active site of porcine pancreatic lipase (McLean *et al.,* 1986b) A triad consisting of Gly-X-Ser-X-Gly has been proposed to have a role in the deacylation of phospholipid substrate, formation of an intermediate Ser-O-acyl moiety and subsequent transfer of the acyl chain to cholesterol (Fielding, 1991).

The primary sequence also contains four predicted sites for N-linked glycosylation at residues 20, 84, 272 and 384 (McLean, *et al.,* 1986a). Previous work in our laboratory has shown that all four N-linked sites are glycosylated and may affect the activity and secretion of the enzyme (O *et al.,* 1993). LCAT has multiple

isoelectric points ranging from pI 3.9 to 4.4, which may be altered by neuraminidase digestion. Careful examination of these bands on isoelectric focusing gels suggest there are 16 sialic acids per LCAT molecule (Doi and Nishida, 1983). Following extensive treatment to remove sialic acids, the apparent molecular weight is reduced by 3,000 and the multiple bands resolve to a single band at pI 5.2 (Doi and Nishida, 1983). Removal of the negatively charged residues through desialation appears to enhance interaction of LCAT with its substrates, resulting in an apparent increase in LCAT specific activity.

There are six cysteine residues in human LCAT. Chemical analysis has identified two cysteine residues with free sulfhydral groups (Yang et al., 1987). The remaining four residues are bridged between Cys-50 to Cys-75 and Cys-313 to Cys-356 (see figure 4).
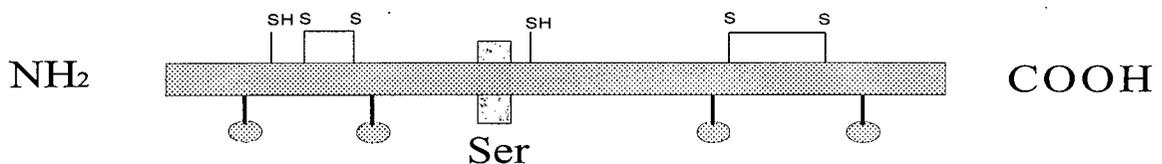
Figure 4. LCAT structural features. The relative positions of major components of the LCAT protein are shown. The catalytic lipase site, including Ser-181 is identified by the box, while the bridged and free cysteine residues are indicated above the line. The four N-linked glycosylation sites are indicated by the ovals below the line.

The predicted secondary structure, supported by circular dichroism measurements, suggests that LCAT is unique among lipoproteins in that it contains no long or medium length α-helices or β-sheets in the amino terminus (Yüksel et al., 1989; Chong et al., 1983). The predicted secondary structure shows some variation between species. Amino acid sequencing of the carboxyl-terminal region has shown that this region contains the greatest number of substitutions between porcine and human LCAT, resulting in the largest differences in conformation

16

between the two species. Most significant was the predicted transformation of the long α-helical region predicted in human LCAT between residues 377-391 into a region containing a β-turn, a β-sheet, and α-helix and a random coil in the porcine enzyme (Yüksel *et al.,* 1989). As this region also contains a predicted N-glycosylation site at Asn-384 (McLean *et al.,* 1986a), alterations of this predicted helix may be functionally significant.

1.3.2   The catalytic mechanism of LCAT

The biochemistry of LCAT has been studied extensively in recent years and has been the subject of several reviews (Barter *et al.,* 1987; Jonas, 1991). As previously mentioned, LCAT catalyses the transfer of an acyl chain from the sn-2 position of phosphatidylcholine to the 3-hydroxyl group of cholesterol, producing cholesteryl esters and lysophosphatidylcholines. Although LCAT shares little sequence identity between other lipases, it contains a Gly-X-Ser-X-Gly motif which is characteristic of the active sites of several other members of this family of enzymes (Brenner, 1988)

The role of Ser-181 and 216, located within different lipase consensus sequences of human LCAT, was investigated using site directed mutagenesis and *in vitro* expression studies by Francone and Fielding (1991a). The exchange of Ser-216 to glycine or threonine reduced, but did not eliminate LCAT specific activity in mutant clones expressing this enzyme. Interestingly, the substitution of Ser-216 with alanine resulted in a 14-fold increase in activity. Following sequence comparison with other lipases, it was suggested that Ser-216 may be at or near the hinge of a helical flap displaced following substrate binding. If this is the case, Ser-216 may be located in a regulatory region for LCAT activity. In contrast, however, substituting Ser-181 with these amino acids produced no detectable catalytic activity. This provided strong evidence that Ser-181 forms part of the active site for LCAT, while it was suggested that Ser-216 has an important but indirect effect in the LCAT catalytic reaction.

In pancreatic lipases, where the three-dimensional structure of the enzyme is

known, the active serine residue contained within this consensus sequence is part of a catalytic Asp-His-Ser triad (Winkler *et al.,* 1990). Interestingly, the esterolytic and cholesterol esterifying activities of both purified LCAT and several species of phospholipase A2 have been inhibited using a monoclonal antibody generated against purified human LCAT. In addition, when LCAT was treated with phenacyl bromide, a reagent with known effects on the active site of phospholipase A2, both the esterolytic activity and the binding ability of LCAT to phospholipase A2 were suppressed. This evidence suggests a similar conformation exists between LCAT and this family of phopholipases, most likely located near or within the esterolytic active site (Khalil *et al.,* 1986).

Site-directed mutagenesis at N-linked oligosaccharide attachment sites designed to prevent attachment of carbohydrates resulted in retention of significant phospholipase and acyltransferase activity in three of the four predicted sites (Asn-20, Asn-84 and Asn-384). Mutation at one site (asn272) produced an enzyme with phospholipase activity that generated fatty acids but no cholesteryl esters (Francone *et al.,* 1993), suggesting this residue was essential for acyltransferase activity. Site directed mutagenesis studies in our laboratory confirmed that all four sites are filled with oligosaccharide moieties (O *et al.,* 1993), Loss of carbohydrate at each site produced varying effects on enzyme activity. Of particular interest was the finding that the N-linked site at Asn-384 had an inhibitory effect on the enzyme. Loss of this site resulted in a two-fold increase in enzyme specific activity. These experiments also demonstrated that elimination of all four N-linked glycosylation sites using a quadruple mutant severely restricted both the specific activity of the enzyme (5% of the wild type) and secretion (10% of the wild-type production rate).

Chemical modifications of Cys, His and Ser residues have also been shown to inhibit LCAT activity (Jauhiainen and Dolphin, 1986). The modification of one histidine residue by diethyl pyrocarbonate or one serine residue by

phenylmethanesulfonyl fluoride inhibited both the acyltransferase and phopholipase activities of LCAT. Evidence obtained by using inhibitors to block sulfhydryl groups on LCAT suggested that the two free cysteine residues on LCAT (Cys-31 and Cys-184) were essential to form thioester bonds prior to the transfer of the acyl group to cholesterol. These two free cysteine residues were shown in a later study (Jauhia-ianen et al., 1988) to be vicinal to each other within the catalytic site.

The studies by Dolphin and coworkers (Jauhiaianen et al., 1988) provided major advances in the understanding of the esterification reaction catalyzed by LCAT and laid the ground work for further study for the structure-function relationship of this enzyme. Subsequent studies using site-directed mutagenesis, however, showed that substitution of the free Cys residues did not affect LCAT activity. The effects of sulf-hydryl inhibitors on these sites were attributed to steric inhibition rather than direct effects on the formation of thioester bonds (Francone and Fielding, 1991b; Qu et al., 1993). In vivo proof of the dispensability of these residues was obtained when chicken LCAT cDNA was shown to lack the codons for these amino acids (Hengstschlager-Ottnad et al., 1995).

Current physical and biochemical knowledge of LCAT suggests there are six sequential steps that are basic components of the enzyme catalytic reaction:

- binding to the lipoprotein surface in a reversible process
- activation by an apolipoprotein (usually apo A-I) to facilitate
  access of the lipid to the active site
- phospholipid substrate deacylation to release lysophophatidylcholine
- formation of an intermediate Ser-O-acyl moiety
- transfer of the acyl chain to cholesterol to produce cholesteryl ester
- and release of cholesteryl ester into the core of the lipoprotein.

LCAT may be inhibited by lysophosphatidylcholine (Fielding *et al.,* 1972b; Smith and Kuksis, 1980). The inhibitory effect of lysophosphatidylcholine is likely the result of either detergent effects or end-product inhibition. Since the majority of lyso-lecithin is thought to be associated with albumin, however, its physiological role on LCAT activity may be limited.

Gas-phase cigarette smoke has also been reported to inhibit LCAT activity. This effect, which did not appear to be due to free radical lipid peroxidation, might be due to modification of the free cysteine residues at Cys-31 and Cys-184 (Bielicki *et al.,* 1995a; Bielicki *et al.,* 1995b). Although an early clinical study suggests that there is little or no effect of cigarette smoke on LCAT activity in human subjects, the true physiological significance of this effect *in vivo* remains to be determined (Ito *et al.,* 1995).

While LCAT preferentially esterifies cholesterol, the enzyme can partially reverse the reaction through the hydrolysis of cholesteryl esters to produce unesterified cholesterol (Sorci-Thomas *et al.,* 1990). In addition, Subbaiah *et al.* (1993) have shown that the enzyme can act reversibly to re-form phosphatidylcholine from lysophosphatidylcholine acylation (LAT). While the physiological significance of the LAT reaction has not been determined, the reaction appears to be largely con-fined to the LDL fraction *in vivo.* This is likely due to the increased affinity of LDL for lysophosphatidylcholine (Subbaiah *et al.,* 1982). This effect, which appears to be due to the reversal of LCAT phospholipase A_2 activity, is dependent not on apo A-I, but rather on the presence of LDL. Trypsin treatment of LDL eliminated the lysolecithin acyltransferase (LAT) reaction, indicating that apoprotein B (apo B), the major struc-tural protein in LDL, appears to be essential for LCAT activation (Subbaiah *et al.,* 1985). LAT activity by LCAT may also be affected by the conformation of apo B , which in turn, is affected by LDL triglyceride concentration (Liu M *et al.,* 1992). *In vitro* studies utilizing proteoliposome substrates have shown that apo A-I and, to a

lesser degree, apo C-I and apo E may be substituted for apo-B in the LAT reaction. The latter apoproteins, however, were 40% and 70% as effective in activating the LAT reaction as apo A-I. The preferential activation of the LAT reaction on LDL by LCAT appears to be due to a higher affinity of lysophosphatidylcholine to LDL than HDL (Liu and Subbaiah, 1993b). While there is a potential for end-product inhibition, this evidence suggests that lysophosphatidylcholine may also compete with unesterified cholesterol as an acyl acceptor.

1.3.3 LCAT Substrates

Although some evidence suggests that lower density lipoproteins may serve as substrates for LCAT (Rajaram 1985; Carlson *et al.,* 1985a; Carlson *et al.,* 1985b), the esterification reaction appears to occur preferentially on the surface of HDL (Barter *et al.,* 1984; Barter *et al.,* 1985; Fielding *et al.,* 1971). Studies in binding and enzyme reactivity of LCAT in different HDL subfractions is complicated by the heterogeneous nature of plasma HDL. In place of endogenous substrates, chemically and physically defined synthetic substrates have been used.

In the original method described by Ho and Nichols (1971) , unilaminar vesicles containing cholesterol, phosphocholine and purified apolipoproteins were combined into stable "proteoliposome" particles. In later work, uniform stable discoidal complexes were produced using the sodium cholate dialysis method (Matz and Jonas, 1982). These methods have provided useful tools for the continued investigation of the kinetic properties, substrate specificity and apoprotein activity of LCAT.

LCAT substrates of physiological significance are found in aggregated form, existing either as native lipoproteins, reconstituted HDL (rHDL) or synthetic lipid vesicles (Jonas, 1986). Monomeric acyl substrates, are non-physiological but are useful for investigations in enzyme kinetics and the LCAT reaction mechanism since they react with LCAT in the absence of a lipid/water environment. (See table 3).

Table 3. Molecular substrates of LCAT. Adapted from Jonas (1991)

Substrates	Physical State	References
Acyl acceptors		
Sterols (cholesterol)	Aggregate	Kitabatake *et al.*, 1979
Lysophospholipids (lyso-PC)	Aggregate	Subbaiah *et al.*, 1982
Alcohols (long chain)	Aggregate	Kitabatake *et al.*, 1979
Water	Monomer	Aron *et al.*, 1978
Acyl donors		
Phospholipids (PC, PE)	Aggregate	Aron *et al.*, 1978
Cholesteryl esters	Aggregate	Sorci-Thomas *et al.*, 1990
Arachidonyl CoA	Micelle	Jauhiainen and Dolphin, 1986
PNP acyl esters	Monomer	Bonelli and Jonas, 1989
C6-NBD-PC	Micelle	Bonelli and Jonas, 1987
D-Py-PC	Monomer	Bonelli and Jonas, 1992

PNP, ρ-nitrophenol; D-Py-PC, 1,2-bis[4-(1-pyreno)-butanoyl]- *sn*-glycero-3-phosphocholine

1.3.3.1   Positional and substrate specificity

The ability of LCAT to react with aggregated substrates is influenced by a number of interrelated factors, including size and shape of the lipoprotein, the apoprotein and lipid composition. The ability of apo-AI and other apoproteins to activate LCAT will be discussed in section 1.3.6   In addition to apoproteins, multiple effects on LCAT activity have been observed due to phospholipid composition. These effects include apoprotein conformation, the interaction of apoproteins to interact with the LCAT active site, and the relative hydration, lipid packing and fluidity of the lipid interface associated with LCAT binding.

1.3.3.2   HDL as a substrate for LCAT

Distinctly different size distributions are observed in reconstituted HDL particles (rHDL) which contain either dipalmitoylphosphatidylcholine (DPPC) or palmitoyloleoylphosphatidylcholine (POPC). This results in differences in the conformation and number of apo A-I molecules located on the rHDL surface, which in

turn will affect LCAT esterification. Phosphatidylcholine in rHDL substrates containing two saturated chains with 16 carbons or less result in optimal reactivity, with decreased esterification rates in longer chains (Pownall *et al.,* 1987). It is difficult to interpret this *in vitro* data with respect to LCAT function *in vivo* as any single phosphatidylcholine type may be influenced by the composition of surrounding phosphatidylcholines (Jonas *et al.,* 1986).

Significantly different LCAT esterification rates have been observed in HDL particles with different size. HDL_3 is generally utilized preferentially by LCAT as an acyl source when compared to larger HDL_2 particles (Fielding and Fielding, 1971; Jahani and Lacko, 1992). *In vitro* studies utilizing reconstituted HDL (rHDL) synthetic discs containing POPC suggest that the differences in substrate utilization between smaller and larger particles may be attributed to alterations in apo A-I conformation (Jonas *et al.,* 1989). When rHDL was prepared using apo A-I and DPPC, the smallest particles (9.7nm) resulted in LCAT activity that was approximately 20-times greater than that of the largest (18.6nm) particles. Interestingly, the conformation of apo A-I was similar, despite the difference in LCAT activity (Hefele Wald *et al.,* 1990). It appears, therefore, that the ability of an HDL particle to interact with LCAT may be independently influenced by size or the surface curvature.

Further, discoidal HDL particles are more reactive with LCAT than native spherical HDL (Marcel *et al.,* 1980). These differences may be attributed to changes in lipid packing and/or apolipoprotein conformation. Using synthetic substrates, Meng *et al.* (1993) demonstrated that large disks containing four molecules of apo A-I were optimal substrates for LCAT with decreasing activity in progressively smaller disks containing three or two molecules respectively. This may be due to the increased potential for synthetic discs to store cholesteryl ester, a possible explanation for additional findings that showed these discs activated LCAT to a greater degree than spherical substrates of a similar composition (Matz and Jonas, 1982).

However, there also appears to be an inverse relationship between LCAT substrate reactivity and particle size that is independent of cholesteryl content (Barter *et al.,* 1985). In later studies utilizing spherical reconstituted HDL with various core cholesteryl ester:triglyceride ratios, Sparks and Pritchard (1989b) showed that high triglycerides compared to cholesteryl ester decreased LCAT V_{max} while the K_m was essentially unaltered. The K_m was increased, however, by increasing particle size and protein content. Increasing unesterified cholesterol content or phospholipid decreased K_m. From these studies, it appears that HDL particle size and shape is affected by the proportion of lipid to apolipoproteins as well as the surface and core lipid composition. Size and shape of the particle, in turn, affects the conformation of the apolipoprotein and these interdependent components have an overall effect on the LCAT esterification rate.

1.3.3.3   LDL as a substrate for LCAT

LCAT may also utilize LDL as a source for unesterified cholesterol (Barter, 1983; Barter *et al.,* 1984; Knipping *et al.,*1986; O K *et al.,* 1993b). In CETP-deficient human plasma, it was found that approx. 73% of esterified cholesterol was located in HDL, 25% in LDL and 1% in VLDL (Rajaram and Barter, 1985). Since pig plasma does not contain CETP, further studies comparing native LCAT and lipoproteins between human and pig species provided additional evidence that LCAT directly interacts with LDL to produce cholesteryl ester (Knipping *et al.,* 1986). While apo B appeared to have some effect on LCAT activity, its removal from LDL did not eliminate LCAT activity. Further, it was found that 60-70% cholesteryl ester produced in pig plasma by LCAT following incubation at 37°C was found in the LDL fraction. This suggests that even in the presence of HDL, porcine LCAT may prefer LDL as a substrate.

1.3.3.4   Effects of phosphatidylcholine on LCAT substrate utilization

Phospholipids, which increase membrane fluidity, are known to increase LCAT cholesterol esterification (Pownall et al., 1985). In the presence of apo A-I, the maximal enzyme activity for LCAT occurs at a phosphatidylcholine:cholesterol ratio of 4:1 (Fielding et al., 1972b). The availability of the phosphatidylcholine species present in plasma lipoproteins largely determines the preference for LCAT to utilize it. Detailed studies utilizing phosphatidylcholine substrates provided evidence that in humans, native LCAT preferentially utilizes plasma acyl groups 16:0>18:1>18:0 in the sn-1 position. Human LCAT also utilizes 18:2>18:1>22:6>20:4 acyl groups in the sn-2 position for cholesteryl ester synthesis. Overall, greater than 90% of cholesteryl esters in plasma are derived from acyl groups in the sn-2 position (Subbaiah et al., 1992). However, if phosphatidylcholines containing 20:4 or 22:6 acyl chains are located at the sn-2 position (chains not utilized well by LCAT), then the percentage of cholesteryl esters derived from the sn-1 position will rise to about 75% of the total cholesteryl esters produced by LCAT. Various potentially confounding factors including the apolipoprotein activator, the ratio of unesterified cholesterol:phospatidyl choline or membrane fluidity did not appear to influence the LCAT preferential specificity for substrate types and position. A possible explanation for these findings is that the larger 20:4 and 22:6 phosphatidylcholine groups do not fit into the active site efficiently, resulting in the use of the lesser-preferred acyl group at the sn-1 position. However, this hypothesis does not explain why 18:0 appear to be utilized to a much lesser extent than 20:4 groups; i.e., the original positional specificity of LCAT for phosphatidylcholine is altered when 14:0-20:4 phosphatidylcholine, 16:0-20:4 phosphatidylcholine or 16:0-22:6 is present (Subbaiah et al., 1992).

1.3.4 Inter-species differences in LCAT substrate specificty

Differences in the ability of LCAT to transfer acyl groups has been observed in a number of different animal species (Grove and Pownall, 1991). Although these results suggested that LCAT conformation of the active site may be different in these species, the experiments utilized synthetic substrates that may not reflect physiological conditions *in vivo.* There is some *in vivo* evidence that, compared to human LCAT, the rat enzyme has a greater specificity for arachidonate (20:4). When the binding affinities of rat LCAT was compared to human LCAT using lecithin-cholesterol vesicles with apo A-I from the two species, it was shown that the rat enzyme has higher affinity to apo A-I containing vesicles. (Furawa *et al.,* 1992). Esterification rates of rat LCAT was two-fold higher when human apo A-I was used to activate LCAT compared to the human enzyme. Rat apo A-I, on the other hand, activated human LCAT with only 18% of the rate observed with human apo A-I.

1.3.5 Activation of the LCAT Reaction

Apo A-I was first demonstrated by Fielding *et al.* (1972) as a requirement for activating the LCAT reaction using egg-phosphatidylcholine and unesterified cholesterol vesicles. Since then, a number of other exchangeable apolipoproteins have also been reported to activate LCAT, albeit to a lesser extent (Jonas and Sweeney, 1984; Steinmetz and Utermann, 1985; Steyrer and Kostner, 1988). Among species, homologous Apo A-I consistently activates homologous LCAT to the greatest degree. Hedgehog apoA-I, for example, was able to activate human LCAT by only 25% of the corresponding values obtained using human apo A-I (Sparrow *et al.,* 1995).

Efforts to determine the regions of apo A-I involved in binding and activating LCAT have been made utilizing monoclonal antibodies (Banka *et al.,* 1991) and apo A-I synthetic peptide analogues (Pownall *et al.,* 1984; Anantharamaiah *et al.,* 1990). There are some structural similarities between exchangeable apolipoproteins which

may be a factor in the ability of these proteins to activate LCAT. Exchangeable apolipoproteins typically contain internal 11-residue-long amino acid repeats. In apoA-I, A-IV and E, which have been shown to activate LCAT, the 11-mer repeats have evolved into 22-mer tandem repeats. Many of these 22-mer tandem repeats contain characteristics of an amphipathic α-helix, a common secondary structural motif in biologically active proteins and peptides, with opposing polar and non-polar faces oriented along its long axis. Because amphipathic alpha helices have the potential to disrupt the water-phospholipid interface to expose the buried substrate to LCAT, it has been suggested that they may play a role in LCAT activation (Bonelli *et al.*, 1989; Segrest *et al.*, 1992). The efficiency of peptides, as well as other apolipoproteins, to activate LCAT is significantly less than apo A-I (generally less than 30%). This suggests that only part of the effects seen in these proteins to activate LCAT is due to conformational properties (Anantharamaiah *et al.*, 1990).

A specific region of apo A-I (residues 66-121) has been identified as having major effects in activating LCAT. When apo A-I specific monoclonal antibodies were used to map epitopes in this region, it was found residues 95-121 were critical for activation of the enzyme (Banka *et al.*, 1991). Using computer analysis, Segrest *et al.* (1992) suggested that unique positions of Glu residues found in residues 66-87 and 99-120 of apo A-I, but not found on other apolipoproteins, may be responsible for the higher LCAT-activating ability of apo A-I. However, subsequent studies suggested that point mutations in this region do not appear to significantly affect apo A-I activation. It is difficult to compare relative reactivity of apolipoproteins and synthetic peptides which, themselves have different lipid binding characteristics; as a result, the specific LCAT activating domain of apo A-I and the mechanism by which apo A-I effects LCAT activation has still not been precisely determined to date.

1.3.6   Expression of human LCAT in transgenic animals

To determine the effects of increased plasma levels of LCAT, Mehlum A *et al.,* (1995) created a transgenic mouse strain which expressed the enzyme at levels approx. 40-fold over normal human plasma. This resulted in a net 50% decrease in plasma triglyceride levels in all plasma lipoproteins. LDL and VLDL levels were decreased by approximately 50% of normal controls, HDL cholesterol levels increased by approximately 20%, with a corresponding increase in apo AI and AII. These studies provided important evidence that overexpression of LCAT can produce major alterations in plasma lipoprotein concentration and composition, resulting in potentially lower levels of atherogenic particles and an increase in anti-atherogenic HDL.

In further studies involving mouse transgenics, Francone et al., (1995) created four lines of transgenic mice expressing human LCAT. The gene was driven either by mouse albumin enhancer or its natural promoter. Plasma activity increased to 1.6-fold higher than control mouse plasma. In vivo effects on plasma lipoproteins included a 20 to 60% increase in total cholesterol and cholesteryl esters found in HDL. Transgenic lines were also created that co-expressed human apo proteins A-I and A-II. Plasma cholesterol was increased up to fourfold in apo-human AI/LCAT transgenic mice and twofold in human AI/AII/LCAT animals when compared to AI and AI/AII transgenic animal controls. HDL particles were predominantly larger in the AI/LCAT and AI/AII/LCAT strains compared to transgenic controls lacking the LCAT gene (Francone *et al.,*1995).

Because mice lack CETP, a rabbit transgenic strain was developed to further assess the effect of overexpression of the LCAT gene in an animal with a lipid metabolism similar to that of humans (Hoeg *et al.,* 1996). The level of plasma LCAT activity on HDL correlated with the number of copies the enzyme integrated into the rabbit DNA. High expressers produced up to a 2.5-fold and in one case a 3.1-fold

increase in the plasma esterification rate, accompanied by increased concentrations of apo E-rich HDL1-sized particles. Particles containing apo B decreased dramatically, indicating that overexpression of LCAT in the presence of CETP can reduce potentially atherogenic lipoproteins and lead to hyperalpha-lipoproteinemia.

1.3.7 Measurement of LCAT Activity and Cholesterol Esterification Rate

There is often confusion in the literature regarding the interpretation of esterification data in plasma assays for LCAT. Esterification of cholesterol by plasma LCAT is routinely measured using two methods which differ with respect to the substrates utilized in the assay.

The first method, measures the LCAT activity in the presence of synthetic substrates and a standardized amount of apo-AI. This exogenous substrate measurement, termed the *LCAT activity assay*, estimates the activity of the enzyme in the absence of plasma constituents and is generally proportional to the amount of LCAT protein in plasma. The substrate used consists of spherical reconstituted HDL consisting of known amounts of apo A-I, [^{3}H]-cholesterol and phospholipid. The reconsititued HDL is added in excess quantity to a small amount of plasma and the rate of conversion of [^{3}H]-cholesterol to [^{3}H]-cholesteryl ester is determined. The resulting estimate for LCAT activity is expressed as nmoles of cholesterol esterified per hour per milliliter plasma.

The second method, the endogenous *cholesterol esterification rate* (CER) determines the rate of cholesterol esterified from plasma cholesterol in the absence of exogenous substrates. In this assay, [^{3}H]-cholesterol is equilibrated with the pool of endogenous unesterified cholesterol in the plasma sample. Equilibration is performed at 4°C to prevent esterification activity until the start of the assay. The plasma sample is subsequently incubated at 37°C. As with the LCAT activity assay, the CER is calculated as the rate of [^{3}H]-cholesterol converted to cholesteryl esters (nmoles [^{3}H]-cholesterol esterified per hour per milliliter plasma). CER, however, provides an

estimate of the endogenous (or net) synthesis rate and is influenced by not only the quantity of LCAT present but also by the composition of the lipoprotein substrates, cofactors and other plasma constituents.

1.3.8 LCAT Gene Structure and Expression

The gene for LCAT is located on the long arm of chromosome 16 and spans 4.2 kb of genomic DNA, over six exons (McLean *et al.*, 1986b). The first 59 nucleotides of exon 5, a region that may potentially form an α-helix, shares a 66% sequence homology with the 3' coding region of the apo E gene. Functional analysis of deletions between -2000 and -300 in 2.9 kb of the 5' flanking region in the LCAT gene produced no change in promoter activity. A 50% reduction in promoter activity occurred when deletions were made to position -71 and 100% following deletion to position -42 (Meroni *et al.*, 1991). There are two putative Sp1 binding sites in the 71bp promoter region. Site directed mutagenesis directed towards the two sites indicate promoter activity is dependent on these sites.

Southern blot hybridization suggests that a single gene for LCAT is present in humans. Human LCAT mRNA is expressed predominantly in the liver and has been detected in HepG2 cells (McLean *et al.*, 1986b). An interesting feature of LCAT mRNA is that the 3' untranslated region contains only 23 bases and the poly(A) signal overlaps the carboxyl-terminal glutamic acid and stop codons (McLean, *et al.*, 1986a). Northern blot experiments in the rat demonstrated that, like humans LCAT mRNA was expressed predominantly in the liver. However, it was also detected in the brain and testes (Warden *et al.*, 1989). In Rhesus monkeys, *in situ* hybridization has further localized LCAT expression to the basal cell layer of the dermis, in addition to hepatocytes and brain tissue (Smith *et al.*, 1990). In the brain, mRNA was expressed in a discrete cell layer of the cerebellum, as well as in scattered epididymal cells, neuroglial cells and neurons. In baboons, the relative levels of mRNA expressed in these neural tissues was determined by RNAse protection assay

(Hixson *et al.,* 1993). These results showed the highest levels of LCAT were present in the cerebellum. The liver expressed 33% of the LCAT mRNA found in the cerebellum, with only trace levels located in the cerebral cortex, spleen and ileum. It appears, therefore, that LCAT is also active in lipid transport in the brain, with most activity in the cerebellum.

A high degree of gene sequence identity exists between all species cloned to date. In addition to the rabbit and porcine LCAT cDNA presented in this thesis, these include LCAT sequences reported for the mouse (Warden *et al.,* 1989), rat (Meroni *et al.,* 1990) , baboon (Hixson *et al.,* 1993), chicken (Hengstschlager-Ottnad E *et al.,* 1995).

All major structural features of LCAT, including glycosylation sites, Cys residues and the catalytic Ser site are conserved with the exception of chicken LCAT. In chicken LCAT, two Cys residues that were at one time thought to be important in mammalian LCAT (Cys-31 and Cys-184, in human LCAT) are absent in the chicken enzyme. As previously mentioned, this provided additional, *in vivo* evidence that these Cys residues do not have a major role in the LCAT reaction (Hengstschlager-Ottnad, et al., 1995).

1.4   Genetic abnormalities affecting LCAT esterification

1.4.1   Natural mutations of the LCAT gene

The importance of the LCAT reaction is underlined by the profound physiological changes in plasma cholesterol homeostasis noted in studies of patients with LCAT deficiency syndromes (Carlson *et al.,* 1979; Frohlich *et al.,* 1986), apo A-I deficiency and Tangier Disease (Schaefer, 1984). Familial defects in the LCAT gene result in the phenotypic expression of LCAT deficiency or a related disorder, Fish Eye Disease (FED). The latter disorder, FED, is characterized by decreased LCAT activity and corneal opacities. Familial LCAT deficiency generally results in a more severe phenotype due to increased unesterified cholesterol levels in patient plasma. In addi-

tion to corneal opacities, patients with familial LCAT deficiency may exhibit mild haemolytic anemia, proteinuria, progressive renal insufficiency which may eventually result in renal failure.

In patients with LCAT deficiency syndromes, normal maturation and metabolism of all serum lipoproteins is impaired, resulting in low levels of HDL. Homozygotes for familial LCAT deficiency have generally low total cholesterol levels, nearly all of which is unesterified cholesterol. Interestingly, despite the clear relationship between low HDL and atherosclerosis in the general population, patients with LCAT deficiency syndromes are not at high risk for developing atherosclerosis (Assmann *et al.,* 1990; Frohlich *et al.,* 1988). The reasons for this lack of association are not clear. In contrast to complete LCAT deficiency, patients with fish eye disease (FED) are able to utilize unesterified cholesterol from LDL and VLDL substrates for esterification. The cholesterol esterification rate in FED plasma is nearly normal but when measured in vitro with an exogenous substrate activated with apo A-I it is only 10-15% of controls (McIntyre, 1988; Skretting *et al.,* 1992). This has led to the hypothesis that LCAT has two types of activity: an activity which esterifies free cholesterol from HDL, termed α-LCAT, and an activity which esterifies free cholesterol from LDL and VLDL, termed ß-LCAT. Fish-eye disease has thus been postulated to result from abnormal α-LCAT activity (but normal ß-LCAT activity) while patients with complete LCAT deficiency lack both α and ß activities (Carlson *et al.,* 1987; Funke *et al.,* 1991b). Interestingly, in vitro supplementation of plasma from a patient with FED using purified LCAT results in normalization of HDL particles, including cholesterol content and a corresponding increase in HDL particle size, suggesting that in vivo plasma supplementation with LCAT may be of therapeutic value in some patients (Holmquist *et al.,* 1988). The value of such therapy remains controversial as most FED patients require little clinical intervention.

Biochemical and clinical data from families affected with these disorders indi-

cate that they are inherited as an autosomal recessive trait. Since the cloning and sequencing of the human LCAT gene by McLean *et al.* (1986a), a number of laboratories have reported a large variety of gene defects that appear to be causative for FED and LCAT deficiency (See table 4). These mutations appear to be distributed across all six exons of the LCAT gene. The majority of these mutations are single base changes leading to single amino acid substitutions. Only one mutation (Gly-183→Ser) appears to directly affect the catalytic site by disrupting the structural motif Gly-X-Ser-X-Gly found in many lipases (Brenner, 1988).

Site directed mutagenesis and the *in vitro* expression of recombinant LCAT (rLCAT) have been used to recreate natural mutations of the LCAT gene in order to determine their functional significance. The first LCAT gene defect reported, Arg147 → Trp (Taramelli *et al.,* 1990) was also the first to be expressed, using a transient transfection in COS-1 cells. Although the mutation associated with LCAT deficiency produced similar levels of mRNA to that of the wild type, the culture medium detected only LCAT protein and activity for the wild type construct. It was suggested that a change in the protein structure resulted in decreased enzyme stability inside or outside the cell. In a later study, utilizing site directed mutageneis to express natural mutants in human embryonic kidney-293 cells, a Tyr156 → Asn substitution, also producing LCAT deficiency, was found to inefficiently secrete the enzyme, which itself was only partially inactive (Klein *et al.,* 1993a). In this study, it was suggested that the mutation disrupted a predicted α-helical region spanning LCAT residues 156-159, thus disrupting enzyme function. Additionally, it was proposed the mutation caused irregular folding of the protein, resulting in decreased secretion and/or enzyme degradation. A further report by Klein *et al.* (1993b) describing a Leu300 deletion, also expressed in human embryonic kidney-293 cells, showed the mutant to secrete very low amounts of rLCAT which otherwise produced normal specific activity and normal mRNA and intracellular LCAT concentrations. In this patient, it was sug-

gested that FED-like symptoms were the result of a defect in quantitative enzyme levels rather than a functional deficiency.

Hill and O produced a variety of natural LCAT mutants in both transient transfections and stable cell lines (Hill *et al.,* 1993; O K *et al.,* 1993b). These included eight gene defects associated with LCAT deficiency (Pro10→Leu, Ala93→Thr, Ala93→Thr/Arg158→Cys, Arg135→Trp, Arg158→Cys, Leu209→Pro, Met252→Lys, Ile375→frameshift), and three defects associated with FED (Thr123→Ile, Leu300, Thr347→Met, Asn391→Ser). Three mutants clinically associated with FED (Pro10→Leu, Thr123→Ile, and Asn391→Ser) produced LCAT specific activities (using HDL-analogue substrates) that were between 11-31% of those observed for the wild-type enzyme. All other mutants produced specific activities less than 6% of the wild type. When LDL was utilized as a substrate, however, both homozygous mutants for FED studied (Pro10→Leu, Thr123→Ile) produced activities similar to that of the wild type. All other mutants produced LCAT activities against LDL substrates of less than 10% of the wild-type, with the exception of Asn391→Ser. This mutant produced intermediate results, with low (but not absent) activities against the HDL analogue (18%), and reduced activity against the LDL substrate (53%) when compared to the wild type. These characteristics are unique compared to those observed in FED or familial LCAT deficiency. Interestingly, the proband with this defect was a compound heterozygote for Asn391→Ser / Met252→Lys, the latter of which had been originally identified as a homozygous defect in three of the original LCAT deficiencies reported in Norway (Skretting *et al.,* 1992). Clinical findings on the family were reported as having a unique variant of hypoalphalipoproteinemia resembling FED, but with clinical findings such as erythrocyte abnormalities suggestive of familial LCAT deficiency.

From the above studies, it appears that in a number of mutants located across the LCAT gene, much of the phenotypic expression of FED or LCAT deficiency may

be attributed to the ability of the mutant protein/enzyme to utilize lipoproteins other than HDL to synthesize cholesteryl esters. Recently, a unique form of FED was reported that produced not only a marked loss of LCAT activity in HDL-like proteoliposome substrates but also a 75% reduction in specific activity against LDL (Kuivenhoven JA et al., 1995). In addition to corneal opacities as the major clinical feature, the mutation, a missense substitution (Asn131→Asp), resulted in premature coronary artery disease in two male probands, suggesting a unique FED phenotype. This would indicate that partial LCAT activity against LDL, in the absence of HDL can also produce FED. Together with the occurrence of compound heterozygote defects, and clinical variability of expression in some families, possibly due to environmental factors and other genes, it is difficult to assign mutations in the LCAT gene to FED or LCAT deficiency phenotypes with absolute certainty. In recent years, FED has been more accurately termed "partial LCAT deficiency" as compared to total or "classic" LCAT deficiency (CLD) (Klein et al., 1995). Mutations are spread over the LCAT gene resulting in a range of abnormal LCAT activities between two extremes: 1) the complete loss of LCAT activity as seen in classical LCAT deficiency and 2) a specific loss of activity against HDL as found in FED.

The study of natural mutations has provided a useful basis for the understanding of the structural properties of the LCAT gene. Further characterization of LCAT mutants associated with either total LCAT deficiency (at residues 147, 156, and 228) or fish eye disease (10, 123, 158, 293, 300, and 347) were recently reported by Klein et al. (1995). Of these clones, secretion of three mutants (residues 147, 156, and 300) appeared to be markedly decreased with respect to the wild-type enzyme. The ability of certain mutants to esterify HDL-like proteoliposome particles, including two mutants associated with total LCAT deficiency (residues 147, and 228) and four fish eye disease mutants (residues 10, 23, 293, and 347) was decreased to less than 5%

Table 4. Naturally occurring mutations of LCAT.

Codon	Structural Change	Zygosity	Phenotype	Reference
10	Pro→ Leu	Homozygous	FED	Skretting and Pyrdz, 1992
10	Pro→Gln	Heterozygous	FED	Kuivenhoven et al., 1996
10	Pro→ Frameshift	Homozygous	LCAT def.	Bujo 1991
16	Leu→ Stop	Heterozygous	LCAT def.	Miettinen et al., 1995
32	Leu→ Pro	Heterozygous	LCAT def.	McLean, 1992
83	Tyr→ Stop	Heterozygous	LCAT def.	Klein et al., 1993a
93	Ala→ Thr	Homozygous	LCAT def.	Funke et al., 1993
119	Gly→ Frameshift	Heterozygous	LCAT def.	Gotoda et al., 1991
123	Thy→ Ile	Homozygous	FED	Funke et al., 1991b
131	Asp→ Asn	Homozygous	FED	Kuivenhoven et al., 1995
135	Arg→Gln	Heterozygous	LCAT def.	Kuivenhoven et al., 1996
135	Arg→ Trp	Heterozygous	LCAT def.	Funke et al., 1991b
141	Gly Insertion	Homozygous	LCAT def.	Gotoda et al., 1991
144	Tyr→ Cys	Heterozygous	FED	Contacos et al., 1993
147	Arg→ Trp	Heterozygous	LCAT def.	Taramelli et al., 1990
156	Tyr→ Asn	Heterozygous	LCAT def.	Klein et al., 1993a
158	Arg→ Cys	Homozygous	LCAT def.	Funke et al., 1993
171	Tyr→ Stop	Heterozygous	LCAT def.	Guerin et al., unpublished
183	Gly→ Ser	Heterozygous	LCAT def.	McLean, 1992
209	Leu→ Pro	Homozygous	LCAT def.	Funke et al., 1993
228	Asn→ Lys	Homozygous	LCAT def.	Gotoda et al., 1991
244	Arg→ Gly	Homozygous	LCAT def.	McLean, 1992
252	Met→ Lys	Homozygous	LCAT def.	Skretting et al., 1992
293	Met→ Lys	Homozygous	LCAT def.	Maeda et al., 1991
300	Leu deletion	Homozygous	FED	Klein et al., 1993b
321	Thr→ Ile	Heterozygous	LCAT def.	McLean, 1992
347	Thr→ Met	Heterozygous	FED	Klein et al., 1992
375	Ile→ Frameshift	Heterozygous	LCAT def.	Funke et al., 1993
391	Asn→ Ser	Heterozygous	FED	Pritchard et al., unpublished
399	Arg→Cys	Heterozygous	LCAT def.	Miettinen H et al., 1995

of normal. However, one total LCAT deficiency mutant (residue 156) and two FED mutants (residues 158 and 300) produced an LCAT enzyme specific activity that ranged between 45 to 110% of the wild-type clone. Interestingly, all nine LCAT mutants retained the ability to hydrolyze the water-soluble PNPB substrates. This would indicate that the hydrolytic activity of LCAT was intact in these mutants. It was therefore suggested that the LCAT mutations at residues 147, 156, 228, resulting in total LCAT deficiency, and 10, 123, 158, 293, 300, and 347, resulting in fish eye disease, alter the structural domains involved in lipid binding or transesterification, rather than the functional domain mediating LCAT phospholipase activity.

Our understanding of the structure-function relationships of LCAT will improve by further analyses of mutant recombinant enzymes. This also will help in further investigation of the underlying mechanisms associated with their clinical and biochemical abnormalities.

1.4.2 Laboratory findings in LCAT deficiency and Fish Eye Disease

In heterozygotes for LCAT deficiency, the enzyme activity (determined using proteoliposome substrates) is reduced to 50% of normal, allowing genotype prediction in non-obligate heterozygotes. However, although LCAT activity is reduced in these patients, heterozygotes for LCAT deficiency generally have no major plasma lipoprotein abnormalities. Some erythrocyte abnormalities and hyperlipidemia have been reported in several kindreds (Godin *et al.,* 1978, Torsvik *et al.,* 1968, Borysiewicz *et al.,* 1982). An exception to this was found in a detailed study by Frohlich *et al.* (1988), where a family had significantly lower HDL cholesterol and apo A-I levels and higher fasting plasma triglycerides. These levels were between those for homozygous LCAT patients within the same family and those of normal individuals, suggesting that these findings were due to decreased LCAT activity. Heterozygotes are may be discriminated from normal individuals by utilizing the LCAT activity assay (exogenous substrate assay). Generally, it is not possible, using

patient's plasma as a substrate to determine the cholesterol esterification rate (CER), to differentiate heterozygotes for LCAT deficiency from unaffected family members or from normal individuals.

Similarly, in Fish Eye Disease (FED), the CER alone cannot be used to distinguish heterozygotes from normal individuals. The clinical phenotype of FED is typically indicated by a reduction in LCAT activity to 50% of normal in heterozygotes but with a normal CER. HDL cholesterol levels are generally decreased in heterozygotes. LCAT protein levels in FED, however, are usually within normal range.

1.4.3　　　Pathophysiology of LCAT deficiency and Fish Eye Disease

1.4.3.1　　　Lipoprotein abnormalities

Patients with LCAT deficiency demonstrate multiple abnormalities in plasma lipoprotein composition. All lipoproteins exhibit some abnormalities, underscoring the importance of LCAT in the metabolism of all lipoprotein particles. Typically, patient plasma contains high plasma concentrations of unesterified cholesterol and phosphatidylcholine, together with low concentrations of lysolecithin and cholesteryl esters. Cholesteryl esters that are present are likely to have originated from intracellular cholesteryl ester syntheses in the intestine via acyl coenzyme A:cholesterol acyltransferase (ACAT). ACAT also produces cholesteryl esters with relatively higher proportions of oleic and palmitic acids than linoleic acid, seen in LCAT deficient patients.

Very low density lipoproteins (d<1.006g/mL) are often elevated in this disorder, and contain higher concentrations of unesterified cholesterol and phosphatidylcholine, relative to protein and triglyceride content (Glomset et al., 1973). Abnormalities have also been shown in intermediate density lipoproteins (d=1.006-1.019, IDL). These heterogeneous particles are enriched in triglyceride and unesterified cholesterol, possibly due to a decreased ability of hepatic lipase to hydrolyse triglyceride in these particles. (Glomset, et al., 1973; Murano 1987).

When LDL particles (d=1.019-1.063) are isolated from plasma from LCAT-deficient patients by gel filtration, three subfractions may be detected instead of the single subfraction found in individuals with normal LCAT activity. These subfractions, approx. 90nm, 30-80nm and 20-22nm respectively, appear to be related to dietary fat content (Glomset et al., 1975), and typically are rich in unesterified cholesterol. Both IDL and LDL particles are enriched in triglyceride. In LDL, the triglyceride to cholesteryl ester ratio is ten time higher than normal. In addition, patient LDL_2 (d = 1.019 to 1.063 g/mL) has been reported to include unusually large particles, which following filtration through 2 percent agarose, yield three major subfractions (Glomset et al., 1973). One of these subfracrtions contain abnormal discoid particles (30-80nm), which formed stacks resembling Lp-x particles found in cholestasis (Hamilton et al., 1971). The significance of these particles in LCAT deficiency has yet to be determined.

Patients who are homozygote for LCAT deficiency have markedly lower HDL cholesterol levels. HDL cholesterol levels are typically 10% of normal individuals, with a high level of unesterified cholesterol and high content of Apo E. The total apoprotein content may be reduced up to 90% (Carlson and Holmquist, 1983).

1.4.3.2   Corneal changes

All patients with familial LCAT deficiency develop corneal opacities in early childhood. By the second decade of life, they are usually detectable with the entire corneal stroma containing fine greyish dots producing the appearance of a diffuse clouding of the cornea. The periphery of the cornea has a much denser concentration of these greyish dots, resulting in an arcus-like appearance. Histopathological evidence for the presence of unesterified cholesterol in the corneal stroma of an LCAT deficient patient has been reported (Cogan et al., 1992). Although corneal changes are associated with LCAT deficiency and FED, they are also seen in a

number of different disorders associated with HDL deficiency, including Tangier disease (Chu et al., 1979) , combined apo A-I/C-III deficiency (Norum et al., 1982) and HDL deficiency with planar xanthomas (Gustafson et al., 1979). There does not appear to be a correlation with the degree of opacification and the severity of HDL deficiency or the risk of premature coronary artery disease. It is likely that the specific composition and structure of the abnormal HDL particles may affect the rate and extent of their accumulation in corneal tissue.

1.4.3.3 Hematological abnormalities

A mild normochromic anemia is often detected in homozygous patients with familial LCAT deficiency. This appears to be due to moderate haemolysis and reduced erythropoiesis (Chevet et al., 1978). Anormalities in the lipid composition, morphology and function of erythrocyte membranes have been observed. Peripheral blood film reveals an increased proportion of target cells, occasional poikiolocytosis, anisocytosis and stomatocytes. Erythrocytes from LCAT deficient patients have increased concentrations of unesterified cholesterol and phosphatidylcholine, but decreased sphingomyelin and phosphatidylethanolamine (Norum et al., 1970; Chevet et al., 1978; Godin et al., 1978) The relationship between the abnormal lipoprotein composition and tissue abnormalities observed in patients with LCAT deficiency has not been clearly established. Results of incubation studies with LCAT deficient plasma and normal erythrocytes suggest that the abnormal lipid composition leading to altered membrane function may be related to the high levels of unesterified cholesterol in these patients (Norm and Gjone, 1968).

1.4.3.4 Renal disease

A common finding in familial LCAT deficiency, often detected in the second or third decade of life, is proteinuria, which is frequently accompanied by hematuria. The predominant protein in the urine is albumin, although α-1 and α-2-migrating pro-

teins may also be present. Proteinuria may persist for many years in moderate amounts (0.5-1.5 mg/mL), however, renal function may deteriorate and progression to renal insufficiency may occur rapidly with increasing proteinuria and onset of hypertension. Lipid analysis of renal tissue has shown increased levels of phospholipid and unesterified cholesterol (Stokke et al., 1974). Multilaminar structures have been found in the plasma, cornea, spleen, bone marrow and kidneys of patients with familial LCAT deficiency and these appear to be partly responsible for the pathology observed in these tissues. Accumulation of these membranes and membrane-bound particles in the glomerular capillaries has been suggested as a possible cause for the damage seen to the endothelium and underlying basement membrane (Hovig and Gjone, 1973). Ultrastructurally, these appear as numerous subepithelial vacuolated deposits of material in glomerular and tubular basement membranes, Bowman's capsule, subendothelial space, mesangium and capillary lumina (Magil *et al.,* 1982). Some reports indicate that a few LCAT deficient patients with no proteinuria and with normal renal function contain similar lipid deposits (Flatmark *et al.,* 1977; Borysiewicz *et al.,* 1982). It has therefore been suggested that infiltration of lipid alone may not be sufficient to initiate renal disease (Borysiewicz *et al.,* 1982). It was proposed by these investigators, therefore, that accumulation of lipid deposits may reduce clearance of immune complexes that predispose development of glomerulonephritis, a condition that has been observed in several LCAT deficient patients.

1.4.4 Treatment of Familial LCAT deficiency

Generally, the first form of intervention is dietary fat restriction in order to decrease the plasma concentration of abnormal lipoproteins found in patients with familial LCAT deficiency. To date, however, there are no data on the effectiveness of dietary treatment in prevention or reversal of the renal impairment.

Whole plasma and blood transfusions have been used in some patients with familial LCAT deficiency both to treat anaemia and as an experimental means to increase plasma cholesterol esterification. The first reported treatment consisted of the infusion of 500mL whole plasma and 450mL blood (Norum and Gjone, 1968). This produced an immediate rise in plasma cholesteryl ester, which reached a peak at day 6 followed by a decrease to pre-treatment concentrations in 14 days. Based on these results, the in vivo half life of LCAT in plasma was calculated to be 4.6 days. A replacement therapeutical trial, consisting of an intravenous infusion of 2200mL whole plasma over a period of ten days was reported by Murayama et al. (1984). During this time, LCAT activity increased from 9.4% to only 17.4%. However, this small increase in enzyme activity resulted in significant increases in the cholesteryl ester content of all lipoprotein fractions. Further, the size of the LDL and VLDL particles reverted to near normal, based on electron microscopy (although no such increase was observed in the HDL fraction). The treatment remained effective for seven days following completion of the infusion.

These reports indicate that while LCAT activity may be partially restored by plasma infusion, it is a relatively inefficient form of treatment the benefits of which last for only a short period of time. At this time, the only effective treatment for renal disease due to LCAT deficiency is renal transplantation. Such treatment, of course does not remove the underlying defect and indeed the typical plasma lipoprotein abnormalities in transplanted patients will generally persist. Interestingly, one patient was observed to show a significant reduction in triglyceride following transplantation (Norum et al., 1989). However, this may have been also related to dietary changes. At this time, the only method to correct the biochemical defect in LCAT esterification is to perform a liver transplant; such a high risk procedure would be difficult to justify, however. There remains, therefore, a need to develop a more effective means of therapy for this disorder.

1.5 Rationale

The important role that LCAT plays in reverse cholesterol transport has resulted in continued interest in the structure, function and metabolism of this enzyme. To date, however, few studies have attempted to determine the effects of increasing LCAT activity on cholesterol content in plasma lipoproteins. Furthermore, no studies have been made to date to determine the metabolic turnover, reaction kinetics and lipoprotein binding characteristics of this enzyme. These experiments have been hindered due to the difficulty of obtaining large quantities of purified LCAT through conventional biochemical methods. Recent advances in our laboratory, however, have permitted the production of large quantities of recombinant human LCAT through the stable integration of an LCAT cDNA into eukaryotic cells. This preparation was found to be identical to the human plasma enzyme with respect to all aspects of structure and function studied so far. Therefore, it is now possible to utilize recombinant LCAT (rLCAT) in experiments to determine its metabolic turnover *in vivo*.

This thesis will define the activity and *in vivo* metabolic half-life of rLCAT in a well -established animal model of lipoprotein metabolism, the New Zealand rabbit. These studies will be of particular value providing data that will be used to define the efficacy of rLCAT in the treatment of familial LCAT deficiency. The goal of these types of experiments is to ultimately restore LCAT activity in patients with this disorder, either through enzyme replacement therapy using a recombinant protein or through gene therapy.

1.6 Specific Aims

AIM 1: <u>To clone rabbit recombinant LCAT cDNA.</u> This will both provide a homologous source for *in vivo* studies in the rabbit and provide sequence information that may help in elucidating inter-species differences in enzyme specificity.

AIM 2: <u>To constitutively express rLCAT in a stable cell line.</u> The enzymatically active protein will be subsequently used to characterize the *in vitro* kinetics of the recombinant protein and subsequently be purified in sufficient quantities studies of LCAT structure, function and metabolism.

AIM 3: <u>To produce radiolabeled, biologically active rLCAT.</u> This is required to characterize the recombinant protein by determining its binding properties to lipoproteins

AIM 4: <u>To determine the metabolic turnover rate of rLCAT *in vivo.*</u> This will provide novel biological data on the metabolism of rLCAT in an animal model.

Chapter 2

MOLECULAR CLONING OF LCAT cDNA

2. MOLECULAR CLONING OF LCAT cDNA

2.1 Introduction

In this chapter, work is described in which we cloned full length rabbit rLCAT and near full-length porcine rLCAT as part of our investigation of inter-species differences of this enzyme. The porcine cDNA was obtained from screening a porcine λ-GT 11 library as a product of early investigations in determining inter-species differences in LCAT predicted amino acid sequence. Together with previously published sequence data from other species, the information obtained from the cloned porcine LCAT cDNA led to the production of a set of consensus primers used to reverse transcribe and amplify full-length cDNA from rabbit liver mRNA. At the time of the investigations presented here, no sequence data had been released on the rabbit rLCAT cDNA sequence and about half of the primary structure of porcine LCAT had been determined by tryptic digestion and amino acid sequencing of the purified enzyme (Yüksel *et al.,* 1989). The results presented in this chapter, therefore, were essential to the success of this thesis.

2.2 Materials

A full length human LCAT cDNA inserted into pUC19 was kindly provided by John McLean, Genentech, Inc., San Francisco. Geneclean and MERmaid kits (Bio101, La Jolla, California) were used to purify double stranded DNA fragments. Modification and restriction enzymes were purchased from Pharmacia-LKB Biotechnology (Baie d'Urfe, Quebec), Bethesda Research Laboratories (BRL, Burlington, Ontario), and Boehringer Mannheim Corporation (BMC, Labal, Quebec) Oligonucleotides were prepared by the Oligonucleotide Synthesis Laboratory, Department of Biochemistry, UBC.

DNA sequencing was performed using a kit containing enzymes and reagents from Unites States Biochemical (USB, Cleveland, Ohio). Radiolabeled reagents including [^{35}S]-dATP, [^{35}S]-methionine, [^{3}H]-cholesterol, [^{32}P]-dATP and [^{14}C]-methylated protein molecular weight markers were obtained from Amersham Canada Ltd or from New England Nuclear. Fixed gels were equilibrated with Amplify$_{tm}$ (Amersham Canada Ltd.) before autoradiography. Gels were exposed on X-Omat AR film from Eastman-Kodak.

2.3   Methods and Results

2.3.1   Cloning of Porcine rLCAT

Porcine liver λ–GT 11 cDNA library was screened using a human LCAT cDNA probe obtained from Genentech. Approximately 10^6 bacteriophage λ particles in 1μL were added into 1mL sterile SM buffer (5.8 g NaCl, 2g MgSO$_4$-H$_2$O, 50mL 1M Tris-HCl pH 7.5, 5mL 2% w/v gelatin in 1L dH$_2$O). The mixture was then added to 4mL plating cells and incubated at 37°C for 20 minutes. 1.25mL of the phage/cell solution was added to 50mL of molten agarose kept at 47°C. The mixture was poured rapidly on the agar surface of previously prepared 150mm culture dishes. After the agarose solidified, the dishes were placed in an incubator in an inverted position and the bacterial cells were allowed to grow until plaques were approximately 1.5mm and almost touched eachother. Cultures were stored at 4°C until required.

Bacteriophage λ plaques were immobilized on Hybond-N$_{tm}$ (Amersham) nylon membranes and oriented to the agar by stabbing the agar through the membrane with an 18-guage needle attached to a syringe containing waterproof black drawing ink. After 30-60 second contact with the agar, the filter was peeled off the agar and dena-tured for 1-5 minutes in a shallow tray containing 0.5M NaOH, 1.5M NaCl. The membrane was neutralized in 1.5M NaCl, 0.5M Tris-HCl (pH 7.4) for 5 minutes,

rinsed in 2 X SSC (17.53g NaCl, 8.82g NaCitrate per litre, pH 7.0) , and dried DNA side up on paper towels. The DNA was then fixed to the membrane by exposure to short-wave UV light for 5 minutes.

A ^{32}P-radiolabeled probe was prepared by adding approx. 20ng human LCAT cDNA in pUC 19 to 32.5μL dH$_2$O. The plasmid cDNA was boiled for 5 minutes then quenched in ice water. 10μL 5X OLB buffer (25mM Tris-Cl pH 8.0; 25mM MgCl$_2$; 5mM β-mercaptoethanol; 2mM each dATP, dGTP, dTTP; 1M HEPES (adjusted to pH 6.6 with 4N NaOH; 1mg/mL oligonucleotides), 2μL 10mg/mL BSA (bovine serum albumin Fraction V; Sigma), 5μL ^{32}P-dCTP, followed by 0.5μL Klenow fragment of E. coli DNA polymerase I (5 units). The mixture was incubated 1.5hrs at 37°C.

The filter prepared above was placed in a heat-sealable bag. The filter was moistened with approximately 10mL 2XSSC buffer. The buffer was squeezed out and replaced with 5 to 10mL prehybridization buffer (1%w/v BSA, 0.5M Na$_2$H$_2$PO$_4$, 1mM EDTA, 7%w/v SDS). Following removal of air bubbles, the bag was heat-sealed and pre-hybridized for 30 minutes at 65°C.   Just prior to hybridization, the radiolabeled probe was boiled for 5 minutes, then quenched in ice water. The probe was then added to the hybridization bag which was resealed and hybridized at 65°C overnight. The next day, the filter was washed with 200mL 0.1X SSC/1% w/v SDS 15 minutes at 15°C, then twice with 200 mL 0.1XSSC/0.5% w/v SDS 15 minutes at 64°C. Following a brief rinse with 0.1XSSC, the filter was dried briefly on a pad of paper towels, then covered (while still damp) with Saran Wrap. The filter finally was exposed to X-Omat AR film with one or two intensifying screens at -70°C.

Bacteriophage λ plaques identified as hybridizing to the probe were picked and cultured in sterile LB media and a near-full length clone was identified and sequenced as described below (see figure 5)

Figure 5. Porcine LCAT cDNA sequence

```
              10        20        30        40        50        60
               |         |         |         |         |         |
    1 NNNNNNNNNNCCGGGCTCCCCACGGCAGTGGGTCCTGCTGCTGCTGGGGCTGCTGCTCCCC
   61 CCTGCCGCCCCCTTCTGGCTCCTCAATGTGCTCTTCCCCCCGCACACCACGCCCAAGGCT
  121 GAGCTCAGTAACCACACACGGCCCGTCATCCTCGTACCTGGCTGCCTGGGGAATCAGCTG
  181 GAAGCCAAGCTGGATAAACCAGATGTGGTGAACTGGATGTGCTACCGCAAGACAGAGGAC
  241 TTTTTCACCATTTGGCTGGATCTCAATATGTTCCTACCCCTTGGGGTAGACTGCTGGATT
  301 GATAATACCAGGGTTGTCTACAACCGCACCTCTGGGCGCGTGTCCAACGCACCGGTGTA
  361 GAGATCCGTGTCCCCGGCTTTGGCAAGACCTACTCTGTCGAGTACCTGGACAACAGCAAG
  421 TTGGCAGGTTATATGCACACACTGGTACAAAACCTGGTCAATAATGGGTATGTGCGGGAT
  481 GAGACCGTGCGGGCTGCCCCCTACGACTGGCGGCTGGAGCCCAGCCAGCAGGAAGAGTAC
  541 TACCTGAAGCTTGCTGGGCTGGTGGAAGAAATGCATGCTACTTATGGAAAGCCGGTCTTC
  601 CTCATTGGGCACAGCCTTGGCTGCCTACACTTGCTCTATTTCTTACTACGCCAACCCCAG
  661 GCCTGGAAGGACCGCTTCATTGATGGTTTCATCTCTCTTGGAGCTCCCTGGGGTGGCTCC
  721 ATCAAGCCCATGCTAGTCTTGGCCTCAGGTGACAACCAGGGCATCCCGATCATGTCCAGC
  781 ATCAAACTGAAAGAGGAGCAGCGCATGACAACAACCTCCCCCTGGATGTTTCCCTCCAGC
  841 CACGTGTGGCCCGAGGACCATGTGTTCATTTCCACCCCCAGCTTCAACTACACAAGCCAT
  901 GACTTCCAGCGCTTCTTTGCAGACCTGCACTTTGAGGAAGGCTGGTACATGTGGCTACAG
  961 TCACGTGACCTGCTGGCAGGCCTCCCAGCGCCTGGTGTGGAAGTATACTGTCTGTATGGT
 1021 GTGGGCCTGCCCACACCCCGCACCTACATCTTTGACCACGGCTTCCCCTACACGGACCCT
 1081 GTGGATGTGCTCTATGAGGATGGTGATGACACTGTGGCTACGCGCAGCACCGAACTCTGT
 1141 GCCCGCTGGCAGGGCCGCCAACAGCAGCCTGTGCACCTGCTGCCTCTGCCTGGGACACAG
 1201 CACCTCAATATGGTTTTCAGTAACCAGACACTGGAGCACATCAATGCCATCCTGCTGGGC
 1261 ACCTACAGAAATAGCACCCCAGTATCCCCAAGCACCAGCACAGGGACCCTTCCCCCTGAA
 1321 TAAAGACTTCTTTGCTG

Total number of bases is: 1337
DNA sequence composition:    276 A;   421 C;   340 G;   291 T;  9 OTHER
```

No clone was isolated that contained the complete LCAT cDNA through
sequencing the 5'-end of several clones obtained from the porcine λ-GT 11 library.
The most complete clone was approx. 9 nucleotides short of the start codon. How-
ever, comparison of the porcine nucleotide sequence with human LCAT cDNA
showed these nucleotides to be located within the coding region of the LCAT leader
sequence which is cleaved from the mature protein during post-translational modifi-
cation. Since the region of the mature porcine LCAT cDNA sequence was contained
within the porcine clone, it was possible to express the protein in a stable expression
system using a human non-coding leader sequence. This was achieved by ligating
nine nucleotides from human LCAT cDNA, including the ATG start codon, into the
porcine LCAT cDNA to replace the missing sequences. Together with the three
resultant human LCAT amino acids, the translated sequence of the porcine rLCAT

clone has 416 amino acids (the same number as human rLCAT) with a predicted molecular weight of 47337daltons. As with human rLCAT, there are four predicted N-linked glycosylation sites having the consensus motif of Asn-Xaa-Ser/Thr . These sites occur at positions 20, 84, 272 and 384. The conserved region of the serine residue in the active site of lipases found in human rLCAT is also present in porcine rLCAT at positions 175-184.

2.3.2 Design of inter-species rLCAT cDNA primers

Three cDNA primers were designed from consensus regions having a high degree of sequence identity between five animal species where the LCAT cDNA was previously known. The primers were designed using Oligo 4.0, a computer program that aids in the design of balanced primers by calculating the predicted melting point and Gibbs free energy, based on nucleic acid composition and distribution. Primers were chosen to amplify two sequences with a 60bp overlapping region to facilitate ligation into a full-length clone. PCR cycling conditions for these primers, together with other materials, are given in section 2.3.5.

Figure 6. Design of LCAT consensus sequence primers. Nucleotides with sequence identity to other species are shown in capitals. Wherever a consensus sequence was obtained, this was used to develop the primer. Where there was no consensus, the human LCAT cDNA nucleotide was selected.

LCAT6 primer: (+ strand, -17 to start codon)

Human	tctctgGcagtagGcacCaGGGCTGGAATG
Rat	GgcacgaGgcaCtGGGCTGTAATG
Mouse	TGTgATG
Consensus	------G------G---C-GGGCTGTAATG
LCAT6 (20mer)	TAGGCACCAGGGCTGGAATG

LCAT2 Primer: (- strand, 1236-1252)

Human	CACATCAATGCCATCCT
Baboon	CACATCAATGCtATCCT
Pig	CACATCAATGCCATCCT
Rat	CAtATtAATGCtATCCT
Mouse	CAtATCAATGCCATCCT
Consensus	CACATCAATGCCATCCT
LCAT2 (17mer)	GTGTAGTTACGGTAGGA

300W Primer: (+strand, 954-983)

Human	CTgCAGTCACGTGACCTcCTGGCAGGaCTC
Baboon	CTgCAGTCACGTGACCTcCTGGCAGGCCTC
Pig	CTaCAGTCACGTGACCTgCTGGCAGGCCTC
Rat	CTaCAGTCtCGTGACCTaCTGGCAGGCCTC
Mouse	CTtCAGTCtCGTGACCTaCTGGagcGCCTC
Consensus	CT-CAGTCACGTGACCT-CTGGCAGGCCTC
L300W (30mer)	CTgCAGTCACGTGACCTcCTaGCAGGaCTC

2.3.3   Total RNA extraction from rabbit liver

Fresh rabbit (Oryctolagus Cuniculus) liver was immediately frozen in liquid nitrogen and total rabbit RNA was isolated by the acid guanidinium thiocyanate-phenol-choloform extraction method (modification of Chomczynski *et al.*, 1987). A tissue homogenizer was carefully cleaned with diethylpyrocarbonate-treated water (1mL DEPC per ltre distilled water; swirled and let stand for greater than one hour, followed by autoclaving) . This was followed by cleaning the homogenizer with Stock Solution A (260g guanidinium thiocyanate; 17.6 mL 0.75 M NaCitrate pH 7.0; 26.4 mL 10% Sarcosyl at 65°C; 293mL DEPC-treated water). Approx. 100mg N_2-frozen rabbit liver was then ground into a fine powder using a morter and pestle under liquid nitrogen. The liver tissue was then added into a 15mL DEPC-treated, autoclaved Corex-tube. To the tissue was added 2.0 mL stock D solution (0.36mL 2-Mercaptoethanol in 50mL Stock Solution A) and the tissue was homogenized on ice with 3 cycles at 15 second intervals. The following was then sequentially added, following by mixing: 0.2mL 2M Na Acetate pH 4.0; 2.0 mL phenol; 0.4mL 49:1

choloform:isoamyl alcohol: The suspension was then shaken vigorously for 10 sec-

onds and cooled on ice for 15 minutes. This was followed by centrifugation at 10,000

g for 20 minutes at 4 °C. After centrifugation, the top aqueous layer was removed

(containing RNA) and transfered to a new Corex tube. This was followed by 2.0 mL

isopropanol. The mixture was then cooled for at least one hour at -20°C, followed by

centrifugation at 10,000g for 20 minutes. The sedimented RNA was then dissolved in

0.3mL Solution D, then transfered to a 1.5mL Eppendorf tube and precipitated with

one volume of isopropanol at -20°C. The tube was next centrifuged for 10 minutes at

4°C and the pellet resuspended in 75% ethanol for long-term storage, or in DEPC-

treated water for short term. Storage was at -20°C. Prior to use, the RNA was

precipitated by centrifugation at 14,000 g X 20 minutes, then resuspended in DEPC

treated dH$_2$O. RNA concentration was estimated by multiplying the absorbance value

at 260nm by 45 to produce units in μg/mL. RNA was utilized if the ratio of absor-

bance at 260 nm was greater than absorbance at 280 nm by a factor of 1.8.

2.3.4   Reverse transcription of rabbit liver total RNA

1-5µg of total RNA was diluted in RNAse-free dH$_2$O to a total volume of
11.5µL The RNA was heated to 95°C for 5 minutes, then snap-chilled on ice.
Two µL 10mM dNTP, 2µL 10 X PCR buffer G (Perkin-Elmer Cetus: 500mM KCL;
0.10% gelatin heat in water to dissolve; 100mM Tris pH 8.3; 15mM MgCl$_2$, filter to
sterilize) and 2.5µL dH$_2$O was added. To this was added either 500ng dT(17) or
50ng consensus reverse primer. This was followed by 1µL RNAse inhibitor (10U),
1µL (200U) RT Superscript reverse transcriptase. The mixture was incubated at
room temperature for 10 minutes, followed by 37°C for 60-90 minutes. Following
reverse transcription, the first strand DNA was separated from mRNA by heating to
95°C for 5 minutes, then cooled to 55°C. 2 units RNAse H (2µL) were then added
and the mixture was incubated at 37°C for 20 minutes to digest the mRNA. The
cDNA produced from the dT and consensus primers were labeled 5'cDNA pool and
3'cDNA pool respectively. Three cDNA pools using each primer were prepared in
separate reverse transcription reactions. These were used as templates for the
PCR amplifications below.

2.3.5   PCR amplification of rabbit rLCAT cDNA

Two separate PCR reactions were used to produce overlapping amplified fragments that spanned the full-length rabbit LCAT cDNA (See Figure 7).
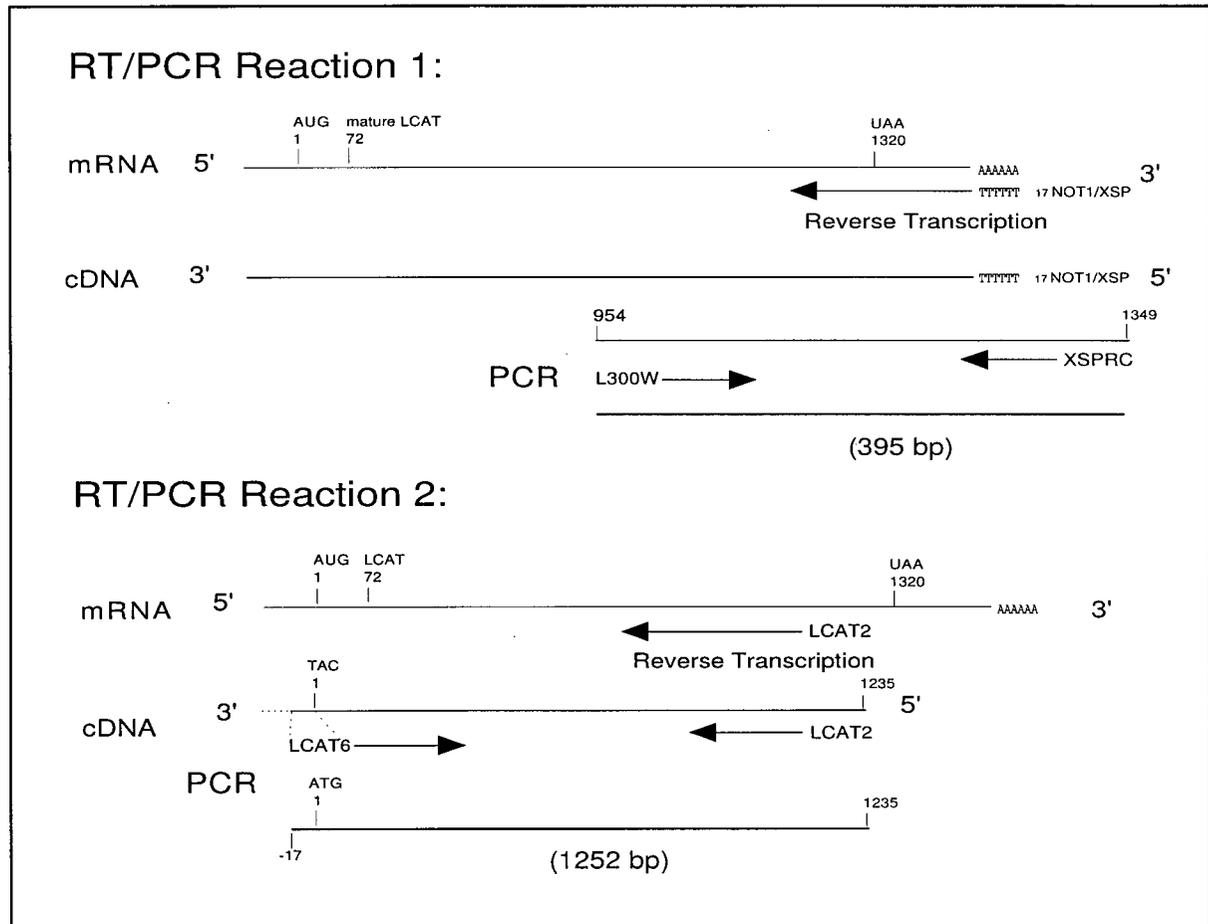
Figure 7. Reverse transcription of rabbit mRNA and PCR amplification of LCAT cDNA. Two separate reverse transcriptions, followed by PCR amplification were used to produce full-length rabbit LCAT cDNA. In reaction 1, a poly-T primer was used to reverse-transcribe mRNA to produce single-stranded cDNA. An inter-species consensus primer (L300W) was used in conjunction with the poly-T primer to amplify the rabbit rLCAT cDNA product. Two inter-species consensus primers were employed in reaction 2, LCAT6 and LCAT2, the latter primer being also used in the initial reverse-transcription. 17NOT1/XSP is an oligo-dT 17 primer to which is attached a NOT1 and XSP restriction site to facilitate cloning into a bacterial or expression vector. XSPRC is a reverse-complement primer lacking the 17 oligodT nucleotides to reduce the opportunity for nonspecific amplification. The PCR amplified products were 395 and 1252. The two products overlap with 281 common sequences which, following restriction digestion and ligation produced full-length rabbit LCAT cDNA.

The first reaction utilized an interspecies-derived consensus primer, L300W, and a dt(17)/NOT/Xsp primer. The latter contains an 17mer oligo-dT sequence to which is attached NOT1 and Xsp restriction sites. These primers amplified the region corresponding between human rLCAT cDNA nucleotide 954 (numbered from the ATG start codon) and the mRNA poly-A tail. The PCR reaction cocktail, prepared on ice, consisted of 0.25μL of first strand cDNA from the 3'cDNA pool obtained above, 5μL 10X buffer D (670mM Tris pH 8.0, 67mM MgSO$_4$, 1.66M (NH$_4$)$_2$SO$_4$, 100mM βMercaptoethanol), 0.5μL 10mM dNTPs, 43μL dH$_2$O, 0.25dH$_2$O Taq DNA polymerase and 0.5μL of each primer (100pmole/μL). The PCR cocktail was placed directly from ice to a preheated PCR machine and the DNA was allowed to melt at 95°C for 3 minutes. This was followed by annealing at 61°C for 45 seconds and extension of the second strand cDNA for five minutes. The PCR was then cycled at 95°C for 45 seconds, 51°C for 45 seconds and 72°C for 1.5 minutes for 35 cycles. The PCR amplification was completed by a final 5 minute extension.

The second PCR amplification utilized two inter-species consensus LCAT-specific primers, LCAT6 and LCAT2. The reaction cocktail, prepared on ice, consisted of 2μL of the 5'cDNA pool, 5μL 10X buffer "D," 8μL 1.25mM dNTP, 0.5μL Taq polymerase and 29.5μL dH$_2$O. 2.5μL of each primer (10mM) were added to the reaction mixture. The PCR cocktail was placed directly from ice to a preheated PCR machine and the DNA was allowed to melt at 95°C for 3 minutes. This was followed by annealing at 61°C for 45 seconds and extension of the second strand cDNA for five minutes. The PCR was then cycled at 95°C 45 seconds, 51°C 45 seconds and 72°C 1.5 minutes for 35 cycles, followed by a final 5 minute extension. The LCAT6 and LCAT2 primers amplified rabbit LCAT cDNA from the ATG start codon (position 1) to position 1235 (referenced in human LCAT cDNA). The region of over-

lap between the first and second LCAT cDNA products was therefore 282 nucleotides.

The PCR-amplified cDNA from the reactions above were isolated from primers and nonspecific products using a 0.8% 1X TAE gel containing ethidium bromide (2.5mL/50mL gel) for cDNA visualization under long-wave UV light. Fragments were purified by Geneclean, placed into 10μL 1X TE buffer, and ligated overnight at 11°C as follows in a mixture of: 3μL cDNA, 1μL BlueScript KS⁻ vector, 2μL 5X ligation buffer, 1μL T4 polymerase and 3μL dH₂O.

The cDNA fragments from each amplification were separately ligated overnight into the BlueScript KS⁺ vector. Three separate PCR amplifications using different reverse-transcribed products were performed to screen for random nucleotide misincorporation errors. The partial amplification products were subsequently cloned, sequenced in both directions, and compared for possible errors. The two partial cDNA strands were ligated into BlueScript to produce complete rabbit LCAT cDNA clone. Both ends of the complete clone and the restriction site used to ligate the two PCR amplification products were sequenced to confirm correct ligation and orientation within the vector.

2.3.6   Culture and transformation of E coli

E. Coli DH5α strains were grown in LB media (5g/L yeast extract, 10g/L NaCl, 10 g/L tryptone). Late log-phase bacterial stocks were frozen -70°C in 20% glycerol. *E. Coli* competent cells were prepared by innoculating one colony in to 20mL TYM broth (5g/L yeast extract, 5.84 g/L NaCl, 1.20g/L MgSO₄, 20 g/L tryptone). Cells were cultured in a shaking incubator at 37°C until midlog phase was reached (OD$_{600}$=0.2-0.8). Cells were then diluted in TYM to 500mL and cultured further. When an OD of 0.6 was reached, cells were rapidly chilled on ice, then pelleted at 5000 x g for 15 minutes. The pellet was then resuspended on ice in 100mL chilled 30mM potassium

acetate, 50mM $MnCl_2$, 10mM $CaCl_2$, 100mM KCl and 15% glycerol. Cells were pelleted again at 5000 x g for 10 min and resuspended in 20mL chilled 75mM $CaCl_2$, 10mM NaMOPS, 10mM KCl and 15% glycerol. 0.1mL and 0.5mL aliquots were frozen in liquid nitrogen and stored at -70°C.

Competent cells were transformed by gently mixing cells with plasmid DNA in an ice water bath for 30 minutes. The mixture was heat shocked at 37°C for 5 min and diluted 1:10 in LB media. Cells were incubated in a gently shaking chamber for 90 minutes at 37°C. The mixture was then plated onto LB-agar plates containing ampicillin [100μg/mL] and incubated inverted for 16h at 37°C. Plasmids containing the β-lactamase gene were utilized in these studies to allow survival of transformants in the presence of ampicillin.

2.3.7 DNA Purification

2.3.7.1 Small scale plasmid preparation

A single colony was inoculated into 5mL LB medium in the presence of 100μg/mL ampicillin. Cells were cultured in a vigorously shaking (300rpm) incubator at 37°C for 20-22 hours. The bacterial culture was pelleted at 12,500rpm in a microcentrifuge and resuspended in two aliquots each containing 200μL Lysis Buffer (50mM glucose, 25mM Tris HCL pH 8.0, 10mM EDTA, 5g/mL lysozyme freshly prepared). The mixture was vortexed 5 seconds then incubated for 5 minutes at room temperature. Following incubation, cells were lysed in 400μL freshly prepared 0.2N NaOH, 1% SDS, then neutralized in 300μL ice cold 7.5M ammonium acetate (pH 7.6). Cellular debris was removed by repeated centrifugation and clear supernatant was removed. DNA was precipitated in 0.6 volumes of isopropanol and resuspended in 100μL 2M ammonium acetate (pH 7.4). Following a second precipitation in 100μL isopropanol, the pellet was washed in 70% ethanol to remove coprecipitating salts. The pellet was then vacuum dried and dissolved in 49μL TE

buffer (10mM Tris HCL, 0.1mM EDTA pH 8.0). To this was added 1μL RNase A. The mixture was then incubated for 15 minutes at 37°C. The plasmid DNA was next dissolved in 25μL 2M ammonium acetate followed by centrifugation. The supernatant was removed, then precipitated again in 200μL 70% ethanol. After centrifugation, the pellet was dissolved in 25μL sterile dH_2O or TE buffer. The relative purity of plasmid DNA was estimated by calculating the ratio of ultraviolet absorbance at 260 and 280nm. If sufficiently pure (A260/A280 ratio ≥1.8), the quantity of DNA was estimated by absorbance at 260nm. An O.D. of 1.0 is equivalent to 50μg/mL double stranded DNA, or 40μg/mL single stranded DNA.

2.3.8   Large scale plasmid preparation

For eukaryotic cell transfections, larger quantities of plasma DNA were prepared. Selective LB broth (250mL) was inoculated with 5mL overnight culture and incubated in a shaking chamber at 37°C for 16 hours. Following incubation, cells were pelleted at 2800 x g and resuspended in chilled 50mM glucose, 10mM EDTA, 5mg/mL lysozyme, and 25mM Tris-HCl pH 8.0. After 20 min incubation on ice, the mixture was transferred to 30mL polycarbonate screw cap tubes. The cells were lysed by gentle inversion in freshly prepared 10mL 0.2M NaOH, 1% SDS. To the mixture was added 7.5mL 5M KAcetate, pH 4.8 and incubated on ice for 10 min. The lysate was next centrifuged at 25,000 x g for 15 min. The supernatant transferred to a 50mL polypropylene screw cap tube and digested with 50μg RNAse A for at 37°C for 20 min. The DNA was then precipitated with two volumes chilled 95% ethanol for 20 min at -20°C and pelleted by centrifugation. The sample was washed in 70% ethanol to remove salts, resuspended in 2mL sterile water, then transferred to a 15mL polypropylene screw cap tube. The DNA was then extracted twice with phenol:chloroform (1:1), followed by a final extraction in chloroform. The DNA solution (1.6mL) was transferred to a 15mL silanized glass Corex tube , to which was

added 2.0mL of 13% polyethylene glycol (PEG-8000) and 0.4mL 5M NaCl. The DNA was allowed to precipitate on ice for 60 minutes, followed by centrifugation at 12,000 x g for 15 minutes. The pellet was redissolved in 200-500μL TE buffer and quantitated by absorbance at 260nm following estimation of purity by A260/A280 ratio.

2.3.9 Isolation of cDNA Fragments

Products from PCR amplification or plasmid fragments from restriction enzyme digestion were purified by agarose gel electrophoresis. Bands of DNA were excised from the gel and extracted using Geneclean or MERmaid (Bio101) protocols. The DNA was quantitated by visualization of ethidium-stained agarose gels.

2.3.10 DNA Sequence analysis

The double-strand enzymatic chain termination method was utilized to determine the DNA sequence of LCAT cDNAs (Sanger *et al.,* 1977). Reactions were performed using a modified T7 DNA polymerase (Sequenase, United States Biochemical), according to manufacturer's instructions. Approximately 2pmol (2-5μg) of plasmid DNA were incubated in 20μL of freshly prepared 0.2M NaOH and 0.2M EDTA for 5 minutes at room temperature. The denatured DNA was neutralized with 2μL 2M ammonium acetate, pH 4.6. The mixture was precipitated with 75μL ethanol and chilled for 10 minutes at -70°C. The supernatant was removed following microcentrifugation, and the remaining pellet was washed in cold 70% ethanol and dried by Speedvac. The DNA was resuspended in 3.8μL dH$_2$O. 1.2μL Sequenase reaction buffer and 5pmol (1μL) annealing primer was added. The primer was annealed to the template DNA by heating for 2 minutes at 65°C, then allowed to cool slowly to less than 35°C over 15-30 minutes. The annealed primer was then simultaneously labeled and extended with Sequenase in the presence of 2.5μCi α-[^{35}S]-dATP, 1.5μM dGTP, dTTP, dCTP and 0.0125M dTT. The reaction was chain

terminated in four separate reactions by adding 2.75μL of the labeling reaction mixture to 1.25μL of a prewarmed solution containing nucleotides plus a dideoxynucleotide corresponding to each nucleotide base. The termination reaction was performed at 37°C for 5 min and stopped by addition of 2.0μL Stop Buffer (95% formamide, 20mM EDTA, 0.05% Bromphenol blue, 0.05% xylene cyanole FF).

The labeled mixture was resolved using a 6% polyacrylamide sequencing gel prepared in 8M urea and 1X TBE (2mM EDTA, 89mM boric acid, 89mM Tris). Following electrophoresis, the gel was mounted by drying on Whatman 3MM chromatography paper and exposed to autoradiographic film for 16-72 hours.

2.4   Results

2.4.1   LCAT cDNA sequence

Clones derived from at least two separate reverse transcription reactions were sequenced in both directions in order to obtain a consensus sequence. Where a disagreement was found between the two clones, likely due to a misincorporation error, a clone from a third reverse transcription reaction was sequenced. Clones with sequence identity between at least two different reverse-trancribed products were then used to develop a consensus sequence and the full-length cDNA for recombinant LCAT expression in eukaryotic cell lines.

The full-length rabbit LCAT cDNA consists of 1345 bases, which have 90.6% sequence identity with that of human cDNA. Compared to human LCAT cDNA, mouse and porcine rLCAT share 84.5% and 88.8% nucleic acid sequence identity, respectively (see Table 5).

Table 5.   **Sequence identity of different species of LCAT.** Percent sequence identity is compared to human LCAT.

Species	Nucleotide	Amino Acid	Reference
Baboon	97%	98%	Hixson et al., 1993
Rabbit	91%	93%	Shaw, this thesis
Pig	89%	92%	Shaw, this thesis
Rat	84%	87%	Merone et al., 1990
Mouse	85%	85%	Warden et al., 1989
Chicken	74%	73%	Hengstschlager-Ottnad, et al., 1995

Figure 8. Rabbit LCAT cDNA sequence

```
              10        20        30        40        50        60
              |         |         |         |         |         |
     1 ATGGGGCCGCCTGGCTCCCCATGGCAGTGGGTGCTGCTGCTGCTGCTGGGGCTGCTGCTC
    61 CCTCCTGCTGCCCCCTTCTGGCTCCTCAATGTGCTCTTCCCCCCGCACACCACGCCCAAG
   121 GCTGAGCTCAGTAACCACACACGGCCCGTCATTCTCGTGCCTGGCTGCCTGGGGAACCAG
   181 CTGGAAGCTAAGCTGGATAAACCAAGTGTGGTGAACTGGATGTGCTACCGCAAGACAGAG
   241 GACTTCTTCACCATCTGGCTGGATCTCAATATGTTTCTACCTCTTGGGGTGGACTGCTGG
   301 ATCGATAATACCAGGGTTGTCTACAACCGCAGCTCTGGGCGCGTGTCCAATGCTCCCGGT
   361 GTACAGATCCGCGTCCCTGGCTTTGGCAAAACCTACTCTGTTGAGTACCTAGACAACAAC
   421 AAGCTGGCAGGTTACATGCACACGCTGGTGCAGAATCTGGTCAACAACGGGTACGTGCGA
   481 GATGAGACCGTGCGAGCTGCCCCCTATGACTGGCGGCTGGAGCCCAGCCAGCAGGAGGAG
   541 TACTACGGGAAGCTCGCTGGGCTGGTGGAGGAGATGCACGCTGCTTACGGGAAGCCCGTC
   601 TTCCTCATTGGGCACAGCCTTGGCTGCCTCCACGTACTCTATTTTTGCTGCGCCAGCCC
   661 CAGTCCTGGAAGGACCGCTTTATTGATGGTTTCATCTCTCTTGGGGCTCCTTGGGGCGGC
   721 TCCATCAAGCCCATGCTGGTCTTGGCCTCAGGTGACAACCAGGGCATCCCACTCATGTCC
   781 AGCATCAAGCTGAGAGAGGAGCAGCGCATAACAACGACTTCCCCCTGGATGTTTCCCTCC
   841 CAGGGGGTGTGGCCTGAGGACCACGTGTTCATTTCCACACCCAGCTTCAACTACACTGGC
   901 CGTGACTTCAAGCGCTTCTTTGAGGACTTGCATTTTGAGGAAGGCTGGTACATGTGGCTC
   961 CAGTCACGTGACCTACTGGCAGGACTCCCCGCCCCGGGCGTGGAAGTGTACTGTCTGTAT
  1021 GGCATAGGCCTGCCCACACCCCACACCTACATCTATGACCACGGCTTCCCCTACACGGAC
  1081 CCTGTGGGTGTGCTCTATGAGGATGGGGATGACACAGTGGCCACACGCAGCACTGAGCTC
  1141 TGTGGCCTCTGGCGAGACCGCCAGCCACAGCCTGTGCACCTGCTGCCCCTGCATGAGACA
  1201 GAGCACCTCAACATGGTCTTCAGCAACCAGACGCTGGAGCACATCAATGCCATCCTGCTG
  1261 GGTGCCTACCGCAGCGGCACTCCTGCCTCCCCGACTGCCAGCCCAGGGAGCCCGCCCCCT
  1321 GAATAAAGAACTTTCTTGCTACTGTAAAAAAAAAAAAAAAA
```
```
Total number of bases to 3'-poly-A tail is: 1345.
DNA sequence composition:     275 A;     427 C;     368 G;     292 T; 0
OTHER;
```

The translated amino acid sequence of the mature protein for our rabbit rLCAT clone has 416 amino acids, the same number as human rLCAT. The mature protein, which has a predicted molecular weight of 47153 daltons, is preceded by a hydro-phobic leader sequence of 24 amino acids. As with human rLCAT and the porcine

rLCAT described above, there are four predicted N-glycosylation sites having the consensus motif of Asn-Xaa-Ser/Thr . These sites occur at positions 20, 84, 272 and 384 (see figure 16). The conserved region encompassing the serine residue in the active site of lipases, also found in known sequences of LCAT of other species, is present in rabbit rLCAT at positions 175-184. Several other potential sites have been identified by searching the PROSITE database for sequence patterns (Bairoch A, 1991). However, a comparison of the observed frequency of occurrence in other potentially related sequences with the theoretical frequency of occurrence of the sequence being analyzed suggests the probability of occurrence is unlikely.

Shortly after our rabbit rLCAT cDNA was cloned and sequenced, independent researchers released an unpublished cDNA sequence. The Genbank entry, which has yet to be published in a peer-reviewed journal, was apparently derived from a λ-GT 10 rabbit liver library and basically confirms the independently derived sequence presented in this thesis (Murata *et al.,* 1993 *unpublished*). There are some significant differences in the coding sequence, however. Most of the differences in nucleic acid sequence were located within the wobble position for nucleic acids and therefore did not affect the amino acid structure. However, our translated amino acid sequence varied from the sequence reported by Murata *et al.* in five locations within the coding region for the mature protein (see table 6).

Table 6. Differences in translated amino acid sequence between cloned rabbit cDNA and genbank data

Amino Acid Position	Rabbit rLCAT		Human rLCAT
	Murata *et al.*	Shaw	Mclean *et al.* (1986a)
-10	-	L	-
90-93	VIS	SNA	SNA
187	L	V	L
351	S	R	R
354	D	E	E
360	G	D	G

A detailed comparison of the differences noted in translated amino acid sequence is given in the next six figures, 9, to 14. Multiple, overlapping sequences were read in both directions using several different clones produced from independent reverse transcriptions:

Figure 9. Amino acid position -10 (non-coding region). The sequences obtained in this thesis are compared with that of Murata *et al.* Lines between the coding sequences indicate sequence identity. The number of clones and reverse transcriptions (RT's) used to obtain the clones are shown. These clones were sequenced and the number of sequencing gels read to confirm the sequence are noted.

```
                                                        gels
                                                        read in
                                                        this
                                                        region:    clones:
                    V  L  L  L  L  L  G    (-15 to -9)
Our rabbit rLCAT:   ggtgctgctgctgctgctggg   (30-50)      8 gels,    5 clones
                    |||||||||||||||||  |||                          (2 RT's)
   Murata et al.:   ggtgctgctgctgct---ggg   30-47)
                    V  L  L  L  L     G    (-14 to -9)
```

Figure 10. Amino acid positions 91-93. The altered amino acids in position 91-93 in the sequence reported by Murata *et al.,* is likely due to three nucleic acid sequencing errors occurring within nine bases. Our results are consistent with all other known mammalian species of rLCAT sequenced in this region:

```
                                                    gels
                                                    read in
                                                    this
                                                    region:  clones:
                     V    S   N   A   P   (90-94)
Our rabbit rLCAT:    gtg-tcca-atgctccc (343-357)    6 gels   4 clones
                     ||| || | || ||||||                      (2 RT's)
    Murata et al.:   gtggtc-atat-ctccc (340-354)
                     V    V   I   S   P   (90-94)
```

Figure 11. Amino acid position 187

```
                                                    gels
                                                    read in
                                                    this
                                                    region:  clones:
                     H     V   L   (186-188)
Our rabbit rLCAT     ca-c-gtactc (631-639)          8 gels   5 clones
                     || | |  |||                             (2 RT's)
    Murata et al.:   catctg--ctc (628-636)
                     H   L   L   (186-188)
```

Figure 12. Amino acid position 351

```
                                                    gels
                                                    read in
                                                    this
                                                    region   clones:
                     T  R  S    (350-352)
Our rabbit rLCAT:    ac-acgcagc (1123-1131)         10 gels  8 clones
                     || | |||||                              (4 RT's)
    Murata et al.    acca-gcagc (1120-1128)
                     T  S  S    (350-352)
```

Figure 13. Amino acid position 354

```
                                                    gels
                                                    read in
                                                    this
                                                    region:  clones:
                     T  E  L    (353-355)
Our rabbit rLCAT:    actgagctctg (1132-1140)        10 gels  8clones
                     ||||| | |||                             4 RT's)
    Murata et al.:   actga-c-ctg (1129-1137)
                     T  D   L   (353-355)
```

Figure 14. Amino acid position 360

```
                                               gels
                                               read in
                                               this
                                               region:  clones:
                           R   D   R   (359-361)
Our rabbit rLCAT:          cgag-accgc  (1153-1161)    8 gels,  5 clones
                           ||||  |||||                         (4 RT's)
      Murata et al.:       cgagg-ccgc  (1150-1158)
                           R   G   R   (359-361)
```

Table 7. Summary of differences in nucleic acid sequence between cloned LCAT cDNA and Genbank data

Nucleic Acid Position	Murata *et al.*	Shaw
45-47	---	GCT
345	G	-
348	-	C
350	T	-
353	-	G
631	T	-
633	T	-
635	--	TA
1124	C	-
1126	-	C
1136	-	G
1138	-	T
1144	T	-
1145	G	-
1150	G	-
1151	-	C
1159	G	-
1160	-	A
1330	-	A

The sequence comparisons above suggest that sequence reading errors may, at least in part be the cause for differences observed between the rabbit LCAT cDNA sequence presented in this thesis and that of Murata *et al.* Because the sequence by Murata *et al.* has yet to be published in a peer-reviewed journal, it is not possible to comment on the techniques they used to obtain and to sequence their clone. Because of the multiple independent confirmations of sequence data used to determine the rabbit LCAT cDNA sequence presented in this thesis, we have confidently submitted a corrected sequence to Genbank.

2.4.2 Phylogenetic comparison of cDNA sequences between species

Using pairwise similarity scores from the CLUSTAL computer program (Higgins *et al.* 1988), a dendogram was created to compare cDNA sequences from known species. The dendogram, or hypothetical phylogenetic tree, plots the degree of similarity between species in graphical form. Rabbit and porcine LCAT cDNA have 91% and 89% sequence identity compared with the human protein, respectively.

Figure 15. Phylogenetic comparison of cDNA sequences.

	Percent Identity
Human	100
Baboon	97
Rabbit	91
Pig	89
Rat	84
Mouse	85
Chicken	74
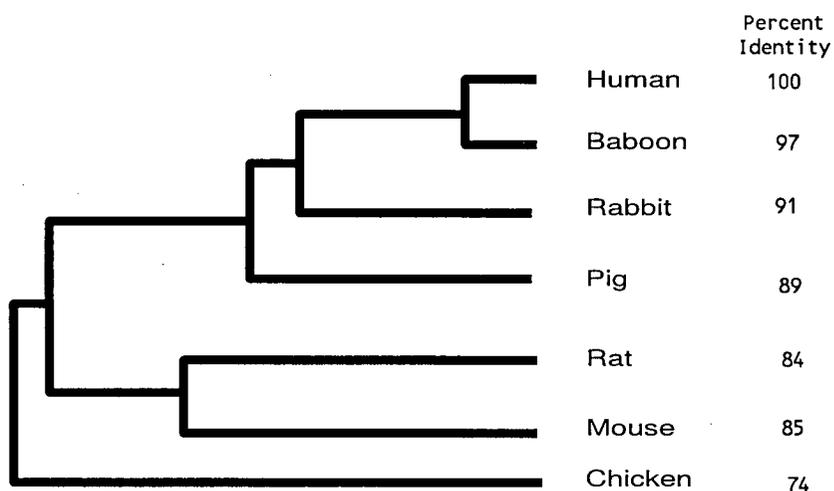
2.4.3 Primary amino acid structure: comparison with rLCAT from other species

The CLUSTAL computer program (Higgins DG *et al.* 1988) was also used to produce a multiple sequence alignment of rLCAT from human, baboon, rabbit, pig, rat, mouse and chicken translated amino acid sequences (see figure 16). Comparison of the primary amino acid sequence has identified specific regions in this highly conserved protein that differ between species. Current work is underway to investigate whether these differences affect the ability of LCAT to esterify various substrates.

2.4.3.1 Amino acid composition

The amino acid composition for rabbit rLCAT is summarized in the table below:

Table 8. Amino acid composition of rabbit rLCAT
The numerical values given are the number of residues located on rabbit rLCAT.

18 Ala	6 Cys	14 His	9 Met	24 Thr
20 Arg	14 Gln	16 Ile	19 Phe	12 Trp
18 Asn	23 Glu	47 Leu	35 Pro	20 Tyr
21 Asp	34 Gln	12 Lys	25 Ser	29 Val

Based on the amino acid composition, the calculated molecular weight is 47153 daltons. SDS polyacrylamide electrophoresis of the purified plasma enzyme produces an observed molecular weight of approx. 67000 daltons, due to glycosylated residues. The total number of negatively charged residues (Asp + Glu) in rabbit rLCAT is 44. The total number of positively charged residues (Arg + Lys) is 32. Using the Physchem computer program module in PC/GENE, the estimated charge at pH 7 is -10.96. The estimated isoelectric point (pI) for the protein is 5.51, compared with an observed pI of 5.2 in human LCAT when stripped of sialic acid residues.

Figure 16. Multiple sequence alignment of LCAT amino acid sequences between animal species. Differences in sequence are highlighted in bold type. N-linked glycosylation sites and cysteine residues are shaded. The interfacial lipase binding region is located between aa 174-192 . A region between 234-302 may affect enzyme substrate specificity (Pritchard *et al.*, unpublished data).

```
           1                   10                  20                  30                  40
human      F W L L N V L F P P H T T P K A E L S H T R P V I L V P G C L G N Q L E A K L
baboon     F W L L N V L F P P H T T P K A E L S H T R P V I L V P G C L G N Q L E A K L
rabbit     F W L L N V L F P P H T T P K A E L S H T R P V I L V P G C L G N Q L E A K L
pig        F W L L N V L F P P H T T P K A E L S H T R P V I L V P G C L G N Q L E A K L
rat        F W L L N V L F P P H T T P K A E L S H T R P V I L V P G C M G N R L E A K L
mouse      F W L L N V L F P P H T T P K A E L S H T R P V I L V P G C L G N R L E A K L
chicken    F W L F N V L F P P T T T P E A P P T S T P P W C L V P G F L G N Q L E A K L
CONSENSUS  F W L L N V L F P P H T T P K A E L S N H T R P V I L V P G C L G N Q L E A K L

                       50                  60                  70                  80
human      D K P D V V N W M C Y R K T E D F F T I W L D L N M F L P L G V D C W I D N T R
baboon     D K P D V V N W M C Y R K T E D F F T I W L D L N M F L P L G V D C W I D N T R
rabbit     D K P S V V N W M C Y R K T E D F F T I W L D L N M F L P L G V D C W I D N T R
pig        D K P D V V N W M C Y R K T E D F F T I W L D L N M F L P L G V D C W I D N T R
rat        D K P N V V N W L C Y R K T E D F F T I W L D F N M F L P L G V D C W I D N T R
mouse      D K P D V V N W M C Y R K T E D F F T I W L D F N L F L P L G V D C W I D N T R
chicken    D K P D V V N W M C Y R K T E D Y F T I W L N L N T F L P V G V D C W I D N T R
CONSENSUS  D K P D V V N W M C Y R K T E D F F T I W L D L N M F L P L G V D C W I D N T R

                       90                  100                 110                 120
human      V V Y R S S G L V S N A P G V Q I R V P G F G K T Y S V E Y L D S S K L A G Y
baboon     V V Y R S S G L V S N A P G V Q I R V P G F G K T Y S V E Y L D S S K L A G Y
rabbit     V V Y R S S G R V S N A P G V Q I R V P G F G K T Y S V E Y L D N N K L A G Y
pig        V V Y R T S G R V S N A P G V E I R V P G F G K T Y S V E Y L D N S K L A G Y
rat        V V Y R S S G H M V S N A P G V Q I R V P G F G K T Y S V E Y L D D N K L A G Y
mouse      I V Y H S S G H M V S N A P G V Q I R V P G F G K T E S V E Y V D D N K L A G Y
chicken    V V Y R T A R K M T N A P G V H I R V P G F G K T Y S V E Y L D Q S K L A G Y
CONSENSUS  V V Y N R S S G   V S N A P G V Q I R V P G F G K T Y S V E Y L D   S K L A G Y

                       130                 140                 150                 160
human      L H T L V Q N L V N N G Y V R D E T V R A A P Y D W R L E P G Q Q E E Y Y R K L
baboon     L H T L V Q N L V N N G Y V R D E T V R A A P Y D W R L E P G Q Q E E Y Y H K L
rabbit     M H T L V Q N L V N N G Y V R D E T V R A A P Y D W R L E P S Q Q E E Y Y G K L
pig        M H T L V Q N L V N N G Y V R D E T V R A A P Y D W R L E P S Q Q E E Y Y L K L
rat        L N T L V Q N L V N N G Y V R D E T V R A A P Y D W R L A P R Q Q D E Y Y Q K L
mouse      L H T L V Q N L V N N G Y V R D E T V R A A P Y D W R L A P H Q Q D E Y Y K K L
chicken    L H T L V Q N L V N N G Y V R D Q T V R A A P Y D W R V G P Q E Q P E Y F Q N L
CONSENSUS  L H T L V Q N L V N N G Y V R D E T V R A A P Y D W R L E P   Q Q E E Y Y   K L

                       170                 180                 190                 200
human      A G L V E E M H A A Y G K P V F L I   G H S L G C L H L L Y F L L R Q P Q A W K D
baboon     A G L V E E M H A A Y G K P V F L I   G H S L G C L H L L Y F L L R Q P Q A W K D
rabbit     A G L V E E M H A A Y G K P V F L I   G H S L G C L H V L Y F L L R Q P Q S W K D
pig        A G L V E E M H A T Y G K P V F L I   G H S L G C L H L L Y F L L R Q P Q A W K D
rat        A G L V E E M Y A A Y G K P V F L I   G H S L G C L H V L H F L L R Q P Q S W K D
mouse      A G L V E E M Y A A Y G K P V F L I   G H S L G C L H V L H F L L R Q P Q S W K D
chicken    K A L I E E M H D E Y Q Q R V F L I   G H S M G N L N V L Y F L L Q Q K Q A W K D
CONSENSUS  A G L V E E M H A A Y G K P V F L I   G H S L G C L H V L Y F L L R Q P Q A W K D

                       210                 220                 230                 240
human      R F I D G F I S L G A P W G G S I K P M L V L A S G D N Q G I P I M S S I K L K
baboon     R F I D G F I S L G A P W G G S I K P M L V L A S G D N Q G I P I M S S I K L K
rabbit     R F I D G F I S L G A P W G G S I K P M L V L A S G D N Q G I P L M S S I K L R
pig        R F I D G F I S L G A P W G G S I K P M L V L A S G D N Q G I P I M S S I K L K
rat        H F I D G F I S L G A P W G G S I K P M R I L A S G D N Q G I P I M S N I K L R
mouse      H F I D G F I S L G A P W G G S I K A M R I L A S G D N Q G I P I L S N I K L K
chicken    Q Y I G G F I S L G A P W G G S V K P L R V L A S G D N Q G I P L M S N I K L R
CONSENSUS  R F I D G F I S L G A P W G G S I K P M L V L A S G D N Q G I P I M S S I K L K

                       250                 260                 270                 280
human      E E Q R I T T T S P W M F P S R M A W P E D H V F I S T P S F N Y T G R D F Q R
baboon     E E Q R I T T T S P W M F P S R L A W P E D H V F I S T P S F N Y T G R D F Q R
rabbit     E E Q R I T T T S P W M F P S Q G V W P E D H V F I S T P S F N Y T G R D F K R
pig        E E Q R M T T T S P W M F P S S H V W P E D H V F I S T P S F N Y T S H D F Q R
rat        E E Q R I T T T S P W M F P A H H V W P E D H V F I S T P N F N Y T G Q D F E R
mouse      E E Q R I T T T S P W M L P A P H V W P E D H V F I S T P N F N Y T V Q D F E R
chicken    E E Q R M T T T S P W M F P T S L A W P E D H V F I S T P S Y N Y T Y R D Y Q R
CONSENSUS  E E Q R I T T T S P W M F P S   V W P E D H V F I S T P S F N Y T G R D F Q R

                       290                 300                 310                 320
human      F F A D L H F E E G W Y M W L Q S R D L L A G L P A P G V E V Y C L Y G V G L P
baboon     F F A D L H F E E G W Y M W L Q S R D L L A G L P A P G V E V Y C L Y G V G L P
rabbit     F F E D L H F E E G W Y M W L Q S R D L L A G L P A P G V E V Y C L Y G I G L P
pig        F F A D L H F E E G W Y M W L Q S R D L L A G L P A P G V E V Y C L Y G V G L P
rat        F F A D L H F E E G W H M F L Q S R D L L A G L P A P G V E V Y C L Y G V G M P
mouse      F F T D L H F E E G W Y M W L Q S R D L L E R L P A P G V E V Y C L Y G V G R P
chicken    F F T D V N L E D G W Y M W E D M K D L L K G L P P P G V D T Y C L Y G T G Y P
CONSENSUS  F F A D L H F E E G W Y M W L Q S R D L L A G L P A P G V E V Y C L Y G V G L P
```

68

Figure 16 (con't).

```
                              330           340           350           360
human      T P R T Y I  Y D H G F P Y T D P V G V L Y E D G D D T V A T R S T E L C G L W Q
baboon     T P R T Y I  Y D H G F P Y T D P V D V L Y E D G D D T V A T R S T E L C G L W Q
rabbit     T P H T Y I  Y D H G F P Y T D P V G V L Y E D G D D T V A T R S T E L C G L W R
pig        T P R T Y I  F D H G F P Y T D P V D V L Y E D G D D T V A T R S T E L C A R W Q
rat        T A H T Y I  Y D H N F P Y K D P V A A L Y E D G D D T V A T R S T E L C G Q V Q
mouse      T P H T Y I  Y D H N F P Y K D P V A A L Y E D G D D T V A T R S T E L C G Q W Q
chicken    T V E T Y I  Y D E H F P Y E D P V D M I Y G D G D D T V N K R S S E L C K R W R
CONSENSUS  T P   T Y I  Y D H G F P Y T D P V   V L Y E D G D D T V A T R S T E L C G   W Q

                              370           380           390           400
human      G R Q P Q P V H L L P L H G I Q H L N M V F S █ L T L E H I N A I L L G A Y R Q
baboon     G R Q P Q P V H L L P L R G I Q H L N M V F S █ Q T L E H I N A I L L G A Y R Q
rabbit     D R Q P Q P V H L L P L H E T E H L N M V F S █ Q T L E H I N A I L L G A Y R S
pig        G R Q Q Q P V H L L P L P G T Q H L N M V F S █ Q T L E H I N A I L L G T Y R N
rat        G R Q S Q G V H L L R M N G T D H L N M V F S █ K T L E H I N A I L L G A Y P H
mouse      G R Q S Q P V H L L P M N E T D H L N M V F S █ K T M E H I N A I L L G A Y R T
chicken    N Q Q K Q K V H V Q E L R G I D H L N M V F S █ L T L T L H Q . . . . . . . . .
CONSENSUS  G R Q   Q P V H L L P L   G T   H L N M V F S N   T L E H I N A I L L G A Y R

                              410
human      G P P A S P T A S P E P P P P E
baboon     G P P A S L T A S P E P P P P E
rabbit     G T P A S P T A S P G S P P P E
pig        S T P V S P S T S T G T L P P E
rat        G T P K S P T A S L G P P P T E
mouse      P K S P A A S P S P P P P E P E
chicken    . . . . . . . . . . . . . H Q
CONSENSUS  G T P   S P T A S P   P P P P E
```

2.4.3.2   Predicted secondary structure comparisons with other species

The translated rabbit rLCAT amino acid sequence was submitted to the Protein Sequence Analysis (PSA) Server for secondary structure predictive analysis. The sequence algorithm is based on probabilistic models to encompass four major folding classes of globular single-domain proteins: "alpha"; "alpha-beta", "beta"; and "irregular". Three potential alpha-helical domains were identified, between aa 118-124, 158-170 and 276-289 (See figures 17 and 18). The probability of a portion of these regions as being in an amphipathic helix was estimated to be 0.6, 0.8, and 0.8, respectively. The strands were classified as "diffuse alpha-beta" due to large standard deviations on both lengths of the strand, the connecting helices, loops loops-plus-turns, and the helix length. The overall predicted secondary structures were virtually superimposable between the human, rabbit and porcine LCAT amino acid sequence. In contrast to results reported by Yüksel *et al.* (1989), the newer PSA predictive algorithms employed in this thesis produced no statistically significant

differences in the predicted secondary structure region between residues 377-391 of porcine and human LCAT amino acid sequences (data not shown).

Other methods to predict secondary structure were compared to determine whether the alpha-helical regions identified above were in agreement with independent predictions. Of the three alpha-helix domains, the sequence between 158-170 was independently identified as having a potential helix domain in methods by four prediction methods (Gibrat *et al.,* 1987, Deleage & Roux 1987., Leven *et al.* 1988., and Geourjon *et al.,* 1994) as calculated by the "Self Optimized Prediction Method" server (Geourjon *et al.,* 1994). Although useful for further study, these predictions must be used with caution due to their inherent inaccuracy and the potential for secondary structure to be altered through post-translational modification.
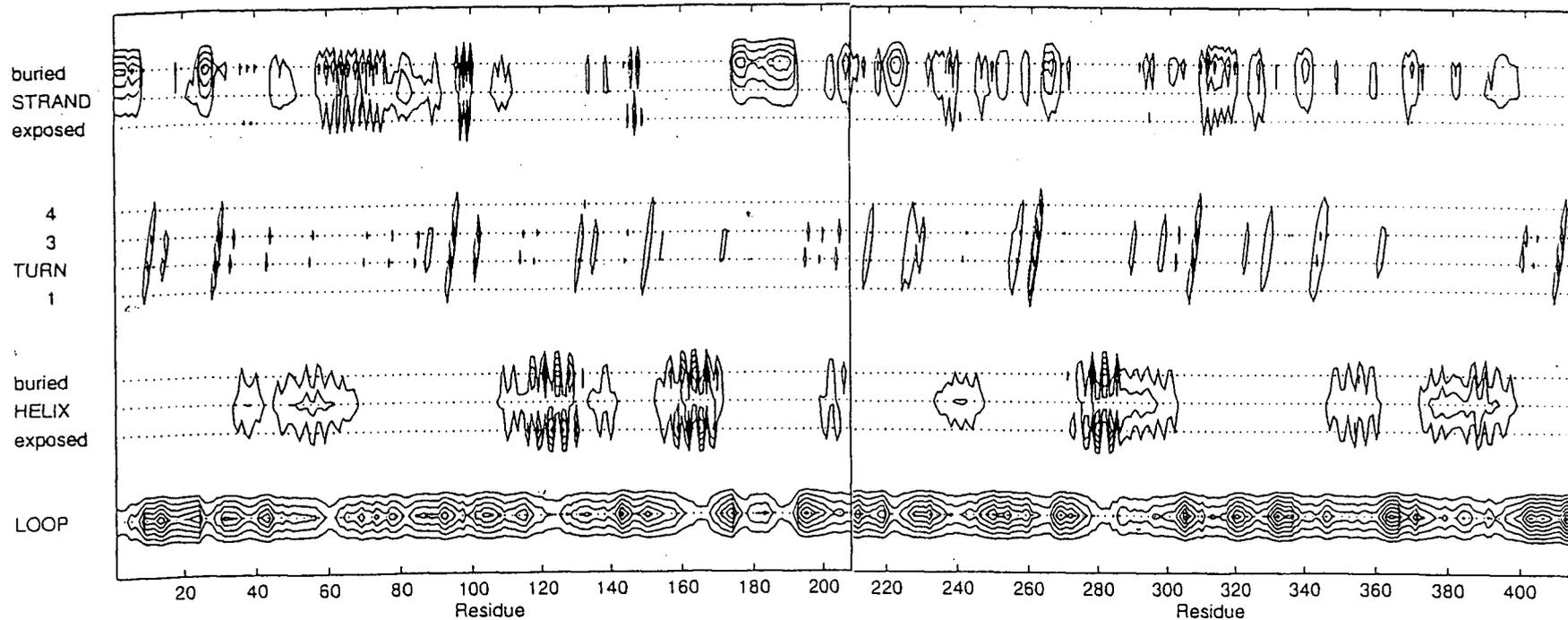
Figure: 17. Contour plot of secondary-structure probabilities for rabbit rLCAT.
Plots were generated by the Protein Sequence Analysis (PSA) System email server ,
psa-request@darwin.bu.edu. The contour lines designate probability increments of
0.1. Potential amphipathic alpha-helical domains with a probability of occurrence
greater than 0.5 were identified between residues 118-124, 158-170 and 276-289

Probability of being in a strand for rLCAT1-416 (psp3.m), 15-Mar-96 (2:1:1)

Probability of being in a strand for rLCAT1-416 (psp3.m), 15-Mar-96 (2:1:1)

Probability of being in a turn for rLCAT1-416 (psp3.m), 15-Mar-96 (2:1:1)

Probability of being in a turn for rLCAT1-416 (psp3.m), 15-Mar-96 (2:1:2)

Probability of being in a helix for rLCAT1-416 (psp3.m), 15-Mar-96 (2:1:0)

Probability of being in a helix for rLCAT1-416 (psp3.m), 15-Mar-96 (2:1:1)

Figure 18. Secondary structure probability distributions for rabbit rLCAT. Plots were generated by the Protein Sequence Analysis (PSA) System email server. The probability of a given residue (on the x-axis) of being in a strand, turn or helix (y-axus) is shown. Potential amphipathic alpha-helical domains with a probability of occurrence greater than 0.5 were identified, between aa 118-124, 158-170 and 276-289

72

2.5 Discussion

This chapter described the successful cloning of rabbit LCAT cDNA using inter-species consensus primers to reverse transcribe mRNA and utilize a PCR-based cloning strategy. This provided novel information regarding the major structural components of rabbit cDNA. It also facilitated a means by which the enzyme might be expressed through a transfected cell line for in vitro and in vivo studies to be described in the following chapters. In addition, the complete porcine LCAT cDNA was cloned, albeit not the initiator methionine and the following two codons in signal peptide, by screening a porcine liver λ-GT 11 library. Sequence data from the porcine clone was used to develop the consensus primers necessary for cloning rabbit LCAT cDNA.

The overall similarity at both the nucleotide and amino acid level of the rabbit and porcine enzyme with other mammalian LCATs, including that of human, mouse, rat, and baboon, is striking. For example, 91% of rabbit LCAT cDNA and correspondingly 93% of the amino acid sequence was identical to that of human LCAT. All major predicted structural components of the enzyme were conserved. The four predicted N-linked glycosylation sites found at positions 20, 84, 272 and 384 are found in identical positions in both the rabbit and porcine amino acid sequence. It is not known whether these sites are glycosylated in the rabbit, however, site directed mutagenesis studies indicate that this is the case in human rLCAT (O et al., 1993). Since the molecular weight observed in SDS-Page gel electrophoresis of the expressed rabbit rLCAT protein (see chapter 3) appears to be the same as human rLCAT, glycosylation of all four sites in rabbit rLCAT appears to be likely. The active Ser 181 of the catalytically active motif GXSXG found in a family of lipases is also conserved (positions 175-184). Ser-216 appears to inhibit LCAT activity when compared with mutant Ala→Ser216. This residue, which may have a regulatory role in LCAT activity, is also preserved. Additionaly, this conservation extends to all six

Table 9. Conservation among species for residues with mutants known to produce FED and LCAT deficiency

Codon	Structural Change	Phenotype	Conserved between species?
10	Pro→ Leu	FED	Yes
10	Pro→Gln	FED	Yes
10	Pro→ Frameshift	LCAT def.	Yes
16	Leu→ Stop	LCAT def.	Yes
32	Leu→ Pro	LCAT def.	Leu→Met, Rat
83	Tyr→ Stop	LCAT def.	Yes
93	Ala→ Thr	LCAT def.	Yes
119	Gly→ Frameshift	LCAT def.	Yes
123	Thy→ Ile	FED	Yes
131	Asp→ Asn	FED	Yes
135	Arg→Gln	FED	Yes
135	Arg→ Trp	LCAT def.	Yes
141	Gly Insertion	LCAT def.	Yes
144	Tyr→ Cys	FED	Yes
147	Arg→ Trp	LCAT def.	Yes
156	Tyr→ Asn	LCAT def.	Yes
158	Arg→ Cys	LCAT def.	Arg→ His, Baboon Arg→ Gly, Rabbit Arg→ Leu, Pig Arg→ Gln, Rat Arg→ Lys, Mouse Arg→ Gln, Chicken
183	Gly→ Ser	LCAT def.	Yes
209	Leu→ Pro	LCAT def.	Yes
228	Asn→ Lys	LCAT def.	Yes
244	Arg→ Gly	CAT def.	Yes
252	Met→ Lys	LCAT def.	Yes
293	Met→ Lys	LCAT def.	Yes
300	Leu deletion	FED	Yes
321	Thr→ Ile	LCAT def.	Yes
347	Thr→ Met	FED	Yes
375	Ile→ Frameshift	LCAT def.	Ile→ Thr, Rabbit Ile→ Thr, Pig Ile→ Thr, Rat Ile→ Thr, Mouse
391	Asn→ Ser	FED	Yes
399	Arg→Cys	LCAT def.	Yes

cysteine residues found in mammalian LCAT, although this thesis did not investigate whether the cysteines are bridged as has been determined in the human enzyme. The conservation of mammalian Cys residues extends to Cys 31, a site thought to be important to maintain LCAT activity but later shown to be nonessential through *in vitro* studies (Francone and Fielding, 1991). This was confirmed *in vivo* when the residue was found to be lacking in the chicken (Hengstschlager et al., 1995).

Of the mammallian species with known LCAT sequences, those most closely related phylogenetically (see Figure 15) also express CETP (human, baboon, rabbit). Pig, rat and mouse do not express CETP. Interestingly, these animals were more distantly related to human, baboon or rabbit by phylogenetic comparison of cDNA sequences although not necessarily by evolution of the species. As CETP and LCAT are found on chromosome 16, it is possible that genetic adaptation to CETP may be partially responsible for the preservation of LCAT sequence identity between species.

Nearly all amino acids in LCAT with known mutations have resulted in some form of altered esterification activity. Since LCAT natural mutations are scattered throughout the human LCAT amino acid sequence it would appear that most of the amino acid residues of the enzyme are essential for its function. Table 9 shows the degree of conservation between species for amino acids in which mutations are known to produce clinical LCAT deficiency or FED. The only three residues in which variation have been tolerated were natural mutations known in man. The mutants located at Leu-32 and Ile-375 appear to have produced either a conformational alteration or a frameshift mutation.

An exception is codon 158, a residue in LCAT where most animal species do not appear to have conserved amino acids. In 1993, Funke *et al.* reported a patient with familial LCAT deficiency in which two different mutations were present on each allele (Ala93→Thr, Arg158→Cys). To determine the cause of the phenotypic expression of LCAT deficiency in this patient, mutants were created individually and

in combination and expressed in COS-1 cells (Hill *et al.,* 1993). It was shown that the Ala93→Thr mutation produced a specific activity of less than 10% of wild type for both HDL-analogue and plasma substrates. Arg158→Cys, however, produced a specific activity of greater than 80% for both substrates when compared to the wild type. Among the species noted in table 9, codon 158 includes residues which are hydrophilic, hydrophobic and positively charged. It has been suggested that the Arg-158 residue may be located on the hydrophilic face within a predicted α-helix region between 156 and 169 (Klein *et al.,* 1993). Given the lack of conservation between species and the *in vitro* expression of the Arg158→Cys mutant which had similar activity to the wild type, it would appear that this residue does not have a major role in maintaining a hydrophilic face on an amphipathic α-helix.

The LCAT sequence for rabbit cDNA from this work was similar to that of Murata et al., but with some notable differences. Following a thorough examination of these differences at the cDNA level, I feel confident in the accuracy of the data presented here. Together with known sequence data, the data obtained through cloning porcine and rabbit LCAT cDNA in this thesis has provided useful information on specific regions of the enzyme that may be responsible for differences in substrate specificity and utilization between animal species. Furthermore, it has provided LCAT cDNA clones which were the foundation for the *in vitro* and *in vivo* work in the following chapters.

Chapter 3

CHARACTERIZATION OF

RECOMBINANT RABBIT AND PORCINE LCAT

3. CHARACTERIZATION OF RABBIT AND PORCINE rLCAT

3.1 Introduction

The purpose of the work described in this chapter was to demonstrate that the
LCAT cDNA clones isolated (as described in chapter 2) could be used to produce
active rLCAT by transient transfection of COS cells and stable integration into BHK
cells. In order to partially characterize the biochemical properties of these recombi-
nant enzymes, I have studied the ability of these proteins to esterify cholesterol in
both native and artificial substrates. In addition, I have studied the requirement of full
enzyme activity for apoprotein A-I.

3.2 Methods and Materials

3.2.1   Materials

COS-1 cells, an SV40-transformed African Green Monkey kidney cell line,
were purchased from the American Type Culture Collection (Rockville, Md.) Dr. Ross
MacGillivray, Department of Biochemistry, UBC kindly provided the BHK cells and the
pNUT vector (Funk *et al.,* 1990, Palmiter *et al.,* 1987). Tissue culture reagents,
including Dulbecco's Modified Eagle Medium (DMEM), fetal bovine serum (FBS) and
reduced serum medium (Opti-MEM$_{tm)}$ were purchased from Gibco-BRL (Mississauga,
Ontario). Methotrexate used in selecting transformants (Cyanamid Canada, Inc.,
Montreal, Quebec) was obtained in sterile saline from Children's Hospital Pharmacy.

3.2.2   Construction of Expression Vector

A short non-coding human cDNA sequence encoding for the LCAT ribosome
binding site was ligated onto the full-length rabbit LCAT cDNA in pUC 19 prior to
incorporation into an expression vector.   A unique NcoI site found in human LCAT
cDNA was preserved in the rabbit clone and the translated amino acid sequence was

identical well beyond this region. The NcoI restriction site is 26 bases downstream from the start codon and is situated within the region coding for a 24-base hydrophobic leader sequence. Comparison of human and rabbit LCAT indicates the leader sequence is identical for both species (see figure 16). The NcoI site was therefore used to ligate the human ribosomal binding site to the full-length rabbit LCAT cDNA. The completed cDNA in pUC 19 was then purified and digested with Xho I and Bam HI restriction enzymes to produce a cDNA insert . Following purification by Geneclean, the insert was ligated into a pNUT mammalian expression vector (Palmiter *et al.*, 1987) and the plasmid DNA transformed into competent bacterial cells. Following purification of the plasmid cDNA, both ends of the previously sequenced insert were sequenced again through the restriction site to confirm the correct orientation. The purified plasmid cDNA was then used to prepare transfections of mammalian cells. Stable transfections are induced through the presence of SV40 and mouse metallothionine promoters in the pNUT vector. The vector also allows the selection of stable transfected cells by their survival in high concentrations of methotrexate due to the presence of a mutant form of the dihydrofolate reductase (DHFR) gene (Funk *et al.*, 1990).

3.2.3 Eukaryotic Cell Culture

BHK and COS-1 cells were cultured in Dulbecco's Modified Eagle Medium (DMEM) supplemented with 10% fetal bovine serum (FBS). Prior to use, FBS was heat-inactivated at 56°C for 30 minutes. Cells were incubated in a humidified chamber in atmosphere containing 5% CO_2.

3.2.3.1 Transient transfection of COS-1 cells

COS-1 cells were transiently transfected using DEAE-dextran (Kriegler, 1990) with a pNUT expression vector containing rabbit or porcine LCAT cDNA. COS-1 cells

grown to 70-80% confluency in 60mm dishes were washed twice with transfection buffer (140mM NaCl, 1mM $CaCl_2$, 0.5mM $MgCl_2$, 3mM KCL, 0.9mM Na_2HPO_4 and 25mM Tris-HCl, pH 7.4). Approx. 7.6 μg plasmid DNA in 1.5mL warm DEAE-dextran (500μg/mL transfection buffer) were added, followed by incubation at 37°C for 30 minutes. The DNA/transfection solution was replaced by DMEM containing 10% FBS and 80μM chloroquine and the cells were incubated for 3 hours. The procedure was completed by incubating the cells in DMEM containing 10% dimethylsulfoxide (DMSO) at room temperature for 3 minutes. The cells were washed with transfection buffer, then incubated in DMEM containing 10% FBS for 12 hours. This was followed by incubation in serum-free medium (Opti-MEM$_{tm}$) for 48 hours.

3.2.3.2   Stable transfection of BHK Cells

Stable transfections were produced in BHK cells using coprecipitates of $CaPO_4$ and plasmid DNA (Kriegler, 1990). BHK cells were cultured to an approximately 50% confluent monolayer in a 100mm dish. Prior to transfection, approx. 5μg plasmid DNA in 450μL sterile dH_2O were added dropwise to 2X HEPES buffered-saline (40mM HEPES, 280nM NaCl, 10mM KCl, 1.5mM Na_2PO_4 and 10mM glucose, pH 6.96) while vortexing. 50μL 2.5M $CaCl_2$ were added in a similar dropwise manner and the calcium-phosphate DNA mixture was incubated at room temperature for 30 minutes. 1.0mL of the transfection mixture was added to the culture dish containing 9mL of DMEM/10% FBS. The cells were incubated overnight at 37°C at 5% CO_2. The cells, in transfection media, were selected over 10-14 days in DMEM/10% FBS containing 500μM methotrexate. Individual colonies surviving methotrexate selection were identified microscopically and transferred to 20mM culture wells. Cells were grown to confluency under methotrexate treatment and clones were screened for LCAT expression by exogenous enzyme activity assay.

3.2.4 Purification of recombinant rLCAT

Small-scale preparations of purified rLCAT were prepared by hydrophobic chromatography. A 0.5X9cm Phenyl-Sepharose column was equilibrated in 300mM NaCl/0.05M phosphate buffer, pH 7.4 at a flow rate of 0.5mL/min. Up to 40mL serum-free cell culture media from BHK cells expressing rLCAT were applied to the column at the same flow rate. The column was then washed with equilibration buffer until the absorbance at 280nm was less than 0.02. rLCAT was then eluted as a single peak in dH_2O.

3.2.5 Preparation of plasma and lipoproteins

Plasma was obtained from normal volunteers or laboratory animals by collecting 12 hour fasting blood samples in EDTA, followed by low speed centrifugation (1,200g for 20 minutes). Lipoproteins were isolated by sequential centrifugation, based on their relative buoyant density (VLDL = d<1.006 g/mL, LDL = 1.006<d<1.063 g/mL, or total lipoprotein-depleted plasma = <1.21 g/mL). The density of plasma solutions were adjusted using NaBr, and samples were ultracentrifuged using a Ti-75 rotor at 40,000rpm for 24 to 48 hours (for LDL/VLDL and HDL respectively).

3.2.6 Protein analysis
3.2.6.1 SDS-Polyacrylamide Gel Electrophoresis

Samples containing protein were mixed 1:1 with 2X SDS sample buffer (2% SDS, 40% glycerol, 0.1M Tris-HCl, pH 6.8) containing 1% bromphenol blue and 10% β-mercaptoethanol. Non-radiolabeled samples were run concurrently using commercial molecular weight markers (BioRad Laboratories). [14C]methylated protein molecular weight markers were used as standards for radiolabeled samples. Mixtures were boiled for 5 minutes, applied to a 10% polyacrylamide gel, and

electrophoresed at a 14mA/gel constant current for 45 minutes. Gels were stained for protein with Coomassie G250 (BioRad Laboratories, 0.1% w/v) in ammonium sulfate (8% w/v), phosphoric acid (1.6% w/v) in 20% methanol. Alternatively, gels containing radiolabeled proteins were fixed in methanol, then equilibrated with Amplify (Amersham Canada Ltd). Gels were dried onto Whatman 3MM chromatography paper. Autoradiograms were exposed for 16-72 hours using X-Omat AR film (Eastman Kodak.).

3.2.6.2   Quantitation of LCAT protein

Human LCAT was quantitated by solid-phase immunoassay. Samples containing serum-free cell culture medium (Opti-MEM$_{tm}$) were bound to nitrocellulose membranes (0.45μM pore size) using a BioRad slot blot apparatus. Human purified recombinant LCAT was included as standards. Following protein binding, the membrane was blocked with 5% non-fat dry milk in PBS at 37°C for 30 minutes. Polyclonal goat anti-human LCAT antibodies (obtained from Andreas Lacko, University of Texas) were diluted in PBS containing 0.5% non-fat dry milk. The mixture was added to the membranes and incubated overnight at room temperature. The membrane was then rinsed in PBS containing 0.02% Tween three times (5 minutes each), then reacted for 60 minutes with Protein G conjugated to horseradish peroxidase. The membrane was again washed three times, then developed in 50mL PBS containing 15mg $CoCl_2$, 25mg diaminobenzidine (Sigma Chemical Company) and 0.010mL 30% H_2O_2. The blots were scanned using a BioRad Video Densitometer (Model 620). The inter-assay coefficient of variation was 7.3% for a single protein measurement in nine separate assays.

The anti-human rLCAT antibody, however, does not cross-react with rLCAT from other species, in particular, the rabbit and porcine enzyme. To achieve compatibility between proteins of different species, total protein determinations were

performed on human, rabbit and porcine rLCAT with a BioRad protein assay kit using bovine immunoglobulin standards.

3.2.6.3 Immunoblot Analysis

Proteins separated by polyacrylamide gel electrophoresis were electroblotted onto nitrocellulose paper ($0.45\mu M$) in a water-cooled chamber containing blot buffer (20% methanol, 192mM glycine, 25mM Tris) for one hour. Sites not bound with protein were blocked using block buffer (5% non-fat powdered milk in PBS) for 30 minutes. The membranes were then incubated sequentially using polyclonal goat anti-human LCAT antibodies and Protein G-horse radish peroxidase to detect the specific protein.

3.2.7 Measurement of LCAT activity

3.2.7.1 Exogenous Substrates

LCAT enzyme activity was determined using synthetic HDL-like proteoliposomes containing apolipoprotein A-I, phosphatidylcholine and [^{3}H]-cholesterol. The radiolabeled liposome was prepared by ethanol injection of egg yolk phosphatidylcholine:cholesterol using the method of Batzri and Korn (1973). The liposome was added to human or rabbit apo A-I to produce a concentration of $7.5\mu g$ apo-AI, 4.66 nmol [^{3}H]-cholesterol ($0.03\mu Ci/nmol$), and 18.46 nmol phosphatidylcholine in 10mM Tris-HCL/150mM NaCl/5mM EDTA (pH 7.4). It was then preincubated for 30min at $37^{\circ}C$. 5mM β-mercaptoethanol and 1.5% essentially fatty acid-free bovine serum albumin were added to the substrate and the reaction started through the addition of either $15\mu L$ plasma, or $50\mu L$ transfected BHK cell culture media, $100\mu L$ COS-cell culture media or $10\mu g$ purified recombinant LCAT. Following incubation at $37^{\circ}C$, the reaction was terminated through the addition of 1.5mL ethanol. The time of incubation was determined empirically and varied according to the sample used. Following termination of the reaction, the precipitated protein was removed and the ethanol-lipid extract was separated by thin-layer

chromatography on silica gel layers incubated in petroleum ether:diethyl ether:acetic acid (70:12:1). The radioactivity of the isolated free and total cholesterol was determined by liquid scintillation spectrophotometry

3.2.7.2 Endogenous Substrates

The esterification activity of rLCAT was also estimated using substrates consisting of [^{3}H]-cholesterol labeled plasma or lipoprotein fractions. The substrates were prepared by heat-inactivation of the endogenous enzyme in plasma or lipoproteins as previously described. The substrates were then pre-equilibrated with [^{3}H]-cholesterol at 4°C according to the method of Dobiasova *et al.,* (1992). Purified rLCAT was added to the radiolabeled substrate (100-150 nmol unesterified cholesterol/mL), 1.5% essentially fatty acid free bovine serum albumin and 5mM β-mercaptoethanol. The mixture was incubated for four hours at 37°C. The reaction was ended by adding 2mL ethanol. Following centrifugation, lipids were removed from the protein precipitate. Unesterified cholesterol and cholesteryl esters were then separated by thin-layer chromatography and radioactivity counted by liquid scintillation. The esterification activity was expressed as nmoles of cholesteryl ester produced per hour per μg of rLCAT protein as determined by BioRad assay.

3.3 Results

3.3.1 Production of Recombinant LCAT in a transient expression system.

Cell culture media was collected 48 hours following transient transfection and assayed for LCAT activity. Controls included transient transfections utilizing human pNUT LCAT cDNA and vector lacking LCAT, labeled pNUT. Media were assayed in triplicate, and in the presence and absence of apo-AI. Immunoblot assays performed at this time showed that the rabbit LCAT did not cross-react with the goat anti-human LCAT polyclonal antibodies used to routinely assay human LCAT protein concentra-

tion. This finding, similar to previous experience in our laboratory with recombinant

porcine and mouse LCAT, suggests that the expressed enzyme was

nonhuman. As a result, however, it was not possible to determine the mass of

rLCAT secreted into the cell culture media. Results were therefore expressed as

moles cholesterol esterified per hour/mL cell culture media (see figure 19).
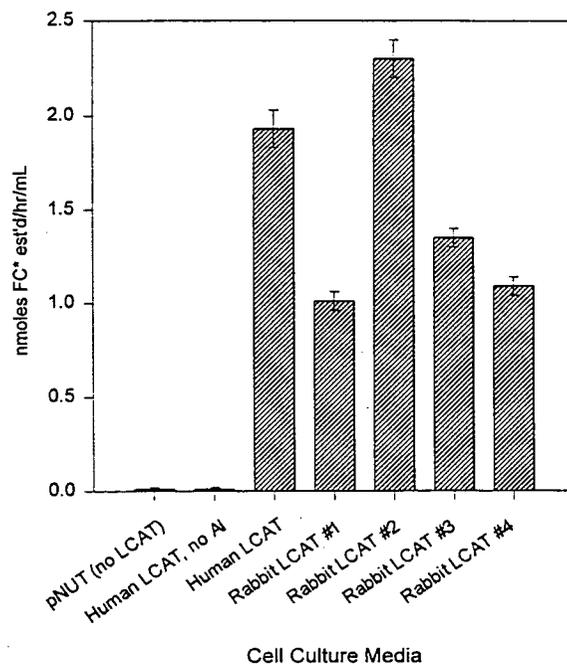
Cell Culture Media

Figure 19. LCAT activity in COS cell transient transfections. All transfected cells
secreted enzyme with esterification activity, expressed as nmoles free cholesterol
esterified per hour/mL cell culture media.   As with human LCAT, no esterification
activity was noted in the absence of apo A-I (data not shown). Assays were per-
formed in triplicate.

3.3.2   Expression of Recombinant LCAT in BHK cells

Following successful transient transfection, BHK cells were stably transfected with

recombinant rLCAT in pNUT. After approx. six weeks cell culture in methotrexate to

select and establish clones, serum-free cell culture media was collected and

assayed for LCAT activity as previously described. Results are shown below for five

clones screened for LCAT activity following 48 hour incubation in serum-free Opti-

MEM$_{tm}$. Assays were performed in triplicate. A human rLCAT control was not

85

transfected to prevent the possibility of cross-contamination of rabbit clones with human LCAT stable transformants. Negative controls included stable transfection of an empty vector and serum free media only (DMEM).
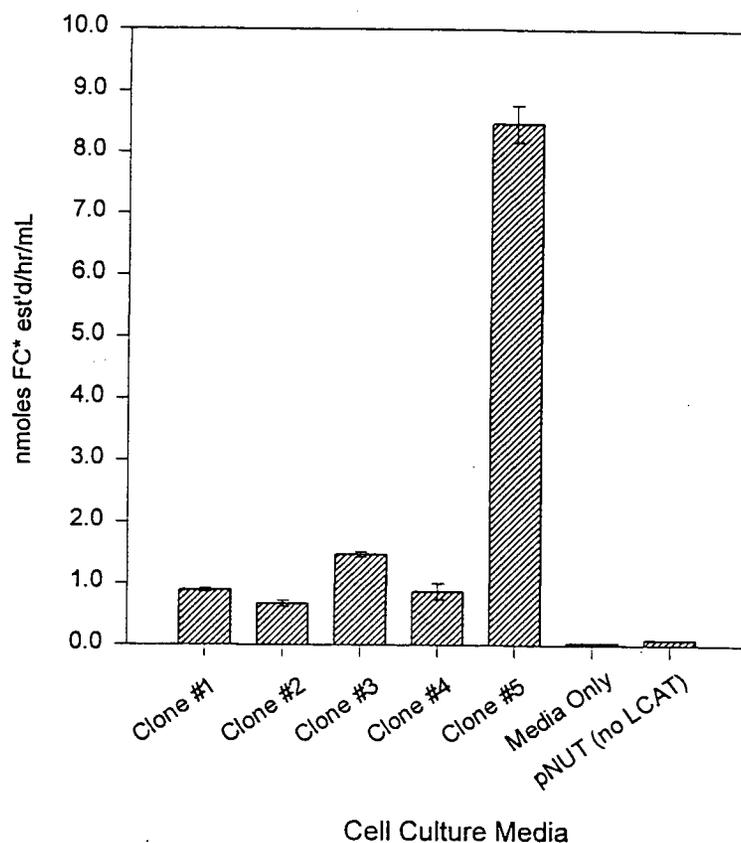
Figure 20. LCAT activity in BHK cell stable transfections. Five clones producing LCAT were assayed for cholesteryl esterification activity, measured as nmoles cholesteryl esters produced per hour per mL cell culture media following 48 hours of confluent growth. Of the clones assayed in the above transfection, clone 5 appeared to secrete rLCAT with relatively high esterification activity. Controls included LCAT activity assay of DMEM cell culture media and a stable BHK cell line transformed with an empty pNUT vector.

3.3.3   Purification of recombinant LCAT

Small-scale purification of human or rabbit rLCAT secreted into serum-free Opti-MEM$_{tm}$ cell culture media from the highest producing clones were collected following 48 hour incubation and were partially purified by phenyl sepharose

chromatography. A typical elution profile is shown in Figure 21. Larger scale purifications were utilized to obtain rLCAT in sufficient quantity for in vitro experiments and provided the data in table 10.
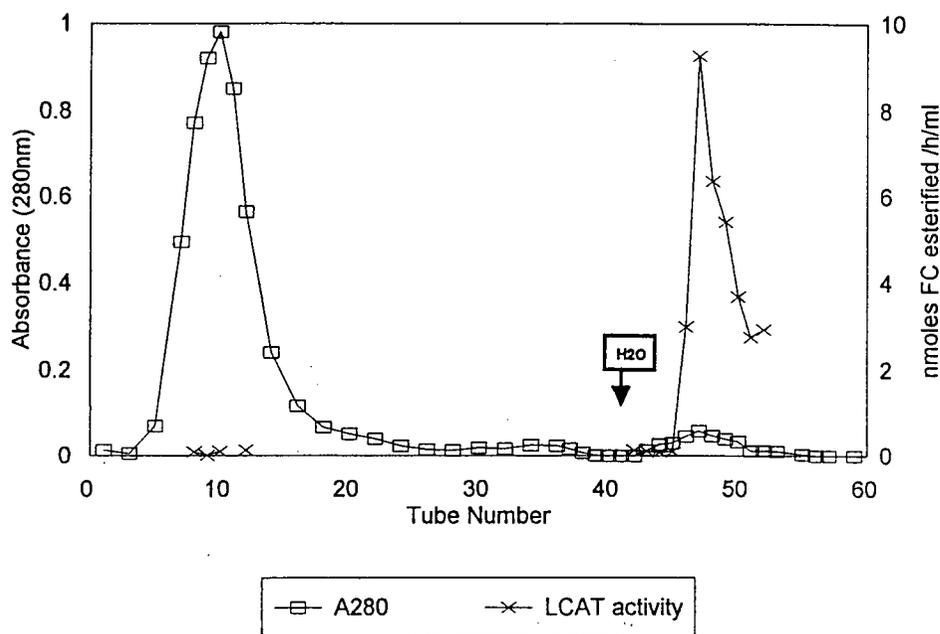
Figure 21. Elution profile of Phenyl Sepharose CL-4B chromatography. 10mL of serum-free cell culture medium containing human rLCAT secreted from BHK cells was applied to a phenyl sepharose CL-4B column (1.5X18cm) previously equilibrated with 0.3M sodium chloride in 0.005M potassium phosphate buffer (pH 7.4). The column was subsequently washed with buffer and the absorbance (280nm) monitored. When the absorbance fell below 0.01, rLCAT was eluted from the column in deionized water (see arrow). The LCAT activity expressed in nmoles cholesterol esterified per hour per mL was determined in each fraction. Virtually identical results were obtained for purification of rabbit recombinant LCAT.

The rabbit recombinant LCAT produced a single band when stained by Coomassie Blue G250 for protein following SDS-polyacrylamide gel electrophoresis, with an observed molecular weight between 64,000 and 67,000 (see figure 22). The results obtained were similar to those previously determined for purified human recombinant and native plasma LCAT. (O, *et al.* 1995; Marcel, 1982).

Table 10. Partial purification of rabbit rLCAT secreted by transfected BHK cells

Fraction	Volume (mL)	Protein (mg)	Specific Activity *(units/mg)	Purification (fold)	Yield (%)
Opti-MEM$_{tm}$ Culture Media	670	372	1.5	-	100
Phenyl-Sepharose eluent	20	9.8	47.5	32	83

3.3.4   Activation by apoprotein A-I

The major activator of LCAT is apoprotein A-I. Studies were undertaken to determine the amount of apo-AI required to obtain maximal activity for LCAT for the recombinant proteins expressed. Purified apo-AI obtained from human and rabbit plasma was titrated into equivalent protein concentrations (10ug/tube) of purified human or rabbit rLCAT. LCAT activity was then measured and expressed as nmoles FC esterified per hour per mL. Human and rabbit rLCAT produced similar activation curves with maximal activation of the enzyme reached for either species of apo-AI of approx. 10-20 ug per reaction tube. In contrast to the rabbit enzyme, porcine rLCAT was activated to a lesser degree than equivalent amounts of human rLCAT, using either human or rabbit apo A-I activating proteins. (see figures 23 and 24).
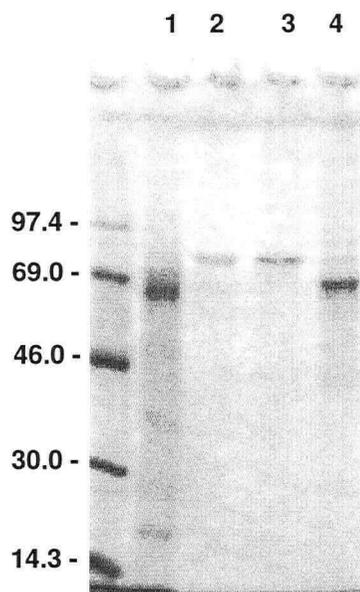
Figure 22. 10% SDS polyacrylamide gel electrophoresis of rabbit rLCAT. The gel was stained for protein using Coomassie Blue. Lane 1 is partially purified human rLCAT (MW=67,000 daltons) as a control. Lanes 2 and 3 are Opti-MEM$_{tm}$ cell culture medium containing transferrin (MW= 76,000-81,000 daltons) and rabbit rLCAT prior to loading the Phenyl-Sepharose column. Lane 4 is the pooled peak containing rabbit rLCAT following purification.
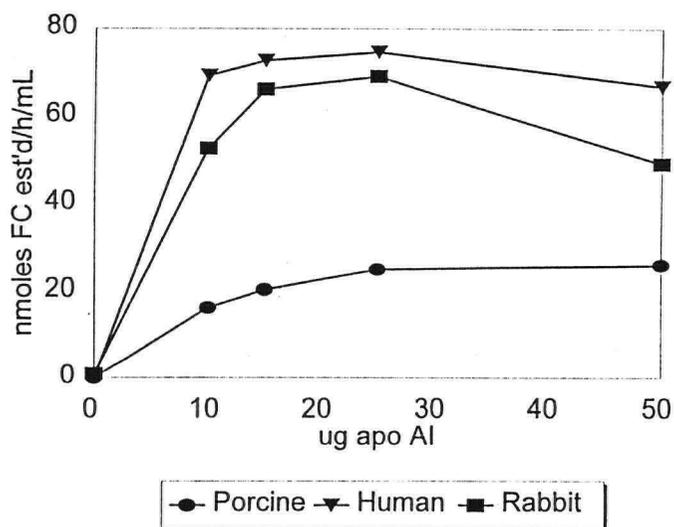
Figure 23. Activation of purified rLCAT by human apo A-I. Substrates used in the assay were single bilayer cholesterol:lecithin (1:4) vesicles. LCAT activity was determined using 10ug of porcine, human or rabbit rLCAT per tube and was expressed as nmol of cholesteryl ester produced per hour per mL. Data points are the means of triplicate assays during a single series of experiments.
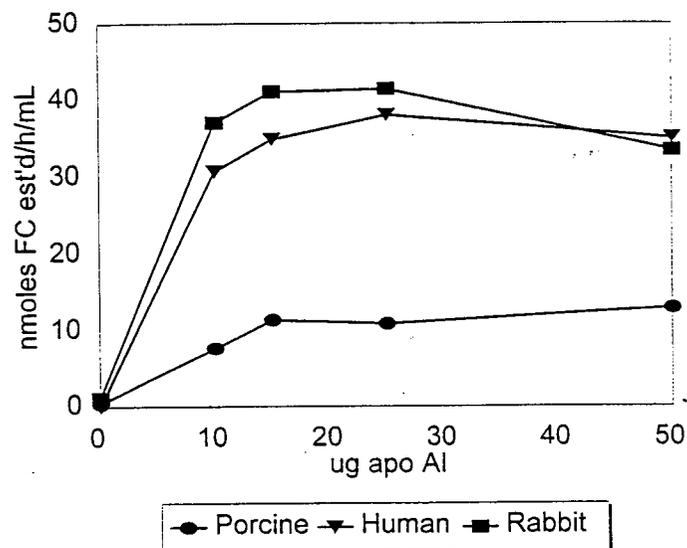
Figure 24. Activation of purified rLCAT by rabbit apo A-I. Substrates used in the assay were single bilayer cholesterol:lecithin (1:4) vesicles. LCAT activity was determined using 10ug of porcine, human or rabbit rLCAT per tube and was expressed as nmol of cholesteryl ester produced per hour per mL. Data points are the means of triplicate assays during a single series of experiments.

3.3.5 Immunoreactivity

As previously mentioned, purified rabbit and porcine recombinant LCAT failed to be detected by goat polyclonal antibodies raised against human LCAT using immunoblot (slot blot) assays. A western blot confirmed the non-reactivity of rabbit rLCAT using partially purified protein produced by transfected BHK cells (see figure 25).

Since several laboratories have reported difficulties in raising specific antibodies to this protein, efforts were were made to raise anti-rabbit IgY polyclonal antibodies in chickens. To date, double immunodiffusion screening experiments have failed to demonstrate presence of rabbit LCAT-reactive antibodies in chicken serum. Recent reports describing development of chicken-rLCAT antibodies using an anthranilate synthase-LCAT fusion protein have been described

(Hengstschlager-Ottnad E, *et al.,* 1995). This technique may prove useful in developing other species-specific anti-LCAT antibodies.

SDS PAGE (Coomassie Stain)   Western Blot (anti-human rLCAT antibody)

A   **B**
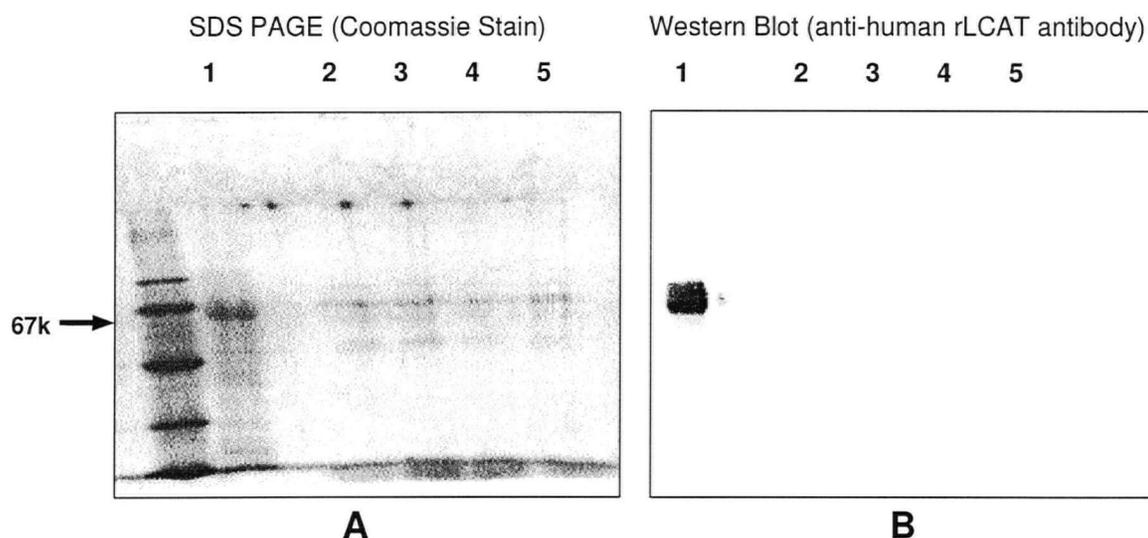
Figure 25. Western blot of rabbit rLCAT. Partially purified rabbit rLCAT was identically applied to lanes 2 to 5 on two separate 10% SDS polyacrylamide gels. Human rLCAT was applied to lane 1 as a control. The gels were then electrophoresed (see methods). Gel "A" was subsequently stained for protein by Coomassie Blue. A Western blot was performed on gel "B" using goat anti-human rLCAT antibodies. Only the human rLCAT (lane 1) produced a positive reaction.

3.3.6   Esterification activity of rLCAT

The enzyme activity of human and rabbit LCAT was studied using two substrates; a synthetic substrate with defined constituents, and species-specific plasma substrates. The apparent Km and Vmax of the enzyme reactions were estimated from double reciprocal plots in an attempt to numerically characterize variations in the ability of LCAT to esterify cholesterol between species.

3.3.6.1   Activity of recombinant LCAT in free cholesterol plasma substrate

The ability of LCAT to esterify cholesterol in an endogenous plasma substrate was compared between human and rabbit recombinant proteins using human or rabbit endogenous plasma substrates respectively. Similar quantities of rLCAT (10ug per

assay tube as determined by BioRad protein measurement) were added to increasing

amounts of free cholesterol which has been added to a heat-inactivated plasma .

A serum blank tube (no rLCAT) was included for each level of free cholesterol.

Results comparing the observed esterification rate and the amount of unesterified

cholesterol between human and rabbit proteins are shown in figure 26.   Similar

activity was observed for both human and rabbit rLCAT, with no apparent increase in

LCAT esterification activity in free cholesterol concentrations greater than approx.

120 nmols free cholesterol per ug LCAT. Since different substrates were used for

each enzyme, it was not possible to compare the kinetic rate constants derived from

these experiments directly.
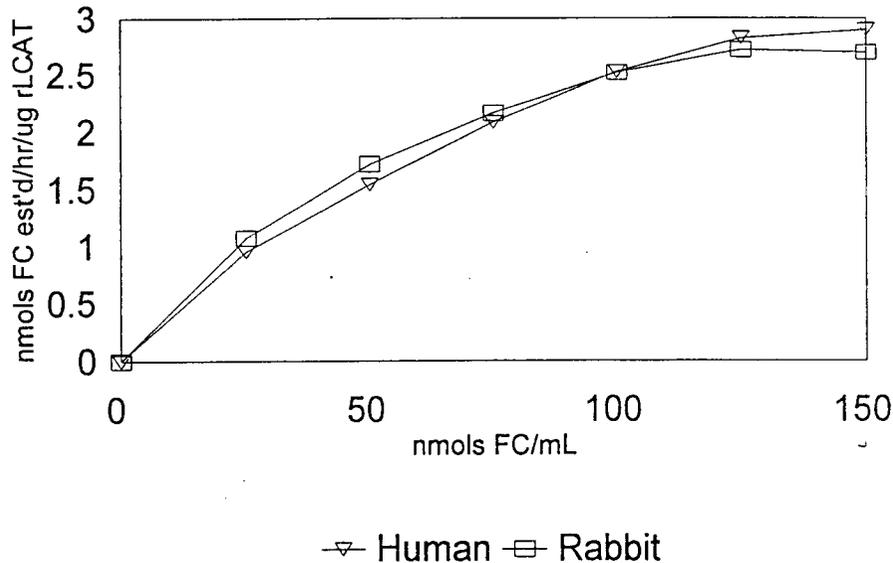
**Figure 26. Activity of rLCAT on free cholesterol (FC) in endogenous plasma
substrates.** Assays were performed using heat-inactivated native plasma substrates
pre-equilibrated with labeled and unlabeled FC to produce the final concentrations
shown. Into each reaction tube, containing rabbit or human plasma, was added 10ug
phenyl-sepharose purified rabbit or human rLCAT respectively and incubated as
described in section 2.6.7.2. Assays were performed in triplicate with the results
were expressed as nmols FC esterified per hour per ug rLCAT.

3.3.6.2   Activity of recombinant LCAT in synthetic liposome substrates

To compare the kinetic rate constants of human and rabbit rLCAT under defined conditions, LCAT activity was assessed using synthetic liposomes consisting of human apo-AI, free cholesterol and phospholipids. Rabbit apo-AI was not included as these experiments were designed to directly compare enzyme activity of each species on the same substrate. Results were plotted to compare LCAT esterification rate with free cholesterol substrate concentration (see figure 27). Utilizing similar quantities of human or rabbit rLCAT as in the endogenous plasma substrate experiments, maximal LCAT activity was reached at approximately 150nmol/mL free cholesterol. K_m and V_{max} were calculated from double-reciprocal Lineweaver-Burk plots in figure 28 and displayed on table 11.
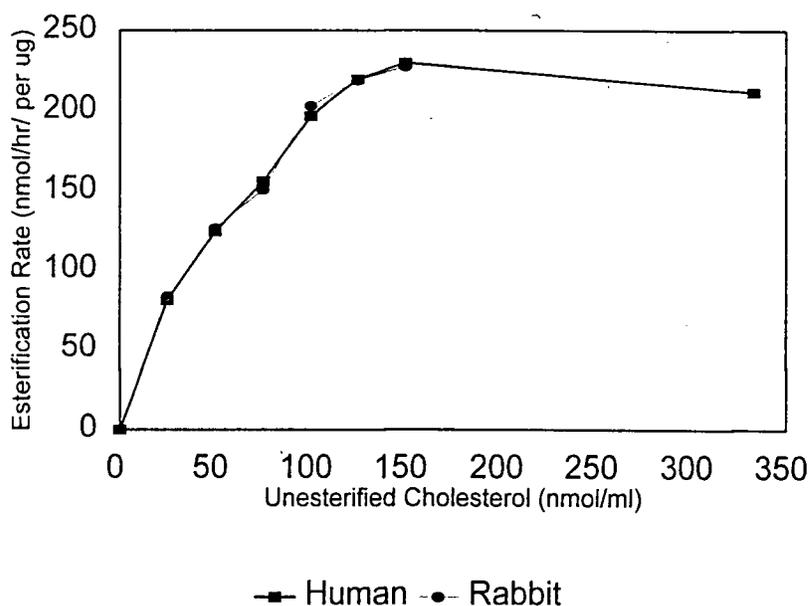
Figure 27. Activity of recombinant LCAT in liposome substrates. Assays were performed using single bilayer cholesterol:lecithin vesicles at FC concentrations given. To the reaction mixture was added human apo-AI and 10ug purified rabbit or human rLCAT (depending on the substrate) per assay. Results were expressed as nmols FC esterified per hour per ug rLCAT.
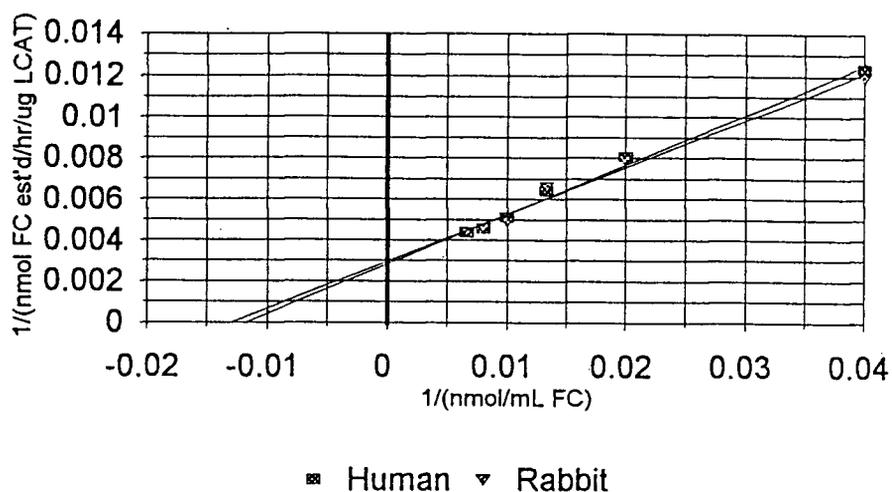
Figure 28. Lineweaver-Burk plot: kinetic rate constants of human and rabbit rLCAT esterification rate in synthetic liposome substrates. Data from this plot were used to calculate the apparent K_m and V_{max} shown in table 11.

Data obtained from the Lineweaver-Burk plot were used to calculate the K_m and V_{max} values from the x- and y-intercepts, respectively (see table 11).

	Human	Rabbit
K_m	85.1±13.2	76.9±11.7
V_{max}	351.7±38.5	335.4±47.9
V_{max} / K_m	4.13±1.12	4.36±1.26

Table 11. Kinetic rate constants of human and rabbit rLCAT esterification rate in synthetic free cholesterol plasma substrates. The apparent K_m is expressed as nmol/mL free cholesterol. Apparent V_{max} is expressed as nmol free cholesterol esterified/hr/ug LCAT. The difference between human and rabbit K_m and V_{max} is not statistically significant.

3.4 Discussion

There was a striking similarity between human and rabbit rLCAT in amino acid sequence homology, their ability to be activated by apo-AI, and in the apparent K_m and V_{max}. However, the two enzymes displayed marked differences in protein antigenicity. It is possible that differences in post-translational glycosylation result in antigenically distinct proteins. However, since the same COS and BHK cell lines were used to produce the human and rabbit recombinant protein, it is more likely that alterations in the primary or secondary structure of the protein are sufficient to prevent the anti-human polyclonal antibody from binding with the rabbit enzyme during immunoblot assays.

Observations using endogenous substrates suggest that both rabbit and human recombinant LCAT activity increases with increased availability of free cholesterol. It appears, therefore, that the capacity of both recombinant enzymes to esterify cholesterol is well above the plasma concentration of free cholesterol when the enzyme is added at physiological concentrations similar to native human LCAT in plasma. Since different enzymes are acting on essentially different substrates, these experiments should be interpreted with caution. Therefore, a direct comparison of the kinetic parameters of the endogenous assays for rabbit and human rLCAT is not possible.

To reduce, although not completely eliminate, confounding factors that may result in misinterpretation of kinetic data, enzyme assays were also performed using defined synthetic liposome substrates. The calculated K_m and V_{max} of the rabbit and human enzymes in these experiments were not statistically different, suggesting that the enzymes esterify cholesterol in a similar manner when presented with the same substrate and apo A-I activator. Km and Vmax of the LCAT reaction for various plasma and synthetic substrates vary considerably between laboratories. For example, the Km and Vmax for native HDL was reported by Fournier *et al.* (1995) to

be 51.1 ± 4.2 μM and 12.9 ± 2.4 nmol/mL/h, respectively. Increasing the cholesterol content in homogeneous recombinant HDL increased the apparent Km from 0.5 to 3.5μM cholesterol and the apparent Vmax increased from 3.1 to 9.2 nmol cholesteryl esters produced per hour per unit of LCAT (Sparks *et al.,* 1995). These differences in kinetic parameters are likely due to different lipid binding properties of diverse apolipoproteins and peptides. Results, therefore, between laboratories are often not comparable (Jonas, 1991).

Further analysis to determine the effect of either rabbit or human apo A-I on the enzyme using similar proteoliposome substrates to those derived for the kinetic data indicates that the two enzymes are indeed similarly activated by apoproteins from either species. All three species studies showed increases in dose-dependant esterification activity in the presence of apo A-I, indicating esterification is dependent on the characteristically LCAT-specific interaction of these recombinant enzymes and this apoprotein. The rabbit and human recombinant enzymes, however, appear to esterify cholesterol more effectively using their native apoprotein activator. Although activated by the rabbit and human apolipoproteins, a similar amount of the porcine recombinant enzyme produced approx. 30% lower esterification activity.

In summary, the data presented in this chapter demonstrates that the full length cDNA clone for rabbit LCAT was used to produce recombinant LCAT through transient transfection of COS cells and stable integration into BHK cells. The result-ing recombinant LCAT was capable of esterifying cholesterol in heat inactivated plasma and defined HDL-analog substrates. Furthermore, apo A-I was required for full activity. These observations demonstrated that the rLCAT is similar to plasma LCAT and that it was a suitable model to study the metabolism of LCAT *in vivo* in the next chapter.

Chapter 4

METABOLISM OF RECOMBINANT LCAT

IN VIVO

4. METABOLISM OF RECOMBINANT LCAT *IN VIVO*

In order to utilize the recombinant rabbit LCAT described in chapter 3 for metabolic studies *in vivo,* two basic questions needed to be answered: Can we prepare radiolabeled rLCAT that has full enzyme activity? And does the recombinant enzyme display similar lipoprotein binding characteristics to that of the native protein? The use of the radiolabeled rLCAT is required to provide sufficient sensitivity for *in vitro* lipoprotein binding and *in vitro* metabolic turnover studies. This requires incorporation of a radiolabeled tracer into the enzyme in such a manner that it does not alter the basic enzymatic properties of the protein.

Two approaches were used to create a radiolabeled protein. The first approach utilized the incorporation of $[^3H]$-Leu into the enzyme by BHK cells during protein synthesis. This method provided a useful technique to add a tracer to a protein with little effect on the specific enzyme activity or its physical characteristics. While rabbit LCAT cDNA was being cloned and sequenced, initial binding studies of recombinant LCAT were performed using the human recombinant protein. These early studies in the association of the recombinant protein included human rLCAT associated with both human and rabbit plasma lipoproteins utilizing Superose-12 size exclusion chromatography and sequential ultracentrifugation at buoyant densities designed to separate lipoproteins. When the rabbit recombinant protein was expressed in stable cell lines, further work on the binding and activity of rLCAT was performed using both human and rabbit rLCAT utilizing ultracentrifugation and 0.5 Mesh Biogel size exclusion chromatography. The latter technique provided greater discrimination between larger HDL subfractions and albumin found in native plasma.

The second approach was to radiolabel the enzyme with $[^{125}I]$ which, due to its short half-life and relatively high specific radioactivity, provides a useful tool for *in vivo* metabolic turnover studies. All methods involving iodination, however, are based on chemical modification of a purified protein. Experience of our own and of other

groups involved in LCAT research has shown that LCAT enzymatic activity is particularly sensitive to the more common methods of iodination, including the use of chloramine-T and the Bolton-Hunter reagent. In this thesis, a third approach, Iodo-beads$_{tm}$ (Pierce Chemical Company) was employed. This method is somewhat gentler than chloramine-T as the oxidizing agent is immobilized, limiting direct contact with the protein.

4.1 Radiolabeling of rLCAT

4.1.1 Methods and Materials

4.1.1.1 Materials

Radiolabeled reagents including [^{3}H]-Leu and Na[^{125}I] were obtained from Amersham Canada Ltd or from New England Nuclear. Leucine-deficient DMEM was obtained from Gibco BRL. Iodobeads$_{tm}$ used in radiodination reactions were purchased from Pierce Chemical Company.

4.1.1.2 Radiolabeling: Incorporation of [^{3}H]-Leu into rLCAT expressed in BHK cell stable transfections

Two 10cm cell culture dishes containing BHK cells expressing rLCAT were grown to 80% confluency in DMEM/FBS/PSF. Just prior to radiolabeling, cells were washed X2 in 3mL serum-free, leucine-deficient DMEM/PSF (DMEM-Leu). Serum-free DMEM-Leu (5 mL) was added to each dish and cells were incubated at 37°C/5% CO_2 for 20 minutes. The medium was then removed and 2mL DMEM-Leu was added. Cells were then radiolabeled using 100μCi [^{3}H]-Leu per dish for 45 minutes, rocking the cells every 15 minutes to ensure cells were adequately exposed to fresh medium. At the end of the incubation period, 8mL DMEM-Leu were added (for at total of 10mL media) and cells were incubated for a further 48 hours. Approx. 9.5mL culture media containing both residual free [^{3}H]-Leu and [^{3}H]-rLCAT secreted

by LCAT-producing BHK cells was then collected and purified by phenyl-sepharose chromatography as previously described, but using a 0.8 X 10cm column with a flow rate of 0.12 mL/min. The elution profile for human [^{3}H]-Leu rLCAT is shown in figure 29. The rabbit rLCAT, obtained and purified under identical conditions, produced a similar profile. Total recovery, based on LCAT esterification assays of eluted fractions, showed approx 89% of LCAT activity to be recovered from the eluted dH$_2$O peak fraction, when compared to the cell culture medium. There was no detectable tritium in the TCA precipitates, indicating that the high levels of radioactivity observed in the 0.3M salt wash were largely due to unincorporated [^{3}H]-Leu. Efficiency of [^{3}H]-Leu incorporation into LCAT was approx. 1-2% when compared to the total [^{3}H]-Leu applied to cell culture.
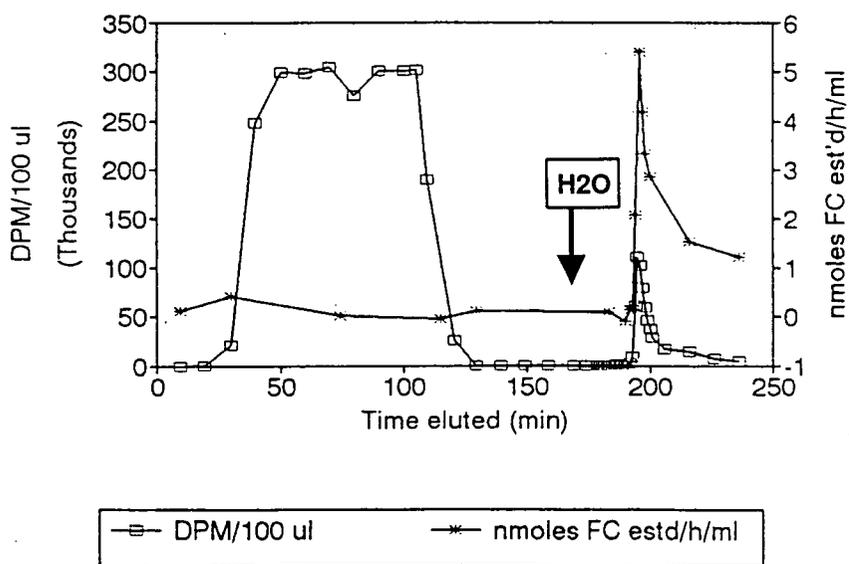
Figure 29. Phenyl-Sepharose CL-4B purification of human [^{3}H]-Leu rLCAT.
Radioactivity (left y-axis) and LCAT esterification activity (right y-axis) of eluted fractions versus elution time. Cell culture media was applied then washed in 0.3M NaCl 0.005M sodium phospate, pH 7.4 until eluted fractions produced an absorbance of less than 0.01 and radioactivity reached background levels. LCAT was subsequently eluted in dH$_2$O (see arrow).
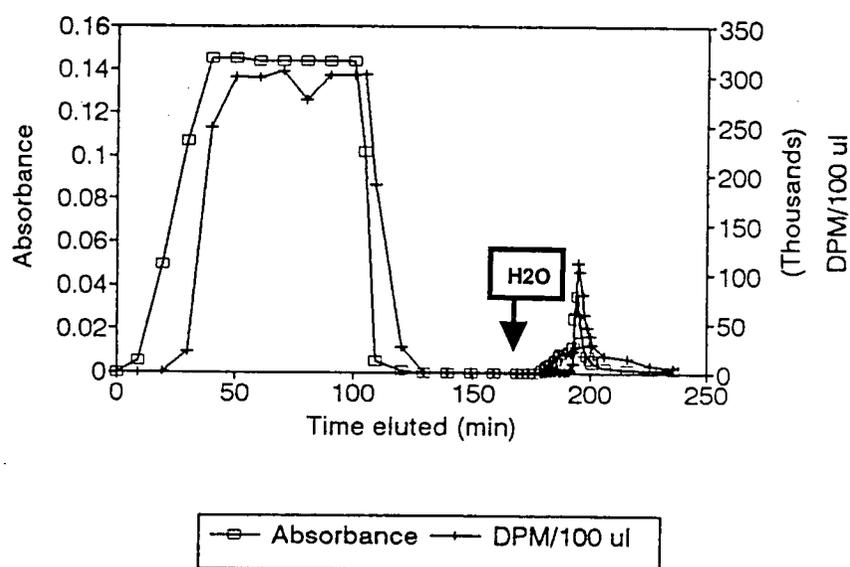
Figure 30. Phenyl-Sepharose CL-4B purification of human [³H]-Leu rLCAT (cont). Absorbance at 280nm (left y-axis) and Radioactivity (right y-axis) of eluted fractions versus elution time.

	Volume (mL)	LCAT Mass (μg/ mL)	LCAT Activity (units/ mL)	Spe-cific Activity (units/ μg)	Mass/ Sample (μg)	Yield (%)	DPM/ ug
DMEM culture media	8.90	0.35	6.10	17.42	3.12	-	-
Pooled Peak	2.25	1.02	9.78	9.58	2.30	73	730366

Table 12. Human [³H]-rLCAT purification from BHK cell culture media. LCAT mass was measured using immunoblot assay (slot blot) using goat anti-human polyclonal antisera. LCAT activity was measured using single bilayer cholesterol:lecithin proteoliposome substrates containing apo A-I, measured as nmols FC cholesterol esterified per hour (one unit) per mL, from which was calculated the specific activity, as nmols FC cholesterol esterified per hour (one unit) per μg. Percent yield was calculated based on the total LCAT mass by immunoblot.

101
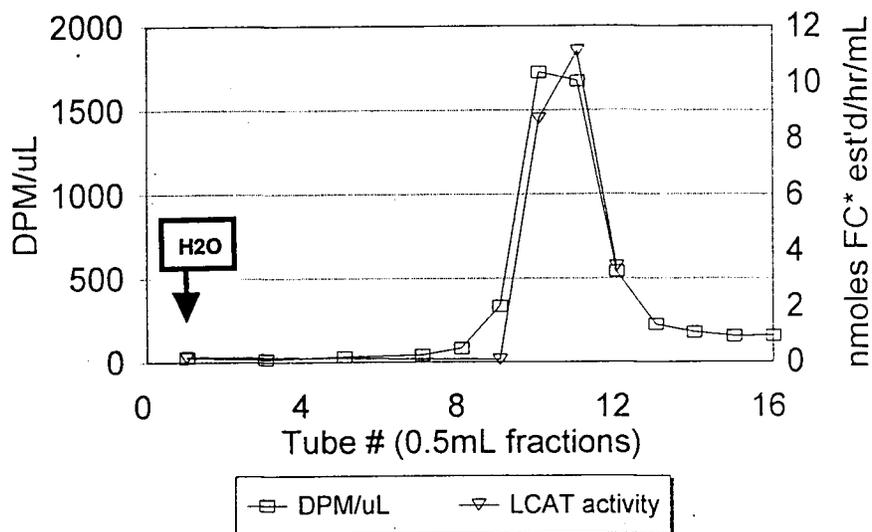
Figure 31. Phenyl-Sepharose CL-4B purification of rabbit [³H]-Leu rLCAT.
Radioactivity (left y-axis) and LCAT esterification activity (right y-axis) of eluted fractions is compared versus elution time. The 0.3M NaCl wash is not shown in this profile. The rabbit rLCAT, with cholesterol esterification activity closely following the radioactivity peak is eluted shortly after the buffer has been changed to dH_2O (see arrow).

Results indicate that endogenously radiolabeled rLCAT derived from either species may be produced and purified with retained esterification activity and sufficiently high specific radioactivity for further biochemical analysis.

SDS-polyacrylamide gel electrophoresis of tritiated rabbit rLCAT, stained for protein by Coomassie Blue showed a single band with a calculated molecular weight of approximately 67,000 daltons To provide a more sensitive estimate of the relative purity of the radiolabeled protein, an autoradiograph was made of the SDS-polyacrylamide gel following electrophoresis as descibed in section 3.2.6.1. Results are shown in figure 32 following 48 hour exposure to the film.
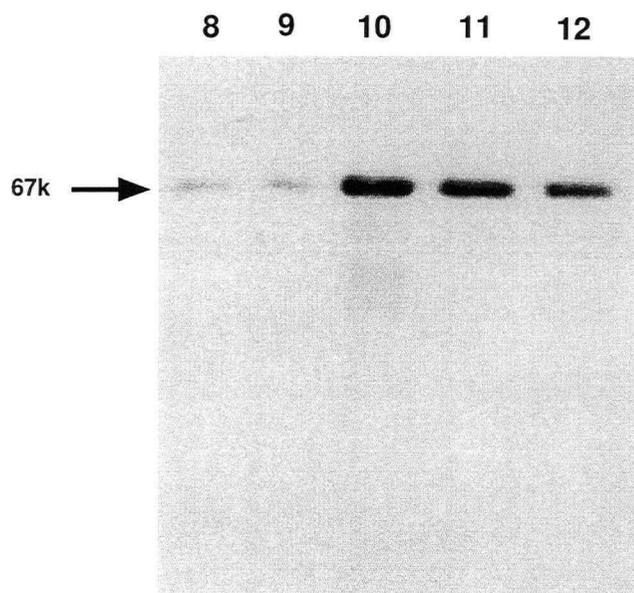
Figure 32. Autoradiograph of purified rabbit [³H]-rLCAT. SDS-polyacrylamide gel electrophoresis was applied to rabbit rLCAT sample tubes eluted in figure 31 and exposed to autoradiograph film for 48 hours following equilibration in Amplify$_{tm}$ (Pierce Chemicals). Lane number refer to fraction tubes in figure 31.

4.1.1.3 Radiolabeling: Iodination of rLCAT

4.1.1.3.1 Conjugation reaction using Iodobead$_{tms}$

Prior to iodination, purified rLCAT was concentrated to 220-260μg/mL using a Centricon$_{tm}$ 10 filter previously pre-equilibrated with 1% BSA. One Iodobead$_{tm}$ (oxidative capacity 0.55μmol/bead) was rinsed twice with phosphate buffered saline, dried on filter paper and placed in a reaction tube. The bead was covered with buffer and allowed to react with 1μCi [¹²⁵I] for five minutes. 1.5mg rLCAT was added and the reaction was continued on ice for five to fifteen minutes at 4°C. The protein was then separated from the Iodobead$_{tm}$ to halt the conjugation reaction and placed in a separate tube. To the radiolabeled reaction mixture was added freshly obtained 1% rabbit plasma in 1XPBS. The radiolabeled rLCAT was finally separated from free [¹²⁵I] using a Sephadex G25 size exclusion column by elution in PBS containing 1% rabbit plasma. Purity of the radiolabeled protein was tested by gamma counts of TCA pre-

cipitates vs supernatant 10% SDS PAGE autoradiography. LCAT esterification activity was measured using a proteoliposome substrate.

Figure 33. SDS-Page Autoradiograph of rabbit [^{125}I]-rLCAT. [^{125}I]-labeled rLCAT was electrophoresed in a 10% SDS polyacrylamide gel following purification by using a Sephadex G25 size exclusion chromatography. The radiolabeled protein was visualized by autoradiography. Unbound [^{125}I], seen in the low-molecular weight band at the base of the gel, indicated by the arrow, was less than 10% of total TCA-precipitable counts.

4.2   Characterization of radiolabeled rLCAT

4.2.1   Esterification activity of radiolabeled rLCAT

The ability of [^{125}I]-rLCAT and [^{3}H]-rLCAT to esterify cholesterol was determined using proteoliposome analogs of HDL containing [^{3}H]-cholesterol, apolipoprotein A-I and phosphatidylcholine. The radiolabeled substrate and esterified products were separated from radiolabeled LCAT by protein precipitation using abso-

lute ethanol followed by thin layer chromatography. Blank assay tubes containing only radiolabeled protein showed only background counts when assayed for free and esterified [3H]-cholesterol. LCAT esterification rates were markedly affected by the oxidative effects of the iodination reaction. Although the method published by Pierce Chemicals suggests some proteins can withstand Iodobead$_{tm}$ iodination for as long as one hour, a timed series of experiments exposing 100μg rLCAT to non-radiolabled iodine together with one Iodobead$_{tm}$ in a 10X75mm tube indicated that as little as five minutes exposure markedly affected esterification activity (see figure 34).
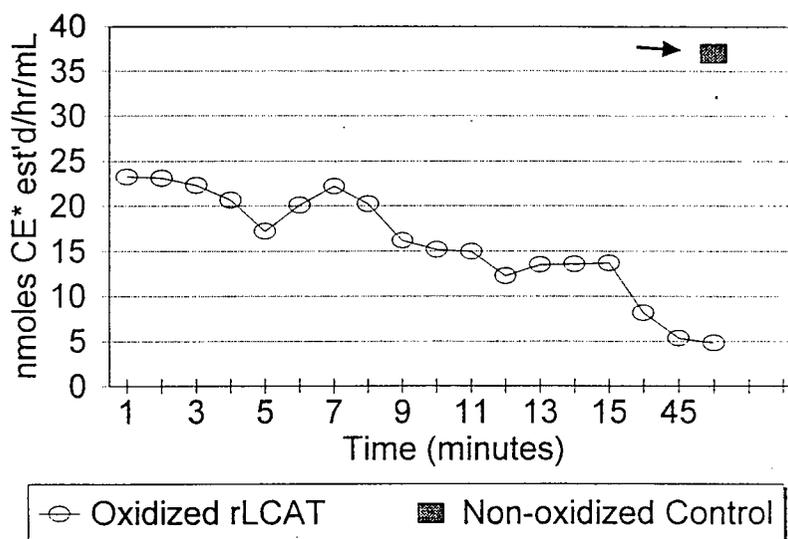
Figure 34. Effects of oxidation on LCAT esterification by exposure to Iodobeads$_{tm}$ (Pierce Chemicals) over time . Purified human recombinant enzyme was subjected to Iodobead$_{tm}$ oxidation over a period of one hour. Following exposure, aliquots were placed on ice then assayed for LCAT esterification activity. Data points are the mean of triplicate assays. A non-oxidized control, left on ice in the absence of an Iodobead$_{tm}$, is shown at 50 minutes (see arrow)

LCAT esterification activity was preserved in [3H]-rLCAT at levels equivalent to the non-radiolabled form (see table 12). However, purified rabbit [3H]-rLCAT, produced under similar conditions, appeared to esterify cholesterol at rates approximately one tenth of that seen with human [3H]-rLCAT. This was expected as previous observations indicated that BHK cell cultures appeared to secrete rabbit rLCAT at significantly lower levels (approx. 30%) compared to the human recombi-

nant protein. Due to the low protein concentration, and the lack of a rabbit-reactive LCAT antibody, it was not feasible to make a direct comparison of the radiolabeled enzyme specific activity compared to that of the human. Comparisons of the purified enzyme esterification rate when using different concentrations of apo A-I and choles-terol substrates, however, suggest that differences in the esterification rates in the secreted cell lines are due to decreased levels of production rather than an effect of the rabbit protein itself.

4.2.2 Binding to lipoproteins *in vitro*

It has been known for some time that native plasma LCAT is both physically and functionally associated with apo A-I containing particles (Pritchard *et al.,* 1988). An important consideration in determining the utility of recombinant LCAT for *in vivo* metabolic studies, and potentially in treatment of LCAT deficient patients is to deter-mine whether differences exist in rLCAT binding to lipoproteins compared to the native protein. Three approaches were taken using classic methods of separating lipoproteins in vitro.

4.2.2.1 Superose 12 chromatography.

Initial studies were performed using human [^{3}H]-rLCAT preincubated with plasma lipoproteins, followed by isolation of lipoprotein constituents using Superose 12 size-exclusion chromatography. This column was chosen due to its theoretical ability to resolve proteins with molecular weights over the range of 1000 to 150,000 daltons. Calibration of the column using defined lipoprotein standards demonstrated that it could resolve HDL from LDL and potentially larger HDL particles from albumin.

To determine if [^{3}H]-rLCAT was able to associate with human and rabbit lipoprotein constituents, both lipoprotein fractions from both species were prepared. Total lipoproteins were obtained through adjusting the plasma to a density of 1.25

g/mL using solid NaBr followed by ultracentrifugation for 48 hours at 42000rpm in a 50.3Ti rotor. The upper layer containing lipoproteins was washed in NaBr solution (d=1.25g/mL) and a portion dialyzed in Tris/NaCl (150mM NaCl, 10mM Tris/HCl, 0.3mM EDTA, 4.6mM NaN$_3$). The lipoprotein fraction (200μL) was then incubated with human [^{3}H]-rLCAT (60μL) for 60 minutes at 37°C and applied to the column in the same buffer at a flow rate of 0.95 mL/min. 700μL of each eluate was counted by liquid scintillation and the results plotted together with the absorbance (280nm) pro-file. (figure 35 and 36). Human [^{3}H]-rLCAT applied with and without rabbit plasma produced similar results. Previous calibration of the column showed that LDL and VLDL elutes as a single sharp peak, essentially in the void fraction. HDL was clearly separated from LDL and VLDL and appears as a broad absorbance peak. Since we know from published data (Pritchard *et al.,* 1988) that plasma LCAT is closely asso-ciated with HDL, one would expect to find the majority of radiolabeled LCAT to be associated with HDL. It was not possible, however, using this particular column, to determine whether a portion of rLCAT is bound to smaller HDL particles that cannot be resolved by the Superose column. A more important drawback, however, is due to the inability of the column to resolve serum albumin from HDL, particularly smaller subfractions. The result (not shown) is an apparent coelution of [^{3}H]-rLCAT with albumin when whole plasma is used.
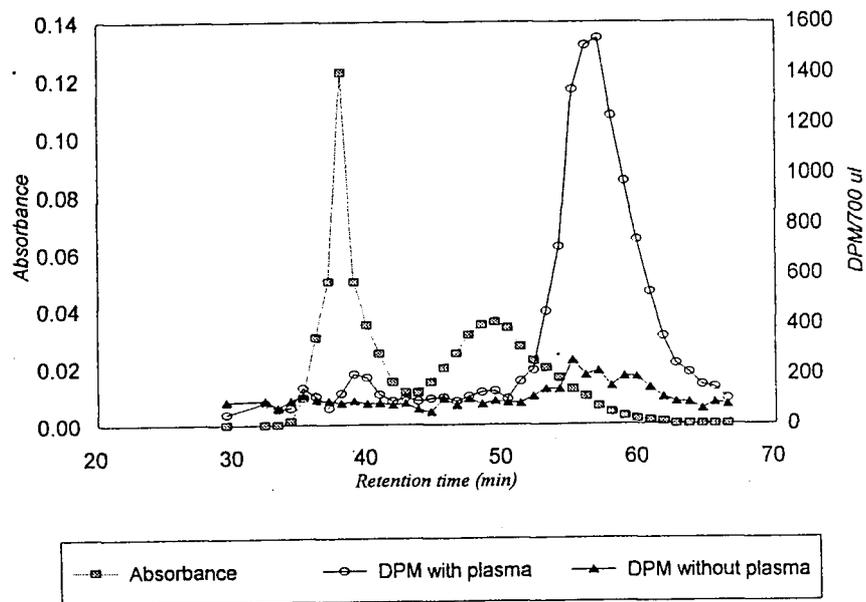
Figure 35. Elution of human plasma lipoproteins with [³H]-Leu human rLCAT by Superose 12 chromatography. Two elutions are shown on each graph, the first in which [³H]-rLCAT is incubated with plasma and the second in which [³H]-rLCAT was introduced directly into the column. Calibration of the column with individual lipoprotein fractions indicates the first absorbance peak (280nm) with a retention time of approx. 38 minutes is a mixture of VLDL and LDL. The second, broader peak with a retention time of approx. 49 minutes is HDL. The majority of [³H]-rLCAT incubated with plasma appears to elute together with either the smallest subfractions of HDL or it eluted as an unbound protein. In the absence of plasma proteins, most [³H]-rLCAT bound to the column and did not elute until the ionic strength of the column had been decreased with 40% ethanol.
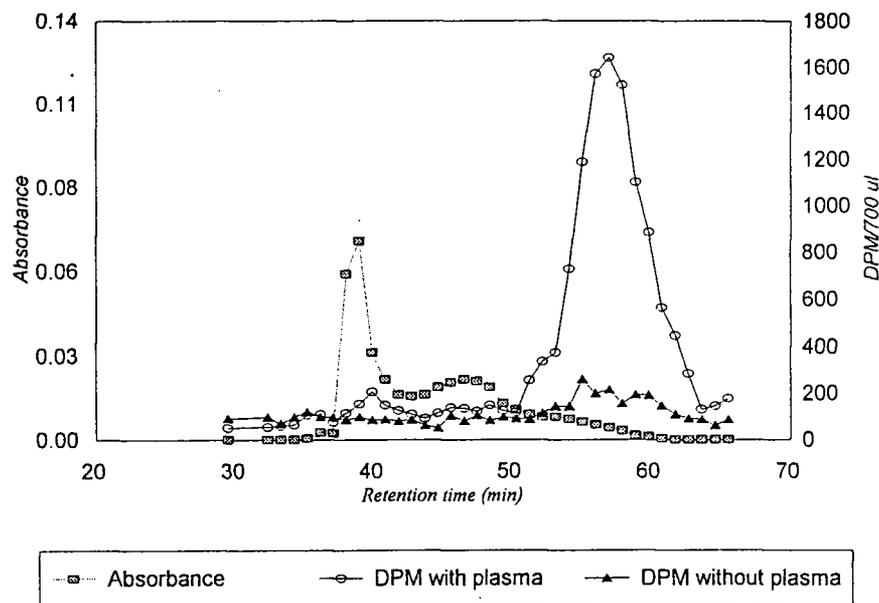
Figure 36. Elution of rabbit plasma lipoproteins with [³H]-Leu human rLCAT by Superose 12 chromatography Analytical conditions were identical to those of figure 35.

4.2.2.2   Ultracentrifugation

Ultracentrifugation has been used both to separate major lipoproteins and to isolate protein constituents associated with these lipoproteins, based on their buoyant density. The following experiments set out to determine whether rLCAT co-migrated into the same region as native plasma LCAT under ultracentrifugation conditions at given adjusted densities. Initial studies utilized human rLCAT. These were followed by similar studies with rabbit rLCAT after it became available through cloning and expression of the enzyme.

In the first experiment, plasma (human or rabbit) was preincubated with radio-labeled rLCAT at either 37°C for 60 minutes or overnight at 4°C. The plasma density was then adjusted to d=1.25g/mL using solid NaBr and ultracentrifuged at 42000rpm in a 50.3Ti rotor for 48 hours. On completion, seven equal fractions were carefully removed from the ultracentrifuged tube, beginning with #1, seen in figure 37. LCAT esterification activity was measured in each fraction. The highest activity was found in the most buoyant fraction, tube #1. At d=1.25 g/mL, this fraction includes HDL, LDL, VLDL and chylomicrons but excludes albumin. The results indicate that the highest [^{3}H]-rLCAT radioactivity is found in the most dense fraction. It is likely that the small amount of LCAT esterification activity noted in the bottom tube is due to the presence of [^{3}H]-rLCAT. This suggests that the recombinant LCAT has not associated with HDL in a similar manner to that of native HDL under these experimental conditions.

These results were further confirmed when [3H]-rLCAT, preincubated with human or rabbit plasma under the same conditions as above, were ultracentrifuged at d=1.21 g/mL (figure 38). At this density under ultracentrifugation, chylomicrons, VLDL, LDL and HDL2 will float to the uppermost fraction. However, native LCAT in denser HDL subfractions will become disassociated with larger HDL pool. This results in an LCAT (and CETP) enriched layer essentially free of other lipoproteins or albu-

min, located approximately in the middle third of the ultracentrifuge tube. Our results indicate that LCAT esterification activity is present in this region, appearing the highest in tubes 3 and 4. The [^{3}H]-rLCAT radioactivity, however, remained localized in the bottommost tube.

Similar results were obtained with rabbit rLCAT, radiolabeled with [^{125}I] and incubated in albumin-deficient rabbit plasma (figure 39). The upper layer containing lipoproteins was washed in NaBr solution (d=1.25). An aliquot was then dialyzed in Tris/NaCl (150mM NaCl, 10mM Tris/HCl, 0.3mM EDTA, 4.6mM NaN$_3$ to remove excess salt. In these experiments, rabbit plasma was ultracentrifuged at d=1.25 g/mL to remove albumin and other dense proteins. A portion of lipoprotein-rich plasma was then dialyzed in Tris/NaCl. Approximately 65,000 cpm rabbit [^{125}I]-rLCAT was incubated with rabbit serum or rabbit lipoproteins (d<1.25) for 18 hours at 4°C. Both dialyzed and undialyzed plasma and lipoprotein samples were incubated to determine whether binding of rLCAT is influenced by ionic strength. A final volume of 0.5mL per sample was adjusted to d=1.21 or 1.25 using NaBr density gradient solution and the samples were ultracentrifuged at 42,000 rpm in a 50.3Ti rotor for 48 hours.

Results (figure 39) indicate that differences in the ionic environment under these conditions do not appear to alter the lack of association observed with recombinant LCAT and native plasma. Had such a physical association been present, there would have been observed an increase of radioactive counts in fractions 2 and 3, similar to that of figure 38.
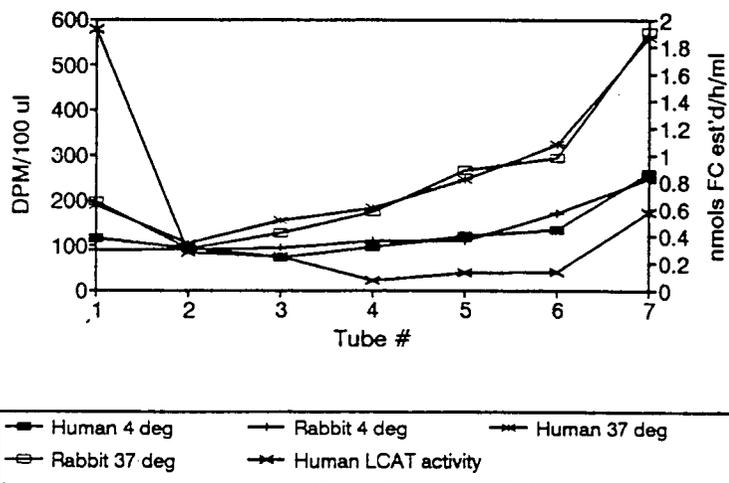
Figure 37. Ultracentrifugation (d=1.25g/mL) of rabbit and human plasma following pre-incubation with human [³H]-rLCAT. Equal fractions were taken from the ultracentrifuge tube after 48 hours at 42,000 rpm in a 50.3Ti rotor. Tube #1 represents the uppermost layer (most buoyant) fraction from the ultracentrifuge tube. Tube #7 was taken from the bottom fraction. LCAT activity, mainly from the native plasma LCAT, was measured in each fraction as nmoles free cholesterol esterified per hour per mL. The other plots represent human [³H]-rLCAT counts measured as DPM/100μL, under various incubation conditions and species of plasma.
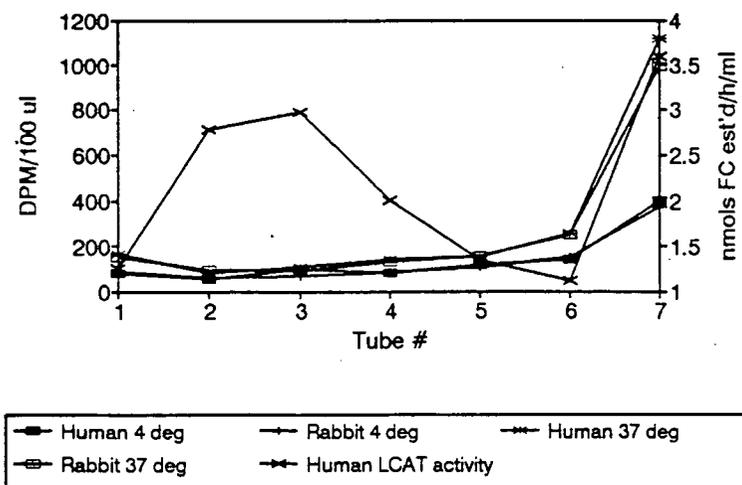
Figure 38. Ultracentrifugation (d=1.21g/mL) of human plasma following pre-incubation with human [³H]-rLCAT. Conditions used in these experiments are similar to that of figure 37. In this experiment, plasma was adjusted to a density of d=1.21 g/mL. At this density, the highest LCAT esterification activity was observed in tubes 2 and 3. The highest radioactivity, however, was found in the most dense tube, tube 7.
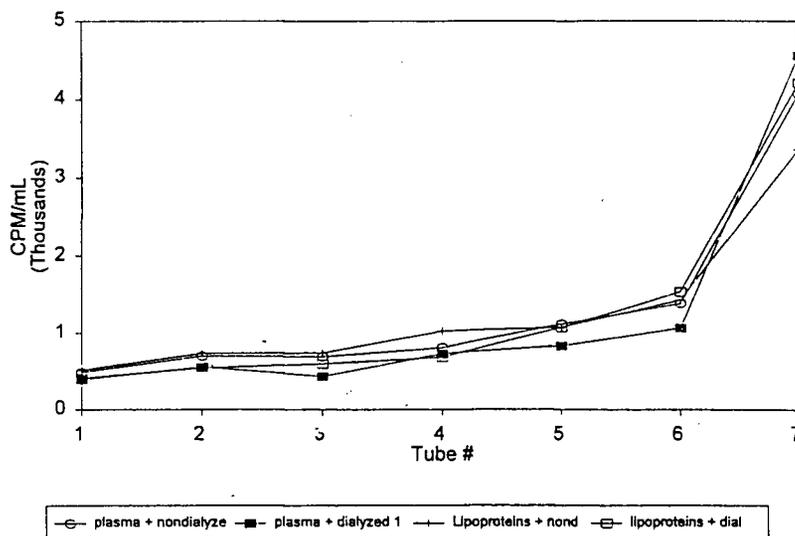
Figure 39. Ultracentrifugation (d=1.21g/mL) of native rabbit plasma and lipoproteins following pre-incubation with rabbit [^{125}I]-rLCAT. Native rabbit plasma and albumin-deficient lipoproteins with density adjusted to 1.25g/mL were incubated with rabbit [^{125}I]-rLCAT with or without extensive dialysis to remove NaBr. The figure shows radioactive counts in thousands of CPM/mL over seven fractions, with least dense fraction labeled tube #1.

4.2.2.3 Biogel size exclusion chromatography.

Based on previous experience in our laboratory, a third approach to determining whether rLCAT may be physically associated with lipoproteins utilized Biogel agarose (0.5 mesh) chromatography. To obtain the adequate resolution between serum lipoproteins, two 1.5 X 95 cm columns were joined in series. Serum samples were preincubated with [^{3}H]-rLCAT, then applied at a flow rate of 0.1mL/min with the first lipoprotein fractions collected approx. 21 hours later (see figure 40). Fractions of the eluted protein were subjected to SDS polyacrylamide gel electrophoresis to determine the relative position of apo A-I compared to radioactivity counted by liquid scintillation.
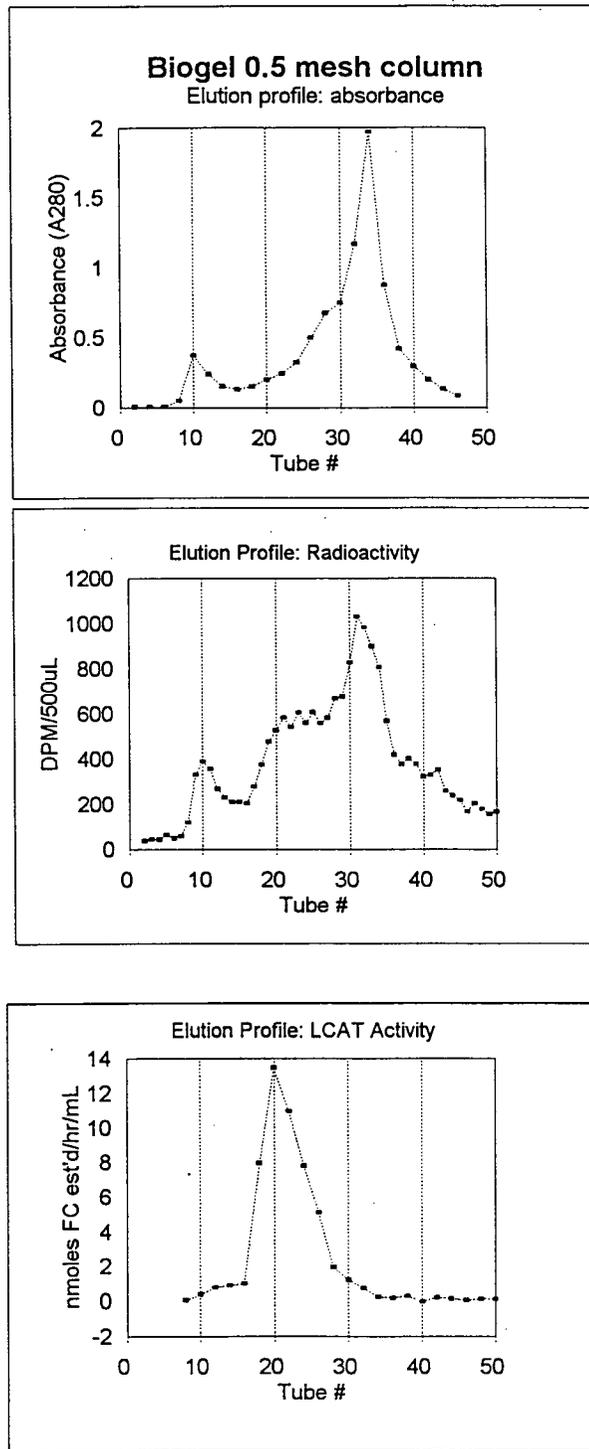
Figure 40. Biogel agarose size exclusion chromatography of human serum incubated with human [³H]-rLCAT. Lanes correspond to lane numbers in figure 41. The three panels compare absorbance (A280nm), radioactivity (DPM/500mL) and LCAT esterification activity with eluted fractions. In this profile, a broad radioactive peak appears to be clearly associated with both LCAT activity and the HDL absorbance shoulder adjacent to the albumin peak between tubes 20 to 28.
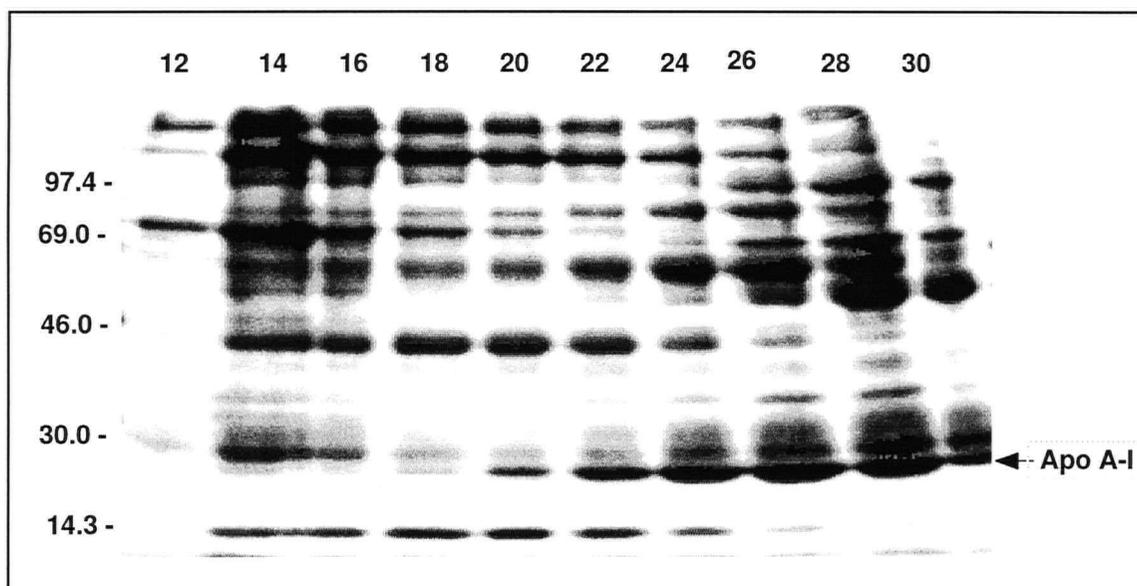
Figure 41. 10% SDS Polyacrylamide gel electrophoresis of human serum eluted from Biogel size-exclusion chromatography. The gel was stained for protein using Coomassie Blue. Lanes correspond to eluted fractions in figure 40. Apo A-I is distinguished as a series of dark bands starting in fraction 18 and extending to fraction 30. (MW=28,300 daltons). Serum albumin (MW=69,000 daltons) is seen to some degree in most lanes, however, is strongest in fractions greater than 24. The distribution of radioactivity in LDL/VLDL, HDL and albumin peaks was 9.4%, 34.9% and 55.7%, respectively.

These results, representative of three similar chromatography runs using human plasma and human [³H]-rLCAT, suggest that a component of the incubated [³H]-rLCAT coelutes with HDL and plasma proteins exhibiting LCAT esterification activity, possibly through a weak form of interaction with plasma HDL. 44.3% of the [³H]-rLCAT coeluted with fractions associated with lipoproteins. Virtually identical results were obtained when using rabbit [³H]-rLCAT and rabbit plasma. The interaction does not appear to be as strong as that of native LCAT, however, as indicated by the lack of binding observed when plasma or lipoproteins containing radiolabeled rLCAT is subjected to physical separation by ultracentrifugation. Despite an observed asso-

ciation with HDL through biochemical activation of LCAT by apo A-I, , it still appears that most of recombinant rLCAT exists as a free form.

4.3   Catabolism of rLCAT: metabolic turnover studies in rabbits

Four metabolic turnover studies utilizing [^{125}I]-rLCAT were completed in rabbits. Although not enzymatically active, useful information could still be obtained following injection of the iodinated recombinant enzyme, particularly if the sites on LCAT which associate with HDL-containing particles are not involved in region(s) associated with esterification. The [^{125}I]-rLCAT experiments were complemented with three [^{3}H]-rLCAT turnover studies using biologically active rabbit radiolabeled enzyme.

4.3.1   [^{125}I]-rLCAT turnover studies.

0.5 - 1.0 µCi pooled [^{125}I]-rLCAT was incubated with 1.0 mL freshly drawn rabbit serum for 60 minutes at 37°C to equilibrate the sample. A 10µL sample was taken to estimate total radioactivity. The rest was injected into a 2.5-3.0kg female New Zealand white adult rabbit and plasma samples were drawn by ear vein over timed intervals. The samples were then measured for total and TCA precipitable [^{125}I] radioactivity using a gamma counter.

4.3.2   [^{3}H]-rLCAT turnover studies

Between 0.5-1.0 mCi purified rabbit [^{3}H]-rLCAT was added to 1.0 mL freshly drawn rabbit serum and incubated for 60 minutes hour at 37°C. A 10µL sample was taken for estimating total radioactivity. The rest was injected into a 2.5-3.0kg female New Zealand white adult rabbit. Plasma samples were drawn by ear vein over timed intervals. The samples were then measured for total radioactivity by liquid scintillography. Due to the lower counts present when using [^{3}H]-rLCAT, TCA precipitation was not performed on these samples.

As a preliminary experiment, human [3H]-rLCAT was utilized in the first turnover study, prior to the availability of the rabbit recombinant enzyme. Two additional studies were then performed using rabbit [3H]-rLCAT (Turnovers #6 and #7).

Results of the turnover studies are found in figures 42 and 43, and are summarized in table 13. While the data was not robust enough for SAAM modeling, two distinct phases in the catabolism of the recombinant enzyme may be evident. The first component was removed very rapidly from the plasma compartment. Using regression analysis, the half-life of this component is between 2.1 to 5.8 hours. The second component was removed from plasma more slowly, with a calculated half-life between 52.7 and 62.6 hours. The wide variation in half-life calculated for these experiments is likely due to difficulty of measuring low levels of radioactivity with inherent error of analysis. The first experiment, a preliminary trial, was excluded from the above estimate for this reason.

Table 13. Calculated half life (hours) from rLCAT turnover studies in the New Zealand rabbit.

Human [3H]-rLCAT calculated half life

Total Counts	Component 1	Component 2
Turnover #1	2.5	N/A

Rabbit [125I]-rLCAT calculated half life

TCA ppt	Component 1	Component 2
Turnover #1	2.2	36.7
Turnover #2	5.2	55.5
Turnover #3	5.8	62.6
Turnover #4	4.3	52.7

Rabbit [3H]-rLCAT half life

Total Counts	Component 1	Component 2
Turnover #6	3.5	55.3
Turnover #6	2.1	55.9

Figure 42. Rabbit [125I]-rLCAT metabolic turnover studies. Two graphs are shown per experiment. The first graph, a simple plot, emphasizes the extremely rapid loss of enzyme within the first few hours following injection. The second graph is a log-transform of the data which permitted calculation of the half-life following regression analysis.

Metabolic Turnover Study#2
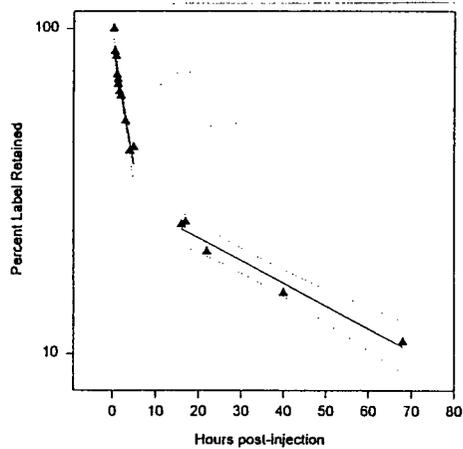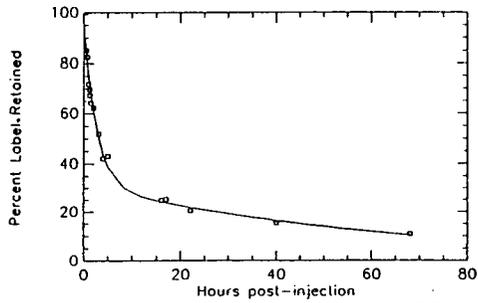
Metabolic Turnover Study#3
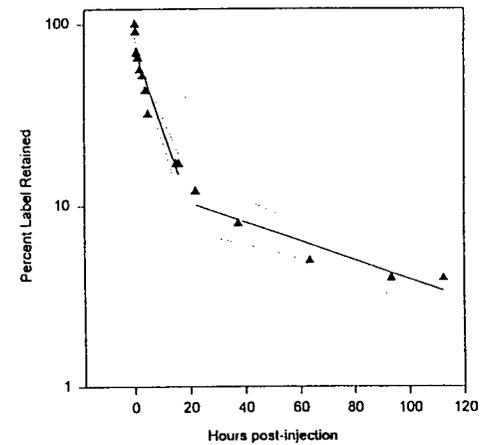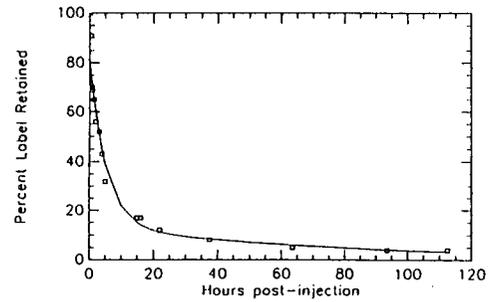
Metabolic Turnover Study#4
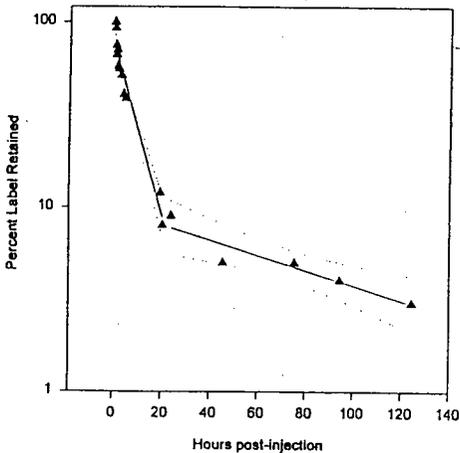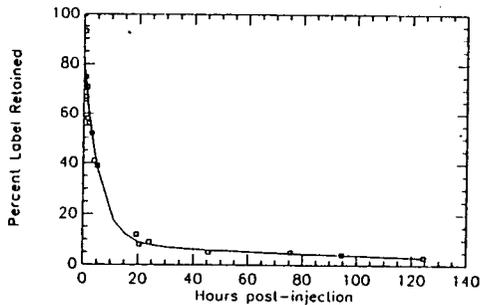
Metabolic Turnover Study#5

117
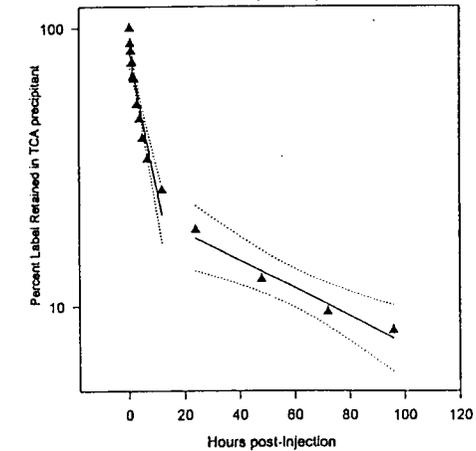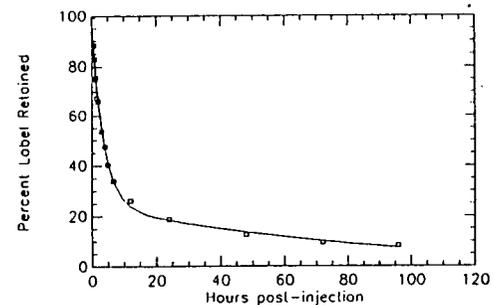
Figure 43. Rabbit [³H]-rLCAT metabolic turnover studies. Two graphs are shown per experiment. The first graph, a simple plot, emphasizes the extremely rapid loss of enzyme within the first few hours following injection. The second graph is a log-transform of the data which permitted calculated of the half-life following regression analysis.


118
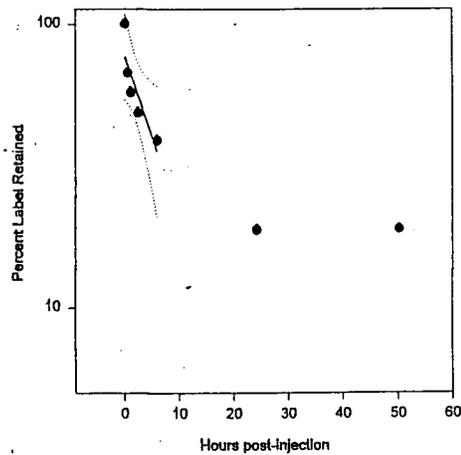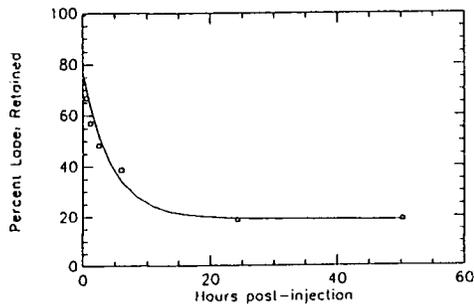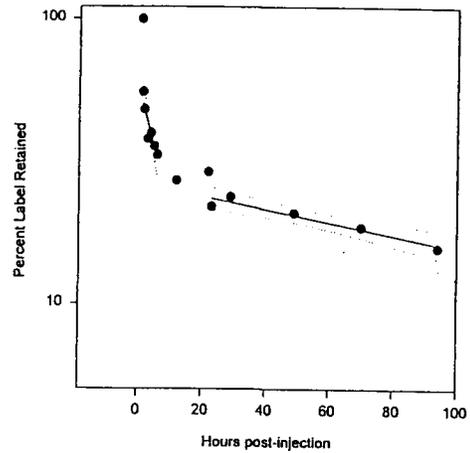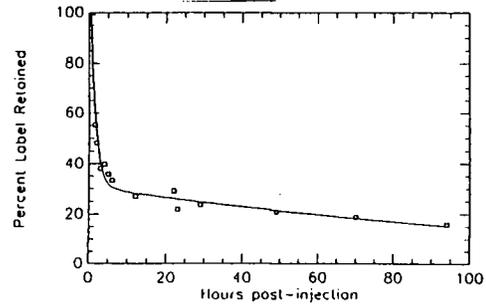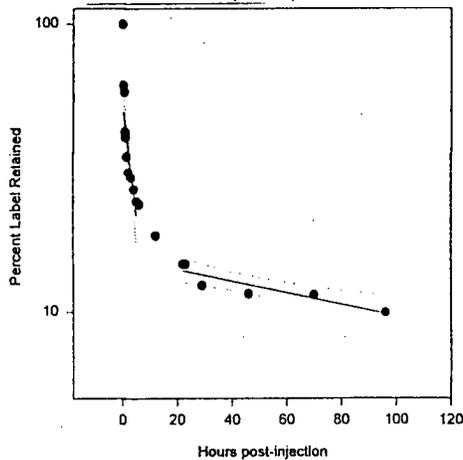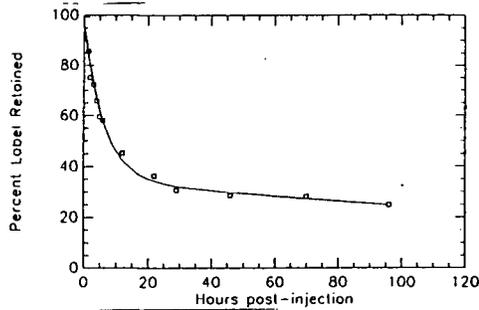
Chapter 5

DISCUSSION

5.   DISCUSSION

The successful cloning of rabbit and porcine LCAT cDNA has provided useful genetic material with which to conduct *in vitro* and *in vivo* studies on the structure-function relationship of this enzyme. Comparison of the cDNA sequence obtained from these clones with that of other species has shown this enzyme to be remarkably conserved through evolution. In this thesis, it was possible to take advantage of this feature by designing consensus PCR primers that potentially may be used to amplify reverse-transcribed mRNA from a number of animal species. The inter-species comparison of cDNA clones complements the ongoing work currently being done using site-directed mutagenesis on predicted structural components and on natural mutations known to affect enzyme production and/or function. It is interesting to note, for example, that of virtually all of the amino acid residues in which mutants have been known to affect LCAT activity or secretion are conserved across all species.

Recombinant rabbit LCAT was compared to the human recombinant enzyme with respect to its utilization of both HDL-analogue and endogenous (plasma) substrates, activation of the esterification reaction by apo A-I and its immunoreactivity. The Km and Vmax of rabbit rLCAT were comparable to those of the human enzyme using HDL-like proteoliposome substrates. However, the rabbit protein failed to react with polyclonal antibodies raised against the human enzyme. While this helped to confirm that the protein expressed in cell culture was a nonhuman LCAT, it presented technical difficulties in measuring protein mass. It was therefore necessary to purify the human and rabbit proteins in order to provide kinetic data that could be compared between species. Until such a mass assay is available, however, it will be difficult to compare the kinetic data obtained through studies of this type with those of other workers.

The further characterization of the radiolabeled enzyme, in chapter 4, utilized a number of techniques to determine its ability to interact with lipoproteins as a biologically active enzyme. Interestingly, although human and rabbit recombinant enzymes esterified cholesterol with activities comparable to that of the purified native human protein, they do not bind to lipoproteins in a similar manner. Experiments utilizing sequential ultracentrifugation showed that the recombinant enzymes did not co-migrate with lipoproteins as did the native LCAT. Furthermore, the association of rLCAT with lipoproteins did not appear to be increased when the ionic environment was changed. Size-exclusion chromatography using Biogel, in contrast to Superose 12, was able to resolve lipoproteins. Using this method, a significant fraction of the recombinant enzyme co-migrated not only with HDL but also with LDL fractions. The interaction of rLCAT with lipoproteins appears to be considerably weaker than that of the native enzyme. There could be a number of reasons for this effect. Since the native LCAT is already located on HDL, it may be conceivable that the recombinant enzyme is unable to compete for a limited number of apoprotein binding sites. If so, a possible future experiment would be to utilize LCAT-deficient plasma in similar incubation experiments as those done in this thesis to determine whether the recombinant protein is more readily incorporated into the lipoprotein particle. Secondly, it is possible that recombinant LCAT is secreted from cell culture in a different manner to that of the native protein. If, for example, the enzyme, which is highly hydrophobic, incorporates lipid material from the cell membrane during secretion, it may not interact with other lipids in a similar manner. Additionally, differences in postranslational modification between native LCAT produced in hepatic cells and recombinant LCAT produced in baby hamster kidney cells may affect carbohydrate content on the recombinant LCAT, which in turn, may alter its ability to interact with lipoproteins.

The metabolic studies utilizing radiolabeled rLCAT provided useful information to assess the utility of the recombinant protein as a possible therapeutic agent for

treatment of familial LCAT deficiency. It is not known whether the marked difference in the manner in which rLCAT binds to lipoproteins influenced the catabolic rate observed when the radiolabeled recombinant protein was utilized in rabbit metabolic turnover studies. Should the lack of binding to lipoproteins be the result of the presence of native LCAT on the lipoprotein, the only valid experiment for a turnover study of this kind would be the use of an LCAT deficient animal, or patient with LCAT deficiency. Alternatively, it may be necessary to develop further methods to increase the association of the recombinant protein with lipoproteins in order to reduce the catabolic rate of the administered enzyme to a rate sustainable under therapeutic conditions.

The second component of the decay curve observed during these metabolic studies resulted in a calculated half-life of 4-6 days, comparable to that of human apo A-I. While this may be suggestive that some rLCAT is metabolized together with HDL lipoproteins, it was not possible, given the rapid loss of the radiolabeled enzyme and resultant low counts in serum, to determine whether the protein was associating with a specific lipoprotein fraction. Nor was it possible to determine the production rate of the enzyme as antibodies were not available to measure LCAT mass in plasma.

5.1   Perspectives for Future Study

Although most of the initial objectives for this thesis were met, the technical difficulties encountered, particularly with respect to obtaining sensitive and specific antibodies that react with rabbit, porcine mouse and other species of LCAT complicated the study and limited its design objectives. With the production of large amounts of recombinant protein through stable transfection, an immediate goal would be to develop antibodies suitable for mass assay in plasma.

A second requirement for further work on the *in vivo* metabolism of LCAT would be to develop anti-apo A-I immunoaffinity columns with sufficient capacity to retain the majority of LCAT associated with this apoprotein in plasma. This apoprotein-specific method would provide more sensitive and accurate means of assessing the association of rLCAT with lipoproteins in the presence of other proteins such as albumin.

The availability of large quantities of homogeneous recombinant enzyme produced in several species, should facilitate the further investigation of some of the physical properties of this protein, for example, through conformational studies using circular dichroism and NMR spectroscopy, the qualitative and quantitative analysis of LCAT with lipid monolayers and ultimately, LCAT crystallization and X-ray diffraction analysis. The latter should resolve details regarding its three-dimensional structure, allowing specific structure-function relationships of LCAT to be proposed and further studied.

Finally, the development of inter-species consensus primers should make possible the cloning of LCAT in other species. Comparison of differences and similarities of the LCAT cDNA and translated amino acid sequence further down the evolutionary tree would extend our current understanding of the structural regions on LCAT that may be related to function of this enzyme.

Chapter 6

REFERENCES

6.   REFERENCES

Acton S, Rigotti A, Landschulz K, Xu S, Hobbs H, and Krieger M. 1996. Identification of scavenger receptor SR-BI as a high density lipoprotein receptor. Science 271: 518-520.

Agnani G, and Marcel Y. 1993. Cholesterol efflux from fibroblasts to discoidal lipoproteins with apolipoprotein A-I (Lp A-I) increases with particle size but cholesterol transfer from Lp A-I to lipoproteins decreases with size. Biochemistry 32: 2643-2649.

Albers JJ, Lin J, and Roberts GP. January 1979. Effect of human plasma apolipoproteins on the activity of purified lecithin: cholesterol acyltransferase. Artery 5 (1): 61-75.

Anantharamaiah GM, Venkatachalapathi YV, Brouillette CG, and Segrest JP. 1990. Use of synthetic peptide analogues to localize lecithin:cholesterol acyltransferase activating domain in apolipoprotein A-I. Arteriosclerosis 10 (1): 95-105.

Aron L, Jones S, and Fielding CJ. 1978. Human plasma lecithin- cholesterol acyltransferase. Characterization of cofactor-dependent phospholipase activity. Journal of Biological Chemistry 253 (20): 7220-7226.

Assmann G, von Eckardstein A, and Funke H. 1990. Clinical, biochemical and genetic heterogeneity of lecithin:cholesterol acyltransferase deficiency syndromes. In Disorders of HDL. Proceedings of the International Symposium held at Karolinska Hospital, Stockholm, 7-8 June 1990. Carlson LA, editor. 169-175. Smith-Gordon: London.

Atger V, Giral P, Simon A, Cambillau M, Levenson J, Gariepy J, MegnienJL, and Moatti N. 1995. High-density lipoprotein subfractions asmarkers of early atherosclerosis. PCVMETRA Group. Prevention Cardio-Vasculaire en Medecene du Travail. American Journal of Cardiology 75(2): 127-31.

Bairoch A. 1991. PROSITE: a dictionary of sites and patterns in proteins. Nucleic Acids Research 19 Suppl: 2241-5.

Banka CL, Bonnet DJ, Black AS, Smith RS, and Curtiss LK. 1991. L ocalization of an apolipoprotein A-I epitope critical for activation of lecithin-cholesterol acyltransferase. Journal of Biological Chemistry 266 (35): 23886-23892.

Barter PJ, Hopkins GJ, Gorjatschko L, and Jones ME. 1984. Competitive inhibition of plasma cholesterol esterification by human high-density lipoprotein-subfraction 2. Biochimica et Biophysica Acta 793: 260-268.

Barter PJ. 1983. Evidence that lecithin:cholesterol acyltransferase acts on both high-density and low-density lipoproteins. Biochimica et Biophysica Acta 751: 261-270.

Barter PJ, Hopkins GJ, and Gorjatschko L. 1985. Lipoprotein substrates for plasma cholesterol esterification: Influence of particle size and composition of the high density lipoprotein subfraction 3. Atherosclerosis 58: 97-107.

Barter PJ, Hopkins GJ, and Ha YC. 1987. The role of lipid transfer proteins in plasma lipoprotein metabolism. American Heart Journal 113: 538-542.

Batzri S, and Korn ED. 1973. Single layer lipoposomes prepared without sonication. Biochimica et Biophysica Acta 1042: 310-314.

Bielicki JK, McCall MR, van den Berg JJ, Kuypers FA, and Forte TM. 1995. Copper and gas-phase cigarette smoke inhibit plasma lecithin: cholesterol acyltransferase activity by different mechanisms. Journal of Lipid Research 36 (2): 322-31.

Bielicki JK, Forte TM, and McCall MR. 1995. Gas-phase cigarette smoke inhibits plasma lecithin-cholesterol acyltransferase activity by modification of the enzyme's free thiols. Biochimica et Biophysica Acta 1258 (1): 35-40.

Blanche PJ, Gong EL, Forte TM, and Nichols AV. 1981. Characterization of human high-density lipoproteins by gradient gel electrophoresis. Biochimica et Biophysica Acta 665: 408-419.

Bonelli FS, Kezdy KE, and Jonas A. 1987. A continuous fluorescence assay for lecithin cholesterol acyltransferase. Analytical Biochemistry 166: 204-207.

Bonelli FS, and Jonas A. 1989. Reaction of lecithin cholesterol acyltransferase with water-soluble substrates. Journal of Biological Chemistry 264 (25): 14723-14728.

Bonelli FS, and Jonas A. 1992. Continuous Fluorescence Assay for Lecithin-Cholesterol Acyltransferase Using a Water-Soluble Phosphatidylcholine. J Lipid Res 33 (12): 1863-1869.

Borysiewicz LK, Soutar AK, Evans DJ, Thompson GR, and Rees AJ. 1982.Renal failure in familial lecithin: cholesterol acyltransferase deficiency. Quarterly Journal of Medicine 51 (204): 411-426.

Brenner S. 1988. The molecular evolution of genes and proteins: a tale of two serines. Nature 334: 528-530.

Brewer HB, Rader D, Fojo S, and Hoeg JM. 1990. Frontiers in the analysis of HDL structure, function, and metabolism. In Disorders of HDL. Carlson LA, editor. 51-58. London: Smith-Gordon and Company Limited.

Bujo H, Kusunoki J, Ogasawara M, Yamamoto T, Ohta Y, Shimada T, SaitoY, and Yoshida S. 1991. Molecular defect in familial lecithin: cholesterol acyltransferase (LCAT) deficiency: a single nucleotide insertion in LCAT gene causes a complete deficient type of the disease. Biochemical & Biophysical Research Communications 181 (3): 933-940.

Burstein M, Fine A, Atger V, Wirbel E, and Girard-Globa A. 1989. Rapid method for the isolation of two purified subfractions of high density lipoproteins by differential dextran sulfate-magnesium chloride precipitation. Biochimie 71 (6): 741-6.

Carlson LA, and Philipson B. 1979. Fish-eye disease. A new familial condition with massive corneal opacities and dyslipoproteinaemia. Lancet 2 (8149): 922-924.

Chevet D, Ramee MP, Le Pogamp P, Thomas R, Garre M, and Alcindor LG. 1978. Hereditary lecithin cholesterol acyltransferase deficiency. Report of a new family with two afflicted sisters. Nephron 20 (4):212-219.

Carlson LA, and Holmquist L. 1985. Paradoxical esterification of plasma cholesterol in Fish Eye disease. Acta Medica Scandinavica 217: 491-498.

Carlson LA, and Holmquist L. 1985. Evidence for the presence in human plasma of lecithin:cholesterol acyltransferase activity (beta-LCAT) specifically esterifying free cholesterol of combined pre-beta- and beta-liproteins. Acta Medica Scandinavica 218: 197-205.

Carlson LA, Holmquist L, and Assmann G. 1987. Different substrate specificities of plasma lecithin: cholesterol acyl transferase in fish eye disease and Tangier disease. Acta Medica Scandinavica 222 (4): 345-50.

Castro GR, and Fielding CJ. 1988. Early incorporation of cell-derived cholesterol into pre-beta-migrating high-density lipoprotein. Biochemistry 27 (1): 25-29.

Chen C, Applegate K, King WC, Glomset JA, Norum KR, and Gjone E. 1984. A study of the small spherical high density lipoproteins of patients afflicted with familial lecithin: cholesterol acyltransferase deficiency. Journal of Lipid Research 25 (3): 269-282.

Chen CH, and Albers JJ. 1982. Distribution of lecithin-cholesterol acyltransferase (LCAT) in human plasma lipoprotein fractions. Evidence for the association of active LCAT with low density lipoproteins. Biochemical and Biophysical Research Communications 107:1091-1096.

Cheung MC, and Albers JJ. 1984. Characterization of lipoprotein particles isolated by immunoaffinity chromatography. Particles containing A-I and A-II and particles containing A-I but no A-II. Journal of Biological Chemistry 259 (19): 12201-9.

Chomczynski P, and Sacchi N. 1987. Single-step method of RNA isolation by acid guanidinium thiocyanate-phenol-choloform extraction. Analytical Biochemistry 162: 156-159.

Chong KS, Jahani M, Hara S, and Lacko AG. 1983. Characterization of lecithin-cholesterol acyltransferase from human plasma. Three chemical properties of the enzyme. Canadian Journal of Biochemistry and Cell Biology 61: 875-881.

Chu FC, Kuwabara T, Cogan DG, Schaefer EJ, and Brewer HB Jr. 1979. Ocular manifestations of familial high-density lipoprotein deficiency (Tangier disease). Arch Opthal 97: 1926-1928.

Cogan DG, Kruth HS, Datilis MB, Martin N. Corneal opacity in LCAT disease. Cornea 1992; 11:595-599.

Contacos C, Neely RDG, Funke H, Assmann G, and Sullivan DR. 1993.Postprandial lipoprotein metabolism in fish eye disease [Abstract].

Deleage G, Roux B. An algorithm for protein secondary structure prediction based on class prediction. Protein Engineering 1987; 1:289- 294.

Dobiasova M, Stribrna J, Pritchard PH, and Frohlich JJ. 1992. Cholesterol esterification rate in plasma depleted of very low and low density lipoproteins is controlled by the proportion of HDL2 and HDL3 subclasses: study in hypertensive and normal middle-aged and septuagenarian men. Journal of Lipid Research 33 (10): 1411-8.

Doi Y, and Nishida T. 1983. Microheterogeneity and physical properties of human lecithin-cholesterol acyltransferase. Journal of Biological Chemistry 258: 5840-5846.

Duverger N, Rader D, and Brewer HB. 1994. Distribution of subclasses of HDL containing apoA-I without apoA-II (LPA-I) in normolipidemic men and women. Arteriosclerosis & Thrombosis 14 (10): 1594-1599.

Eisenberg S. 1984. High density lipoprotein metabolism. Journal of Lipid Research 25: 1017-1066.

Emmanuel F, Steinmetz A, Rosseneu M, Brasseur R, Gosselet N, Attenot F, Cuine S, Seguret S, Latta M, Fruchart JC, and Denefle P. 1994. Identification of specific amphipathic α-helical sequence of human apolipoprotein A-IV involved in lecithin-cholesterol acyltransferase activation. Journal of Biological Chemistry 269 (47): 29883-29890.

Espeland MA, Hoen H, Byington R, Howard G, Riley WA, and Furberg CD. 1994. Spatial distribution of carotid intimal-medial thickness as measured by B-mode ultrasonography. Stroke 25 (9): 1812-9.

Fielding CJ, and Fielding PE. 1971. Purification and substrate specificity of lecithin-cholesterol acyltransferase from human plasma. FEBS Letters 15: 355-358.

Fielding CJ, Shore VG, and Fielding PE. 1972. A protein cofactor of lecithin:cholesterol acyltransferase. Biochemical & Biophysical Research Communications 46 (4): 1493-8.

Fielding CJ, Shore VG, and Fielding PE. 1972. Lecithin: cholesterol acyltransferase: effects of substrate composition upon enzyme activity. Biochimica Et Biophysica Acta 270 (4): 513-518.

Fielding CJ, and Collet X. 1991. Phospholipase activity of lecithin-cholesterol acyltransferase. Methods In Enzymology 197: 426-33.

Fielding CJ, and Fielding PE. 1981. Regulation of human plasma lecithin:cholesterol acyltransferase activity by lipoprotein acceptor cholesteryl ester content. Journal of Biological Chemistry 256 (5): 2102-2104.

Fielding PE, Miida T, and Fielding CJ. 1991. Metabolism of low-density lipoprotein free cholesterol by human plasma lecithin-cholesterol acyltransferase. Biochemistry 30 (35): 8551-8557.

Flatmark AL, Hovig T, Myhre E, Gjone E. Renal transplantation in patients with familial lecithin: cholesterol-acetyltransferase deficiency. Transplantation Proceedings 1977; 9:1665-1671.

Forte TM, McCall MR, Knowles BB, and Shore VG. 1989. Isolation and characterization of lipoproteins produced by human hepatoma-derived cell lines other than HepG2. Journal of Lipid Research 30: 817-829.

Fournier N, Myara I, Atger V, Moatti N. Reactivity of lecithin-cholesterol acyl transferase (LCAT) towards glycated high-density lipoproteins (HDL). Clinica Chimica Acta 1995; 234:47-61.

Francone OL, Gurakar A, and Fielding CJ. 1989. Distribution and functions of lecithin:cholesterol acyltransferase and cholesteryl ester transfer protein in plasma lipoproteins. Evidence for a functional unit containing these activities together with apolipoproteins A-I and D that catalyzes the esterification and transfer of cell-derived cholesterol. Journal of Biological Chemistry 264 (12): 7066-7072.

Francone OL, and Fielding CJ. 1991. Structure-function relationships in human lecithin:cholesterol acyltransferase. Site-directed mutagenesis at serine residues 181 and 216. Biochemistry 30 (42): 10074-7.

Francone OL, and Fielding CJ. 1991. Effects of site-directed mutagenesis at residues cysteine-31 and cysteine-184 on lecithin- cholesterol acyltransferase activity. Proceedings of the National
Academy of Sciences of the United States of America 88 (5): 1716-1720.

Francone OL, Evangelista L, and Fielding CJ. 1993. Lecithin-cholesterol acyltransferase: effects of mutagenesis at N-linked oligosaccharide attachment sites on acyl acceptor specificity. Biochimica et Biophysica Acta 1166 (2-3): 301-304.

Francone OS, Gong EL, Ng DS, Fielding CJ, Rubin EM. Expression of human lecithin-cholesterol acyltransferase in transgenic mice. Journal of Clinical Investigation 1995; 96.

Frohlich J, and McLeod R. 1986. Lecithin: cholesterol acyltransferase (LCAT) deficiency syndromes. Advances In Experimental Medicine & Biology 201: 181-94.

Frohlich J, Hoag G, McLeod R, Hayden M, Godin DV, Wadsworth LD, Critchley JD, and Pritchard PH. 1987. Hypoalphalipoproteinemia resembling fish eye disease. Acta Medica Scandinavica 221 (3): 291- 298.

Frohlich J, McLeod R, Pritchard PH, Fesmire J, and McConathy W. 1988. Plasma lipoprotein abnormalities in heterozygotes for familial lecithin:cholesterol acyltransferase deficiency. Metabolism: Clinical & Experimental 37 (1): 3-8.

Frohlich JJ, Pritchard PH, Sparks DL, and Westerlund J. 1990. Primary isolated hypo-alpha-lipoproteinemia: a distinct familial lipoprotein abnormality? *In* Disorders of high density lipoprotein. Carlson L, editor. 177-184. London: Smith - Gordon and Company Ltd.

Fruchart J-C, Ailhaud G, and Bard J-M. 1993. Heterogenity of high density lipoprotein particles. Circulation 87(suppl III): III-22-III-27. Funk WD, MacGillivray RTA, Mason AB, Brown SA, and Woodworth RC. 1990. Expression of the amino-terminal half-molecule of human serum transferrin in cultured cells and characterization of the recombinant protein. Biochemistry 29: 1654-1660.

Funke H, von Eckardstein A, Pritchard PH, Karas M, Albers JJ, and Assmann G. 1991a. A frameshift mutation in the human apolipoprotein A-I gene causes high density lipoprotein deficiency, partial lecithin: cholesterol-acyltransferase deficiency, and corneal opacities. Journal of Clinical Investigation 87 (1): 371-376.

Funke H, von Eckardstein A, Pritchard PH, Albers JJ, Kastelein JJ, Droste C, and Assmann G. 1991b. A molecular defect causing fish eye disease: an amino acid exchange in lecithin-cholesterol acyltransferase (LCAT) leads to the selective loss of alpha-LCAT activity. Proceedings of the National Academy of Sciences of the United States of America 88 (11): 4855-4859.

Funke H, von Eckardstein A, Pritchard PH, Hornby AE, Wiebusch H, Motti C, Hayden MR, Dachet C, Jacotot B, Gerdes U, and et al. 1993. Genetic and phenotypic heterogeneity in familial lecithin: cholesterol acyltransferase (LCAT) deficiency. Six newly identified defective alleles further contribute to the structural heterogeneity in this disease. Journal of Clinical Investigation 91 (2): 677-683.

Furukawa Y, Urano T, Hida Y, Itoh H, Takahashi C, and Kimura S. 1992. Interaction of rat lecithin-cholesterol acyltransferase with rat apolipoprotein A-I and with lecithin-cholesterol vesicles. Journal of
Biochemistry 111 (3): 413-418.

Geourjon C, and Deleage G. 1994. SOPM: a self optimised prediction method for protein secondary structure prediction. Protein Engineering 7: 157-164.

Gibrat JF, Garnier J, Robson B. Further developmentsof protein secondary structure prediction using information theory. New parameters and consideration of residue pairs. Journal of Molecular Biology 1987; 198:425-443.

Glass C, Pittman RC, Civen M, and Steinberg D. 1985. Uptake of high density lipoprotein associated apoprotein A-I cholesteryl esters by 16 tissues of the rat in vivo and by adrenal cells and hepatocytes in vitro. Journal of Biological Chemistry 260: 744-750.

Glomset JA. 1968. The plasma lecithin:cholesterol acyltransferase reaction. Journal of Lipid Research 9 (2): 155-167.

Glomset JA. 1970. Physiological role of lecithin-cholesterol acyltransferase. American Journal of Clinical Nutrition 23: 1129-1136.

Glomset JA, Nichols AV, Norum KR, King W, and Forte T. 1973. Plasma lipoproteins in familial lecithin:cholesterol acyltransferase deficiency. Further studies of very low and low density lipoprotein abnormalities. Journal of Clinical Investigation 52: 1078-1092.

Glomset JA, Norum KR, Nichols AV, King WC, Mitchell CD, Applegate KR, Gong EL, and Gjone E. 1975. Plasma lipoproteins in familial lecithin: cholesterol acyltransferase deficiency: effects of dietary manipulation. Scandinavian Journal of Clinical & Laboratory Investigation 35 (Suppl 142): 3-30.

Godin DV, Gray GR, and Frohlich J. 1978. Erythrocyte membranealterations in lecithin:cholesterol acyltransferase deficiency.Scandinavian Journal of Clinical & Laboratory Investigation 38 Suppl(150): 162-167.

Goldberg DI, Beltz WF, and Pittman RC. 1991. Evaluation of pathways for the cellular uptake of high density lipoprotein cholesterol esters in rabbits. Journal of Clinical Investigation 87 (1): 331-46.

Goldstein JL, Brown MS. The low density lipoprotein pathway and its relation to atherosclerosis. Annual Review of Biochemistry 1987; 46:897-930.

Gordon T, Castelli WP, Hjortland MC, Kannel WB, and Dawber TR. 1977. High density lipoprotein as a protective factor against CHD. American Journal of Medicine 62: 707-714.

Gotoda T, Yamada N, Murase T, Sakuma M, Murayama N, Shimano H, KozakiK, Albers JJ, Yazaki Y, and Akanuma Y. 1991. Differential phenotypic expression by three mutant alleles in familial lecithin:cholesterol acyltransferase deficiency. Lancet 338 (8770): 778-781.

Grove D, and Pownall HJ. 1991. Comparative specificity of plasma lecithin:cholesterol acyltransferase from ten animal species. Lipids 26 (6): 416-420.

Gustafson A, McConathy AW, Alaupovic P, Curry MD, and Person B. 1979. Identification of apolipoprotein families in a variant of human plasma apolipoprotein A deficiency. Scandinavian Journal of Clinical & Laboratory Investigation 39: 25-33.

Hamilton RL, Havel RJ, Kane JP, Blaurock AI, Sata T. Cholestasis: lamellar structure of the abnormal human serum lioprotein. Science 1971; 172:475-478.

Havel RJ, Eder HA, and Bragdon JH. 1955. The distribution and chemicalcomposition of ultracentrifugally separated lipoproteins in human serum. Journal of Clinical Investigation 34: 1345-1353.

Havel RJ, Goldstein JL, and Brown MS. 1980. Lipoproteins and lipid transport. *In* Metabolic
Control and Disease. Bondy PK, and Rosenberg LE, eds. 393-494. Philadelphia: Saunders.

Hefele Wald J, Krul ES, and Jonas A. 1990. Structure of apolipoprotein A-I in three homogenous, reconstituted high density lipoprotein particles. Journal of Biological Chemistry 265: 20037-20043.

Hengstschlager-Ottnad E, Kuchler K, and Schneider WJ. 1995. Chicken lecithin-cholesterol acyltransferase. Molecular characterization reveals unusual structure and expression pattern. Journal of Biological Chemistry 270 (44): 26139-45.

Higgins DG, and Sharp PM. 1988. CLUSTAL: a package for performing multiple sequence alignment on a microcomputer. Gene 73 (1): 237-44.

Hill JS, O K, Wang X, and Pritchard PH. 1919. Lecithin:cholesterol acyltransferase deficiency: identification of a causative gene mutation and a co-inherited protein polymorphism. Biochimica et Biophysica Acta 1993 Jun 1181 (3): 321-3.

Hixson JE, Driscoll DM, Birnbaum S, and Britten ML. 1993. Baboon lecithin cholesterol acyltransferase (LCAT): cDNA sequences of two alleles, evolution and gene expression. Gene 128: 295-299.

Hoeg JM, Vaisman BL, Demonsky SJ, Meyn SM, Talley GD, Hoyt Jr RF *et al.* Lecithin:cholesterol acyltransferase overexpression generates hyperlipoproteinemia and a nonatherogenic lipoprotein pattern in transgenic rabbits. Journal of Biological Chemistry 1996; 271:4396-4402.

Holmquist L, and Carlson LA. 1988. Normalization of high density lipoprotein in fish eye disease plasma by purified normal human lecithin: cholesterol acyltransferase. Lipids 23 (3): 225-229.

Ho WKK, and Nichols AV. 1971. Interaction of lecithin:cholesterol acyltransferase with sonicated dispersions of lecithin. Biochimica et Biophysica Acta 231: 185-193.

Hovig T, Gjone E. Familial plasma lecithin:cholesterol acyltransferase (LCAT) deficiency. Ultrastructural aspects of a new syndrome with particular reference to lesions in the kidneys and the spleen. Acta Pathol Micro Scand 1973; Section A, 81:681-697.

Huang Y, von Eckardstien A, and Assmann G. 1993. Cell-derived unesterified cholesterol cycles between different HDLs and LDL for its effective esterification in plasma. Arteriosclerosis and Thrombosis 13: 445-458.

Ito T, Nishiwaki M, Ishikawa T, and Nakamura H. August 1995. CETP and LCAT activities are unrelated to smoking and moderate alcohol consumption in healthy normolipidemic men. Japanese Circulation Journal 59 (8): 541-6.

Jahani M, and Lacko AG. 1982. Study of the lecithin:cholesterol acyltransferase reaction with liposome and high density lipoprotein substrates. Biochimica et Biophysica Acta 713: 504-511.

Jauhiainen, M., and P. J. Dolphin. 1986. Human plasma lecithin- cholesterol acyltransferase. An elucidation of the catalytic mechanism. Journal of Biological Chemistry 261 (15): 7032-7043.

Jauhiainen M, Stevenson KJ, and Dolphin PJ. 1988. Human plasma lecithin-cholesterol acyltransferase. The vicinal nature of cysteine 31 and cysteine 184 in the catalytic site. Journal of Biological Chemistry 263 (14): 6525-6533.

Jonas A, Sweeny SA, and Herbert PN. 1984. Discoidal complexes of A and C lipoproteins with lipids and their reactions with lecithin:cholesterol acyltransferase. Journal of Biological Chemistry 259 (10):6369-6375.

Jonas, A. 1986. Synthetic substrates of lecithin:cholesterol acyltransferase. Journal of Lipid Research 27: 689.

Jonas A, Kezdy KE, and Wald JH. 1989. Defined apolipoprotein A-I conformations in reconstituted high density lipoprotein discs. Journal of Biological Chemistry 264 (9): 4818-4824.

Jonas A. 1991. Lecithin-cholesterol acyltransferase in the metabolism of high-density lipoproteins. Biochimica et Biophysica Acta 1084 (3): 205-220.

Kadowaki H, Patton GM, and Robins SJ. 1992. Metabolism of high density lipoprotein lipids by the rat liver: evidence for participation of hepatic lipase in the uptake of cholesteryl ester. Journal of Lipid Research 32: 97-106.

Kitabatake K, Piran U, Kamio Y, Doi Y, and Nishida T. 1979. Purification of human plasma lecithin:cholesterol acyltransferase and its specificity towards the acyl acceptor. Biochimica et Biophysica Acta 573: 145-154.

Khalil A, Farooqui J, and Scanu AG. 1986. Antigenic relatedness between lecithin-cholesterol acyltransferase and phospholipases of the A2 family. Biochimica et Biophysica Acta 878: 127-130.

Klein HG, Lohse P, Pritchard PH, Bojanovski D, Schmidt H, and Brewer HB. 1992. Two Different Allelic Mutations in the Lecithin- Cholesterol Acyltransferase Gene Associated with the Fish Eye Syndrome - Lecithin-Cholesterol Acyltransferase (Thr123->Ile) and Lecithin- Cholesterol Acyltransferase (Thr347->Met). J Clin Invest 89 (2): 499-506.

Klein HG, Lohse P, Duverger N, Albers JJ, Rader DJ, Zech LA, Santamarinafojo S, and Brewer HB. 1993a. 2 Different Allelic Mutations in the Lecithin - Cholesterol Acyltransferase (LCAT) Gene Resulting in Classic LCAT Deficiency - LCAT (tyr(83)->stop) and LCAT (tyr(156)->asn). J Lipid Res 34 (1): 49-58.

Klein HG, Santamarina-Fojo S, Duverger N, Clerc M, Dumon MF, Albers JJ, Marcovina S, and Brewer HB Jr. 1993b. Fish eye syndrome: a molecular defect in the lecithin-cholesterol acyltransferase (LCAT) gene associated with normal alpha-LCAT-specific activity. Implications for classification and prognosis. Journal of Clinical Investigation 92 (1): 479-485.

Klein HG, Duverger N, Albers JJ, Marcovina S, Brewer HB Jr, and Santamarina-Fojo S. 1921. In vitro expression of structural defects in the lecithin-cholesterol acyltransferase gene. Journal of Biological Chemistry 1995 Apr 270 (16): 9443-7.

Knipping G, Birchbauer A, Steyrer E, Groener J, Zechner R, and Kostner GM. 1986. Studies on the substrate specificity of human and pig lecithin:cholesterol acyltransferase: role of low-density lipoproteins. Biochemistry 25: 5242-5249.

Kriegler M. 1990. In Gene transfer and expression. A laboratory manual. 96-101. New York: Stockton Press.

Kuivenhoven JA, Stalenhoef AFH, Hill JS, Demacker PNM, Errami A, Kastelein JJP, and Pritchard PH. 1996. Two novel molecular defects the LCAT gene are associated with Fish Eye Disease. Arterioscleros Thrombosis, and Vacular Biology 16 (2): in press.

Kuivenhoven JA, van Voorst tot Voorst EJGM, Wiebusch H, Marovina SM, Funke H, Assmann G, Pritchard PH, and Kastelein JJP. 0995. A unique genetic and biochemical presentation of Fish-Eye disease. Journal of Clinical Investigation 96: 2783.

Kunitake ST, LaSala KJ, and Kane JP. 1985. Apolipoprotein A-I- containing lipoproteins with pre-beta electrophoretic mobility. Journal of Lipid Research 26: 549-555.

Levin JM, Garnier J. Improvements in a secondary structure predictionmethod based on a search for local sequence homologies and its use as a model building tool. Biochimica et Biophysical Acta 1988; 955:283-295.

Lipman DJ, and Pearson WR. 1985. Rapid and sensitive protein similarity searches. Science 227 (4693): 1435-41.

Liu M, and Subbaiah PV. 1993. Activation of plasma lysolecithin acyltransferase reaction by apolipoproteins A-I, C-I and E. Biochimica et Biophysica Acta 1168 (2): 144-152.

Magil A, Chase W, Frohlich J. Unusual renal biopsy findings in a patient with familial lecithin:cholesterol acyltransferase deficiency. Human Pathology 1982; 13:283-5.

Maeda E, Naka Y, Matozaki T, Sakuma M, Akanuma Y, Yoshino G, and Kasuga M. 1991. Lecithin-cholesterol acyltransferase (LCAT) deficiency with a missense mutation in exon 6 of the LCAT gene. Biochemical & Biophysical Research Communications 178 (2): 460-466.

Manninen V, Elo MO, Frick M, Haapa K, Heinonen OP, Heinsalmi P, Helo P, Huttunen JK, Kaitaniemi P, Koskinen P et al. 1988. Lipid alterations and decline in the incidence of coronary heart disease in the Helsinki Heart Study`. JAMA 260 (5): 641-651.

Marcel YL, Vezina C, Emond D, and Suzue G. 1980. Heterogeneity of human high density lipoprotein: presence of lipoproteins with and without apoE and their roles as substrates for lecithin:cholesterol
acyltransferase reaction. Proceedings of the National Academy of Sciences of the United States of America 77 (5): 2969-2973.

Marcel YL. 1982. Lecithin: cholesterol acyltransferase and intravascular cholesterol transport. Advances In Lipid Research 19:85-136.

Matz CE, and Jonas A. 1982. Micellar complexes of human apolipoprotein A-I with phosphatidylcholines and cholesterol prepared from cholate-lipid dispersions. Journal of Biological Chemistry 257: 4535-4540.

Matz CE, and Jonas A. 1982. Reaction of human lecithin cholesterol acyltransferase with synthetic micellar complexes of apolipoprotein A- I, phosphatidylcholine, and cholesterol. Journal of Biological Chemistry 257 (8): 4541-4546.

McLean J, Fielding C, Drayna D, Dieplinger H, Baer B, Kohr W, Henzel W, and Lawn R. 1986a. Cloning and expression of human lecithin cholesterol acyltransferase cDNA. Proc. Natl. Acad. Sci. USA 83: 2335-2339.

McLean J, Wiopn K, Drayna D, Fielding C, and Lawn R. 1986b. Human lecithin-cholesterol acyltransferase gene: complete gene sequence and sites of expression. Nucleic Acids Research 14 (23): 9397-9406.

McLean JW. 1992. Molecular defects in the lecithin:cholesterolvacyltransferase gene. In High density lipoproteins and atherosclerosis, vIII. Miller NE, and Tall AR, editors. 59-65. Amsterdam: Elsevier Science Publishers B.V.

McGill HC Jr, Ed. 1968. The geographic pathology of atherosclerosis. 1-193. Baltimore: Williams & Wilkins.

McIntyre N. 1988. Familial LCAT deficiency and fish-eye disease. Journal of Inherited Metabolic Disease 11 Suppl 1: 45-56.

McLean J, Fielding C, Drayna D, Dieplinger H, Baer B, Kohr W, Henzel W, and Lawn R. 1986. Cloning and expression of human lecithin cholesterol acyltransferase cDNA. Proc. Natl. Acad. Sci. USA 83: 2335-2339.

McLean J, Wiopn K, Drayna D, Fielding C, and Lawn R. 1986. Human lecithin-cholesterol acyltransferase gene: complete gene sequence and sites of expression. Nucleic Acids Research 14 (23): 9397-9406.

Mehlum A, Staels B, Duverger N, Tailleux A, Castro G, Fievet C et al. Tissue-specific expression of the human gene for lecithin: cholesterol acyltransferase in transgenic mice alters blood lipids, lipoproteins and lipases towards a less atherogenic profile. European Journal of Biochemistry 1995 Jun 1901; 230:567-75.

Mendez AJ, Oram JF, and Bierman EL. 1991. Protein kinase C as a mediator of high density lipoprotein receptor dependent efflux of intracellular cholesterol. Journal of Biological Chemistry 266: 10104-10111.

Meng QH, Calabresi L, Fruchart JC, and Marcel YL. 1993. Apolipoprotein A-I domains involved in the activation of lecithin:cholesterol acyltransferase. Importance of the central domain. Journal of Biological Chemistry 268 (23): 16966-16973.

Meroni G, Malgaretti N, Magnaghi P, and Taramelli R. 1990. Nucleotide sequence of the cDNA for lecithin-cholesterol acyl transferase (LCAT) from the rat. Nucleic Acids Research 18 (17): 5308.

Meroni G, Malgaretti N, Pontoglio M, Ottolenghi S, and Taramelli R. 1991. Functional analysis of the human lecithin acyl transferase gene promoer. Biochemical and Biophysical Research Communications 180: 1469-1475.

Miettinen H, Gylling H, Ulmanen I, Miettinen TA, and Kontula K. 1995. Two different allelic mutations in a Finnish family with lecithin: cholesterol acyltransferase deficiency. Arteriosclerosis, Thrombosis & Vascular Biology 15 (4): 460-7.

Miller GC, and Miller NE. 1975. Plasma-high-density-lipoprotein concentration and development of ischaemic heart-disease. Lancet 1 (7897): 16-19.

Miller NE, and Miller GJ. 1984. Current concepts of the role of HDL in reverse cholesterol transport. In Clinical and metabolic aspects of high density lipoproteins. Miller NE, and Miller GJ, editors. 1-459. New York: Elsevier.

Miller NE, LaVille A, and Croak D. 1985. Direct evidence that reverse cholesterol transport is mediated by high-density lipoprotein in rabbit. Nature 314: 109-111.

Murano S, Shirai K, Saito Y, Yoshida S, Ohta Y, Yamamoto S, and Tsuchida H. 1987. Impaired intermediate-density lipoprotein triglyceride hydrolysis in familial lecithin: cholesterolacyltransferase (LCAT) deficiency. [Japanese]. Nippon Naika Gakkai Zasshi - Journal of Japanese Society of Internal Medicine 76 (1):123-7.

Murata,Y., Maeda,E., Yoshino,G. and Kasuga,M. 1993. Rabbit mRNA for lecithin-cholesterol acyltransferase. Genbank D13668 (locus RABLCAT).

Murayama N, Asano Y, Kato K, Sakamoto Y, Hosoda S, Yamada N, Kodama T, Murase T, and Akanuma Y. 1984. Effects of plasma infusion on plasma lipids, apoproteins and plasma enzyme activities in familial lecithin: cholesterol acyltransferase deficiency. European Journal of Clinical Investigation 14 (2): 122-129.

Norum KR, and Gjone E. 1968. The effect of plasma transfusion on the plasma cholesteryl esters in patients with familial lecithin:cholesterol acyltransferase deficiency. Scandinavian Journal of Clinical & Laboratory Investigation 22: 339-342.

Norum KR, Borsting S, and Grundt I. 1970. Familial lecithin: cholesterol acyltransferase deficiency. Acta Medica Scandinavica 188: 323-326.

Norum KR, Gjone E, and Glomset JA. 1989. Familial lecithin:cholesterol acyltransferase deficiency, including fish eye disease. In The metabolic basis of inherited disease. editors Scriver CR, Beaudet AL,Sly WS, and Valle D, 1181-1194. New York: McGraw-Hill, Inc.

Norum RA, Lakier JB, Goldstein S, Angel A, Goldberg RB, Block WD, Nofze DK, Dolphin PJ, Edelglass J, Bogorad DD, and Alaupovic P. 198 Familial deficiency of apolipoproteins A-I and C-III and precocious coronary heart disease. New England Journal of Medicine 306: 1513-1519.

O K, Hill JS, Wang X, McLeod R, and Pritchard PH. 1993a. Lecithin:cholesterol acyltransferase: role of N-linked glycosylation in enzyme function. Biochemical Journal 294 (Pt 3): 879-884.

O K, Hill JS, Wang X, and Pritchard PH. 1993b. Recombinantlecithin:cholesterol acyltransferase containing a Thr123--:Ile mutation esterifies cholesterol in low density lipoprotein but not in high density lipoprotein. Journal of Lipid Research 34 (1): 81-8.

O K, Hill JS, and Pritchard PH. 1995. Role of N-linked glycosylation of lecithin:cholesterol acyltransferase in lipoprotein substrate specificity. Biochimica et Biophysica Acta 1995 Jan 1254 (2): 193-7.

Oram JF. 1990. Cholesterol trafficking in cells. Current Opinion in Lipidology 1: 416-421.

Palmiter RD, Behringer RR, Quaife CJ, Maxwell F, Maxwell IH, and Brinster RL. 1987. Cell lineage ablation in transgenic mice by cell-specific expression of a toxin gene. Cell 50: 435-443.

Park CM, Kudchodkar BJ, Frohlich J, Pritchard H, and Lacko AG. 1987. Study of the components of reverse cholesterol transport in lecithin: cholesterol acyltransferase deficiency. Archives of Biochemistry and Biophysics 258 (2): 545-554.

Patsch JR, Gotto AM Jr, Olivercrona T, and Eisenberg S. 1978. Formation of high density lipoprotein2-like particles during lipolysis of very low density lipoproteins in vitro. Proceedings of the National Academy of Sciences of the United States of America 75 (9): 4519-23.

Patsch JR, Souter AK, Morisett JD, Gotto AM Jr, and Smith LC. 1980. Characterization of human high density lipoproteins by zonal ultracentrifugation. Journal of Biological Chemistry 255: 3178-3185.

Phillips MC, McLean LR, Stoudt GW, and Rothblat GH. 1980. Mechanism of cholesterol efflux from cells. Atherosclerosis 36: 409-422.

Pownall HJ, Gotto AM Jr, and Sparrow JT. 1984. Thermodynamics of lipid-protein association and the activation of lecithin:cholesterol acyltransferase by synthetic model apolipopeptides. Biochimica et Biophysica Acta 793: 149-156.

Pownall HJ, Pao Q, and Massey JB. 1985. Acyl chain and head group specificity of human plasma lecithin:cholesterol acyltransferase. Separation of matrix and molecular specificities. Journal of Biological Chemistry 260: 2146-2152.

Pownall HJ, Pao Q, Brockman HL, and Massey JB. 1987. Inhibition of lecithin-cholesterol acyltransferase by diphytanoyl phosphatidylcholine. Journal of Biological Chemistry 262 (19): 9033-9036.

Pritchard PH, McLeod R, Frohlich J, Park MC, Kudchodkar BJ, and Lacko AG. 1988. Lecithin:cholesterol acyltransferase in familial HDL deficiency (Tangier disease). Biochimica Et Biophysica Acta 958 (2): 227-234.
Qu SJ, Fan HZ, Blanco-Vaca F, and Pownall HJ. 1931. Effects of site- directed mutagenesis on the N-glycosylation sites of human lecithin:cholesterol acyltransferase. Biochemistry 1993 Aug 32 (34): 8732-6.

Rajaram OV, and Barter PJ. 1985. Reactivity of human lipoproteins with purified lecithin:cholesterol acyltransferase during incubations in vitro. Biochimica et Biophysica Acta 835: 41-49.

Reichl D, and Miller NE. 1989. Pathophysiology of reverse cholesterol transport: insights from inherited disorders of lipoprotein metabolism. Arteriosclerosis 9 (6): 785-797.

Rinninger F, and Pittman RC. 1989. Mechanism of the cholesteryl ester transfer protein-mediated uptake of high density lipoprotein cholesteryl esters by Hep G2 cells. Journal of Biological Chemistry 264 (11): 6111-6118.

Rothblat GH, Mahlberg FH, Johnson WJ, and Phillips MC. 1992. Apolipoproteins, membrane cholesterol domains, and the regulation of cholesterol efflux. Journal of Lipid Research 33: 1091-1097.

Rye K-A, Garrety KH, and Barter PJ. 1992. Changes in the size of reconstituted high density lipoprotein during incubation with cholesteryl ester transfer protein: the role of apolipoproteins.
Journal of Lipid Research 33: 215-224.

Sanger F, Nicklen S, and Coulson AR. 1977. DNA sequencing with chain-termating inhibitors. Proc. Natl. Acad. Sci. USA 74: 5463-5469.

Schaefer EJ. 1984. Clinical, biochemical and genetic features in familial disorders of high density lipoprotein deficiency. Arteriosclerosis 4: 303-322.

Schmitz G, Assmann G, Robenek H, and Brennhausen B. 1985. Tangier disease: a disorder of intracellular membrane traffic. Proc. Natl. Acad. Sci. USA 82: 6305-6309.

Segrest JP, Jones MK, De Loof H, Brouillette CG, Venkatachalapathi YV, and Anantharamaiah GM. 1992. The amphipathic helix in the exchangeable apolipoproteins: a review of secondary structure and function. [Review]. Journal of Lipid Research 33 (2): 141-166.

Segrest JP, Garber DW, Brouillette CG, Harvey SC, and Anantharamaiah, GM. 1994. The amphipathic alpha helix: a multifunctional structural motif in plasma apolipoproteins. [Review]. Advances in Protein Chemistry 45: 303-69.

Shepherd J, and Packard CJ. 1984. High-density lipoprotein apolipoprotein metabolism. In Clinical and metabolic aspects of high-density lipoproteins. Miller NE, and Miller GJ, editors. 247-274. New York: Elsevier.

Simard, G., Loiseau D, Girault A, and Perret B. 1989. Reactivity of HDL subfractions towards lecithin-cholesterol acyltransferase. Modulation by their content in free cholesterol. Biochimica et Biophysica Acta 1005 (3): 245-52.

Skretting G, and Prydz H. 1992. An Amino Acid Exchange in Exon-I of the Human Lecithin - Cholesterol Acyltransferase (LCAT) Gene Is Associated with Fish Eye Disease. Biochem Biophys Res Commun 182 (2): 583-587.

Skretting G, Blomhoff JP, Solheim J, and Prydz H. 1992. The genetic defect of the original Norwegian lecithin:cholesterol acyltransferase deficiency families. Febs Letters 309 (3): 307-310.

Smith NB, and Kutsis A. 1980. Stereo chemical substrate requirements of lecithin:cholesterol acyltransferase and its inhibition by entantiometric lysolecithins. Canadian Journal of Biochemistry 58:1286-1291.

Smith KM, Lawn RM, and Wilcox JN. 1990. Cellular localization ofapolipoprotein D and lecithin:cholesterol acyltransferase mRNA in rhesus monkey tissues by in situ hybridization. Journal of Lipid Research 31: 995-1004.

Sorci-Thomas M, Babiak J, and Rudel LL. 1915. Lecithin-cholesterolacyltransferase (LCAT) catalyzes transacylation of intact cholesteryl esters. Evidence for the partial reversal of the forward LCAT reaction. Journal of Biological Chemistry 1990 Feb 265 (5): 2665-70.

Soutar AK, Garner CW, Baker HN, Sparrow JT, Jackson RL, Gotto AM Jr, and Smith LC. 1975. Effect of the human plasma apolipoproteins and phosphatidylcholine acyl donor on the activity of lecithin:cholesterol acyltransferase. Biochemistry 14: 3057-3064.

Sparks DL, Frohlich J, and Pritchard PH. 1988. Cholesteryl ester transfer activity in plasma of patients with familial high-density lipoprotein deficiency. Clinical Chemistry 34 (9): 1812-1815.

Sparks DL, and Pritchard PH. 1989. Transfer of cholesteryl ester into high density lipoprotein by cholesteryl ester transfer protein: effect of HDL lipid and apoprotein content. Journal of Lipid Research 30 (10): 1491-8.

Sparks DL, and Pritchard PH. 1989. The neutral lipid composition and size of recombinant high density lipoproteins regulates lecithin: cholesterol acyltransferase activity. Biochemistry & Cell Biology 67 (7): 358-64.

Sparks DL, and Pritchard PH. 1991. Lipid transfer proteins, hypertriglyceridemia and reduced high density lipoprotein cholesterol. American Heart Journal 122 (2): 601-607.

Sparks DL, Anantharamaiah GM, Segrest JP, Phillips MC. Effect of the cholesterol content of reconstituted LpA-I on lecithin:cholesterol acyltransferase activity. Journal of Biological Chemistry 1995; 270: 5151-7.

Sparrow DA, Laplaud PM, Saboureau M, Zhou G, Dolphin PJ, Gotto AM Jr, Sparrow JT. Plasma lipid transport in the hedgehog: partial characterization of structure and function of apolipoprotein A-I. Journal of Lipid Research 1995; 36:485-95.

Steinmetz A, Barbaras R, Ghalim N, Clavey V, Fruchart JC, and Ailhaud G. 1990. Human apolipoprotein A-IV binds to apolipoprotein A-I/A-II receptor sites and promotes cholesterol efflux from adipose cells. Journal of Biological Chemistry 265 (14): 7859-63.

Steinmetz A, and Utermann G. 1985. Activation of lecithin:cholesterol acyltransferase by human apolipoprotein A-IV. Journal of Biological Chemistry 260: 2258-2264.

Steyrer E, and Kostner GM. 19 February 1988. Activation of lecithin- cholesterol acyltransferase by apolipoprotein D: comparison of proteoliposomes containing apolipoprotein D, A-I or C-I. Biochimica Et Biophysica Acta 958 (3): 484-91.

Stokke KT, Bjerve KS, Blomhoff JP, Oystese B, Flatmark A, Norum KR, and Gjone E. 1974. Familial lecithin:cholesterol acyltransferase deficiency: studies on lipid composition and morphology of tissues. Scandinavian Journal of Clinical & Laboratory Investigation 33 (Suppl 137): 93-100.

Subbaiah PV, Chen CH, Albers JJ, and Bagdade JD. 1982. Studies on the .cofactor requirement for the acylation and hydrolysis reactions catalyzed by purified lecithin-cholesterol acyltransferase. Effect of low density lipoproteins and apolipoprotein A-i. Atherosclerosis 45 (2): 181-90.

Tall AR, and Small DM. 1978. Plasma high-density lipoproteins. New England Journal of Medicine 299: 1232-1236.

Taramelli R, Pontoglio M, Candiani G, Ottolenghi S, Dieplinger H, Catapano A, Albers J, Vergani C, and McLean J. 1990. Lecithin cholesterol acyl transferase deficiency: molecular analysis of a mutated allele. Human Genetics 85 (2): 195-199.

Torsvik H, Gjone E, and Norum KR. 1968. Familial plasma cholesteryl ester deficiency: clinical studies in a family. Acta Medica Scandinavica 183: 387-391.

Warden CH, Langner CA, Gordon JI, Taylor BA, McLean JW, and Lusis AJ. 1989. Tissue-specific expression, developmental regulation, and chromosomal mapping of the lecithin: cholesterol acyltransferase gene. Evidence for expression in brain and testes as well as liver. Journal of Biological Chemistry 264 (36): 21573-81.

Winkler FK, D'Arcy A, and Hunziker W. 1990. Structure of human pancreatic lipase. Nature 343: 771-774.

Yang CY, Manoogian D, Pao Q, Lee FS, Knapp RD, Gotto AM Jr, and Pownall HJ. 1987. Lecithin:cholesterol acyltransferase. Functional regions and a structural model of the enzyme. Journal of Biological Chemistry 262 (7): 3086-3091.

Yüksel KU, Park YB, Jung JH, Gracy RW, and Lacko AG. 1989. Studies on the structure of lecithin:cholesterol acyltransferase (LACT)--comparisons of the active site region and secondary structure of the human and the porcine enzymes. Comparative Biochemistry & Physiology - B: Comparative Biochemistry 94 (2): 389-94.